

---

## CHAPTER 2

# An Introduction to Coupled Cluster Theory for Computational Chemists

T. Daniel Crawford\* and Henry F. Schaefer III

*Center for Computational Quantum Chemistry, Department of Chemistry, The University of Georgia, Athens, Georgia 30602-2525, (present address): \*Institute for Theoretical Chemistry, Departments of Chemistry and Biochemistry, The University of Texas, Austin, Texas, 78712-1167*

---

## INTRODUCTION

Since its introduction into quantum chemistry in the late 1960s by Čížek and Paldus,<sup>1–3</sup> coupled cluster theory has emerged as perhaps the most reliable, yet computationally affordable method for the approximate solution of the electronic Schrödinger equation and the prediction of molecular properties. The purpose of this chapter is to provide computational chemists who seek a deeper knowledge of coupled cluster theory with the background necessary to understand the extensive literature on this important ab initio technique.

In spite of the method's present utility and popularity, the quantum chemical community was slow to accept coupled cluster theory, perhaps because the earliest researchers in the field used elegant but unfamiliar mathematical tools such as Feynman-like diagrams and second quantization to derive working equations. Nearly 10 years after the essential contributions of Paldus and Čížek, Hurley presented a re-derivation of the coupled cluster doubles (CCD) equa-

*Reviews in Computational Chemistry, Volume 14*  
Kenny B. Lipkowitz and Donald B. Boyd, Editors  
Wiley-VCH, John Wiley and Sons, Inc., New York, © 2000

tions<sup>4</sup> in terms which were more familiar to quantum chemists. Soon thereafter Monkhorst<sup>5</sup> developed a general coupled cluster response theory for calculating molecular properties. By the end of the 1970s, computer implementations of the theory for realistic systems began to appear as the groups of Pople<sup>6</sup> and Bartlett<sup>7</sup> each developed and tested spin-orbital CCD programs. A few years later, Purvis and Bartlett derived the coupled cluster singles and doubles (CCSD) equations and implemented them in a practical computer program.<sup>8</sup> Since that pioneering achievement, the popularity of coupled cluster methods has blossomed, and tremendous efforts have been made in the construction of highly efficient CCSD energy codes,<sup>8–14</sup> inclusion of higher excitations in the coupled cluster wavefunction,<sup>15–34</sup> spin-adaptation of open-shell methods,<sup>35–42</sup> as well as development of analytic first<sup>43–54</sup> and second<sup>55–59</sup> energy derivatives, and methods to treat excited states.<sup>60–74</sup>

In the following section, we will use the cluster function approach developed by Sinanoğlu<sup>75</sup> to justify the well-known exponential form of the coupled cluster wavefunction. This task requires use of the mathematical technique known as second quantization (also called “occupation-number” formalism), and we introduce important concepts as they are needed. We then construct the operator equations of coupled cluster theory and address issues such as the Hausdorff expansion, variational approaches, and an eigenvalue perspective on the coupled cluster problem. In the third section, we develop a set of algebraic and diagrammatic tools needed to derive programmable equations for the CCSD method, and, using these tools, we discuss the property of the energy known as size extensivity. Next, we examine the relationship between the coupled cluster equations and those of finite-order many-body perturbation theory, leading to an explanation of the popular (T) correction implemented in many quantum chemical program packages. We then discuss some of the issues associated with an efficient computer implementation of coupled-cluster-like equations, such as matrix formulations, intermediate factorization, spin and spatial symmetry simplifications, and atomic-orbital-based algorithms. Finally, we describe some of the latest developments in the theory, including the implementation of open-shell Brueckner methods, an area of coupled cluster theory which in recent years has proven to be valuable for a number of difficult open-shell symmetry-breaking problems.

We would like to stress that this chapter is a review of coupled cluster *theory*. It is not primarily intended to provide an analysis of the numerical performance of the coupled cluster model, and we direct readers in search of such information to several recent publications.<sup>76–79</sup> Instead, we offer a detailed explanation of the most important aspects of coupled cluster theory at a level appropriate for the general computational chemistry community. Although many of the topics described here have been discussed by other authors,<sup>77,78,80,81</sup> this chapter is unique in that it attempts to provide a concise, practical introduction to the mathematical techniques of coupled cluster theory (both algebraic and diagrammatic), as well as a discussion of the efficient

implementation of the method on high performance computers, in a manner accessible to newcomers to the field.

## FUNDAMENTAL CONCEPTS

In this section we examine some of the critical ideas that contribute to most wavefunction-based models of electron correlation, including coupled cluster, configuration interaction, and many-body perturbation theory. We begin with the concept of the cluster function which may be used to include the effects of electron correlation in the wavefunction. Using a formalism in which the cluster functions are constructed by cluster operators acting on a reference determinant, we justify the use of the “exponential ansatz” of coupled cluster theory.<sup>80</sup>

### Cluster Expansion of the Wavefunction

Consider a model system of four electrons moving in an arbitrary electrostatic field generated by the nuclei in a molecule. For our purposes, it is not necessary to specify the number of these nuclei, their types, or positions; only the general form of the electronic wavefunction is of interest. It is convenient to describe the motions of each electron separately by assigning them to one-electron functions,  $\phi_i(\mathbf{x}_1)$ , where  $\mathbf{x}_1$  is a vector of the coordinates (including spin) of electron 1. In addition, electrons are fermions, so the electronic wavefunction must be antisymmetric with respect to interchange of the coordinates of any pair of electrons. A traditional and very useful starting point for such a four-electron wavefunction is the so-called Slater determinant

$$\Phi_0 = \frac{1}{\sqrt{4!}} \begin{vmatrix} \phi_i(\mathbf{x}_1) & \phi_j(\mathbf{x}_1) & \phi_k(\mathbf{x}_1) & \phi_l(\mathbf{x}_1) \\ \phi_i(\mathbf{x}_2) & \phi_j(\mathbf{x}_2) & \phi_k(\mathbf{x}_2) & \phi_l(\mathbf{x}_2) \\ \phi_i(\mathbf{x}_3) & \phi_j(\mathbf{x}_3) & \phi_k(\mathbf{x}_3) & \phi_l(\mathbf{x}_3) \\ \phi_i(\mathbf{x}_4) & \phi_j(\mathbf{x}_4) & \phi_k(\mathbf{x}_4) & \phi_l(\mathbf{x}_4) \end{vmatrix} \quad [1]$$

where the  $1/\sqrt{4!}$  is a normalization constant. Expansion of this determinant reveals a linear combination of products of the four functions,  $\phi_i$ ,  $\phi_j$ ,  $\phi_k$ , and  $\phi_l$ , with the electronic coordinates  $\mathbf{x}_n$  distributed among them in all possible ways. Since permutation of any two rows in the determinant—which is equivalent to interchanging the coordinates of any two electrons—changes the sign of  $\Phi_0$ , the antisymmetry principle is maintained.

The component functions  $\phi_i$  may be chosen in a variety of ways. For example, if the nuclear field were only a single beryllium nucleus, the one-electron spatial functions could be constructed to mimic the atomic 1s and 2s orbitals. For a molecular system, the functions can be constructed as a linear combination of atomic orbitals (AOs) in which each one-electron function

represents a molecular orbital (MO) whose AO coefficients are optimized via the Hartree–Fock self-consistent field (SCF) procedure.<sup>82</sup> A convenient shorthand notation for this wavefunction consists of a Dirac-notation ket containing only the diagonal elements of the matrix above,

$$\Phi_0 = |\phi_i(\mathbf{x}_1)\phi_j(\mathbf{x}_2)\phi_k(\mathbf{x}_3)\phi_l(\mathbf{x}_4)\rangle \quad [2]$$

where the normalization factor is included implicitly. As discussed in detail elsewhere in *Reviews in Computational Chemistry*,<sup>77</sup> the single-determinant wavefunction fails to account for the instantaneous Coulombic interactions that keep the electrons of opposite spin apart.<sup>82</sup>

How can we improve this so-called independent-particle approximation such that the motions of the electrons are correlated? Often the set of *occupied* orbitals (i.e., those functions that compose the Slater determinant above) is chosen from a larger set of one-electron functions. These “extra” functions are frequently referred to as *virtual* orbitals and may, for example, arise as a by-product of the SCF procedure.<sup>a</sup> Within the space described by the full set of orbitals, any function of  $N$  variables may be written in terms of  $N$ -tuple products of the  $\phi_p$ . For example, a function of two variables may be constructed by using all possible binary products of the set of one-electron functions:

$$f(\mathbf{x}_1, \mathbf{x}_2) = \sum_{p>q} c_{pq} \phi_p(\mathbf{x}_1)\phi_q(\mathbf{x}_2) \quad [3]$$

where the double-summation runs over the entire set of one-electron functions and the notation  $p > q$  indicates that only unique pairs of functions are included. Instead of correlating the motions of a specific pair of electrons, however, we may use a modified form of this expansion to correlate the motions of any two electrons within a selected pair of occupied orbitals—say functions  $i$  and  $j$ —using a two-particle *cluster* function,

$$f_{ij}(\mathbf{x}_m, \mathbf{x}_n) = \sum_{a>b} t_{ij}^{ab} \phi_a(\mathbf{x}_m)\phi_b(\mathbf{x}_n) \quad [4]$$

where the  $t_{ij}^{ab}$  are the cluster coefficients whose specific values are determined via the electronic Schrödinger equation (see the next section on Formal Coupled Cluster Theory). Inserting this into  $\Phi_0$  leads to the somewhat-improved electronic wavefunction

$$\Psi = |[\phi_i(\mathbf{x}_1)\phi_j(\mathbf{x}_2) + f_{ij}(\mathbf{x}_1, \mathbf{x}_2)]\phi_k(\mathbf{x}_3)\phi_l(\mathbf{x}_4)\rangle \quad [5]$$

---

<sup>a</sup>We will denote those functions that are part of the occupied space with the subscripts  $i, j, k, \dots$ , those within the virtual space with  $a, b, c, \dots$ , and arbitrary functions that may lie in either space with  $p, q, r, \dots$ .

where the Dirac shorthand implies a correctly antisymmetrized wavefunction including normalization factors as in Eq. [2]. Inclusion of the cluster function,  $f_{ij}$ , in the wavefunction produces a linear combination of Slater determinants involving replacement of occupied orbitals  $\phi_i$  and  $\phi_j$  by virtual orbitals  $\phi_a$  and  $\phi_b$ , such that

$$\Psi = \Phi_0 + \sum_{a>b} t_{ij}^{ab} |\phi_a(\mathbf{x}_1)\phi_b(\mathbf{x}_2)\phi_k(\mathbf{x}_3)\phi_l(\mathbf{x}_4)\rangle \quad [6]$$

In addition, the determinantal form of the individual terms in this expansion implies antisymmetrization of the cluster coefficients, such that  $t_{ij}^{ab} = -t_{ji}^{ab} = -t_{ij}^{ba} = t_{ji}^{ba}$ .

It should be carefully noted here that the cluster function,  $f_{ij}(\mathbf{x}_1, \mathbf{x}_2)$ , is intended to correlate the motions of *any* pair of electrons placed in orbitals  $i$  and  $j$ , and not just the motions of electrons 1 and 2. Since the Slater determinant produces a linear combination of orbital products, including terms such as

$$[\phi_i(\mathbf{x}_1)\phi_j(\mathbf{x}_2) + f_{ij}(\mathbf{x}_1, \mathbf{x}_2)]\phi_k(\mathbf{x}_3)\phi_l(\mathbf{x}_4) \quad [7]$$

and

$$[\phi_i(\mathbf{x}_3)\phi_j(\mathbf{x}_4) + f_{ij}(\mathbf{x}_3, \mathbf{x}_4)]\phi_k(\mathbf{x}_1)\phi_l(\mathbf{x}_2) \quad [8]$$

which differ only in their distribution of electronic coordinates, the cluster function correlates the motion of *every* pair of electrons found in orbitals  $\phi_i$  and  $\phi_j$ .

Depending on the chemical system of interest, however, it might be more prudent to correlate the motions of electrons in orbitals  $k$  and  $l$  rather than orbitals  $i$  and  $j$ . For example,  $\phi_i$  and  $\phi_j$  might correspond to molecular core orbitals, while  $\phi_k$  and  $\phi_l$  might correspond to the atomic or molecular valence orbitals. Electron correlation can be particularly important in the latter set of functions because the valence orbitals are often directly involved in the formation of chemical bonds. In this case, the wavefunction would be written as

$$\Psi = |[\phi_i(\mathbf{x}_1)\phi_j(\mathbf{x}_2)[\phi_k(\mathbf{x}_3)\phi_l(\mathbf{x}_4) + f_{kl}(\mathbf{x}_3, \mathbf{x}_4)]]\rangle \quad [9]$$

On the other hand, a more intelligent approach might be to correlate all possible pairwise combinations of orbitals in this four-electron system, that is,

$$\begin{aligned} \Psi = & |\phi_i\phi_j\phi_k\phi_l\rangle + |f_{ij}\phi_k\phi_l\rangle - |f_{ik}\phi_j\phi_l\rangle + |f_{il}\phi_j\phi_k\rangle + |\phi_i f_{jk}\phi_l\rangle \\ & - |\phi_i f_{jl}\phi_k\rangle + |\phi_i\phi_j f_{kl}\rangle + |f_{ij}f_{kl}\rangle - |f_{ik}f_{jl}\rangle + |f_{il}f_{jk}\rangle \end{aligned} \quad [10]$$

where the electronic coordinates are now implicit in the notation, and the signs on individual terms arise from the permutations in the orbital ordering needed to define the appropriate cluster functions. However, there is no need to limit this approach to orbital pairs only. Following Harris et al.,<sup>80</sup> we introduce three-orbital cluster functions and include these in our new wavefunction to give

$$\begin{aligned}\Psi = & |\phi_i\phi_j\phi_k\phi_l\rangle + |f_{ij}\phi_k\phi_l\rangle - |f_{ik}\phi_j\phi_l\rangle + |f_{il}\phi_j\phi_k\rangle + |\phi_i f_{jk}\phi_l\rangle \\ & - |\phi_i f_{jl}\phi_k\rangle + |\phi_i\phi_j f_{kl}\rangle + |f_{ij}f_{kl}\rangle - |f_{ik}f_{jl}\rangle + |f_{il}f_{jk}\rangle \\ & + |f_{ijk}\phi_l\rangle - |f_{ijl}\phi_k\rangle + |f_{ikl}\phi_j\rangle + |\phi_i f_{jkl}\rangle\end{aligned}\quad [11]$$

If one continues this process to include all cluster functions for up to  $N$  orbitals (four in the case discussed here), as well as single-orbital “cluster” functions that account for adjustment of the one-electron basis as other cluster functions are added, we could obtain the exact wavefunction within the space spanned by the  $\{\Phi_p\}$ . On the other hand, we might assume that clusters larger than pairs are less important to an adequate description of the system—an assumption supported by the fact that the electronic Hamiltonian contains operators describing pairwise electronic interactions at most.<sup>75</sup> We therefore write a four-electron wavefunction that includes all clusters of only one and two orbitals as<sup>80,83</sup>

$$\begin{aligned}\Psi = & |\phi_i\phi_j\phi_k\phi_l\rangle + |f_i\phi_j\phi_k\phi_l\rangle + |\phi_i f_j\phi_k\phi_l\rangle + |\phi_i\phi_j f_k\phi_l\rangle + |\phi_i\phi_j\phi_k f_l\rangle \\ & + |f_i f_j\phi_k\phi_l\rangle + |f_i\phi_j f_k\phi_l\rangle + |f_i\phi_j\phi_k f_l\rangle + |\phi_i f_j f_k\phi_l\rangle + |\phi_i f_j\phi_k f_l\rangle \\ & + |\phi_i\phi_j f_k f_l\rangle + |f_i f_j f_k\phi_l\rangle + |f_i f_j\phi_k f_l\rangle + |f_i\phi_j f_k f_l\rangle + |\phi_i f_j f_k f_l\rangle \\ & + |f_{ij}\phi_k\phi_l\rangle - |f_{ik}\phi_j\phi_l\rangle + |f_{il}\phi_j\phi_k\rangle + |\phi_i f_{jk}\phi_l\rangle - |\phi_i f_{jl}\phi_k\rangle \\ & + |\phi_i\phi_j f_{kl}\rangle + |f_{ij}f_{kl}\rangle - |f_{ik}f_{jl}\rangle + |f_{il}f_{jk}\rangle + |f_{ij}f_{jk}f_l\rangle \\ & + |f_{ij}f_k\phi_l\rangle + |f_{ij}\phi_k f_l\rangle + |f_{ij}f_j f_l\rangle - |f_{ik}f_j\phi_l\rangle - |f_{ik}\phi_j f_l\rangle - |f_{ik}f_j f_l\rangle \\ & + |f_{il}f_j\phi_k\rangle + |f_{il}\phi_j f_k\rangle + |f_{il}f_j f_k\rangle + |f_{ij}f_{jk}\phi_l\rangle + |\phi_i f_{jk}f_l\rangle + |f_i f_{jk}f_l\rangle \\ & - |f_i f_{jl}\phi_k\rangle - |\phi_i f_{jl}f_k\rangle - |f_i f_{jl}f_k\rangle + |f_i\phi_j f_{kl}\rangle + |\phi_i f_j f_{kl}\rangle + |f_i f_j f_{kl}\rangle\end{aligned}\quad [12]$$

## Cluster Functions and the Exponential Ansatz

The complicated notation of Eq. [12] can be drastically reduced by using a simple analytic form for the cluster functions. Note again that each determinant involving a cluster function is actually a linear combination of determinants each of which differs from the reference,  $\Phi_0$ , by a specific number of orbitals. For example, the 27th term on the right-hand side of in Eq. [12] expands to become

$$|f_{ij}\phi_k f_l\rangle = \sum_{a>b} \sum_c t_{ij}^{ab} t_l^c |\phi_a \phi_b \phi_k \phi_c\rangle \quad [13]$$

where we have inserted the definition of the two-electron cluster function in Eq. [4] and its one-electron counterpart to indicate the pairwise correlation of electrons in orbitals  $\phi_i$  and  $\phi_j$  as well as the “correlation” of electrons in orbital  $\phi_l$ . Note that each determinant in the summation above differs from the reference by exactly three orbitals; orbitals  $\phi_i$ ,  $\phi_j$ , and  $\phi_l$  are replaced by orbitals  $\phi_a$ ,  $\phi_b$ , and  $\phi_c$ , respectively. Hence, each term can be written as the result of some substitution operator (or products of such operators) acting on  $\Phi_0$ . This task is perhaps most easily accomplished using the mathematical technique known as second quantization.<sup>80,82,84</sup>

We will define a *creation* operator by its action on a Slater determinant:

$$a_p^\dagger |\phi_q \cdots \phi_s\rangle = |\phi_p \phi_q \cdots \phi_s\rangle \quad [14]$$

where we have added one more column (orbital) and one more row (electron) to form the new determinant on the right-hand side. We may define an *annihilation* operator in a similar manner to obtain

$$a_p |\phi_p \phi_q \cdots \phi_s\rangle = |\phi_q \cdots \phi_s\rangle \quad [15]$$

where we have removed the first column (orbital) and the first row (electron) from the original function.<sup>b</sup> A given Slater determinant may be written as a chain of creation operators acting on the true vacuum (a state containing no electrons or orbitals), that is;

$$a_p^\dagger a_q^\dagger \cdots a_s^\dagger |0\rangle = |\phi_p \phi_q \cdots \phi_s\rangle \quad [16]$$

Note also that an annihilation operator acting on the vacuum state gives a zero result,

$$a_p |0\rangle = 0 \quad [17]$$

Pairwise permutations of the operators introduce changes in the sign of the resulting determinant, for example,

<sup>b</sup>The annihilation operator  $a_p$  is simply the Hermitian conjugate of the creation operator  $a_p^\dagger$ . An equivalent perspective on Eq. [14], therefore, is the annihilation operator  $a_p$  acting to the left on the bra state,  $\langle \Phi_0 |$ , to give

$$\langle \phi_q \cdots \phi_s | a_p = \langle \phi_p \phi_q \cdots \phi_s | = (\langle \phi_p \phi_q \cdots \phi_s |)^\dagger = (a_p^\dagger | \phi_q \cdots \phi_s \rangle)^\dagger$$

$$a_q^\dagger a_p^\dagger | \rangle = |\phi_q \phi_p \rangle = - |\phi_p \phi_q \rangle = - a_p^\dagger a_q^\dagger | \rangle \quad [18]$$

Therefore, the *anticommutation* relation for a pair of creation operators is simply

$$a_p^\dagger a_q^\dagger + a_q^\dagger a_p^\dagger = 0 \quad [19]$$

The analogous relation for a pair of annihilation operators is

$$a_p a_q + a_q a_p = 0 \quad [20]$$

Therefore, if we change the ordering of a pair of annihilation or creation operators, we must also change the sign of the resulting expression. Finally, it may be shown that the anticommutation relation for the “mixed” product is

$$a_p^\dagger a_q + a_q^\dagger a_p^\dagger = \delta_{pq} \quad [21]$$

where  $\delta_{pq}$  is the conventional Kronecker delta, which equals 1 if  $p = q$  and 0 if  $p \neq q$ .

Using these so-called second-quantized operators, we may define the single-orbital cluster operator

$$\hat{t}_i \equiv \sum_a t_i^a a_a^\dagger a_i \quad [22]$$

where the operator  $a_i$  deletes the orbital  $\phi_i$  from the determinant on which the operator acts, whereas  $a_a^\dagger$  introduces the orbital  $\phi_a$  in its place. (The  $\wedge$  is used to indicate a second-quantized operator.) Similarly, a two-orbital cluster operator that substitutes orbital  $\phi_a$  for  $\phi_i$  and  $\phi_b$  for  $\phi_j$  is given by

$$\hat{t}_{ij} \equiv \sum_{a>b} t_{ij}^{ab} a_a^\dagger a_b^\dagger a_j a_i \quad [23]$$

(Again note that the order of replacement is important for the sign of the resulting determinant.) Hence, the 27th term on the right-hand side of Eq. [12] shown explicitly in Eq. [13] may be written simply as

$$|f_{ij}\phi_k f_l\rangle = \hat{t}_{ij} \hat{t}_l |\Phi_0\rangle \quad [24]$$

The creation operators in Eqs. [22] and [23] are restricted to act only on the virtual orbitals, and the annihilation operators may act only on the occupied orbitals. Therefore, by Eq. [21], the creation–annihilation operator pairs exactly anticommute:

$$a_a^\dagger a_i + a_i a_a^\dagger = \delta_{ia} = 0 \quad [25]$$

since the occupied orbital  $\phi_i$  and the virtual orbital  $\phi_a$  cannot be the same. Therefore, by the equation above as well as the anticommutation relations given in Eqs. [19] and [20], all the creation and annihilation operators in  $\hat{t}_i$  and  $\hat{t}_{ij}$  anticommute. Given the additional fact that the cluster operators always contain even numbers of second-quantized operators, the  $\hat{t}_i$  and  $\hat{t}_{ij}$  operators will exactly commute.<sup>c</sup>

Equations [22] and [23] may be used to rewrite the long one- and two-orbital cluster wavefunction in Eq. [12] above as

$$\Psi = \left( 1 + \sum_i \hat{t}_i + \frac{1}{2} \sum_{ij} \hat{t}_i \hat{t}_j + \frac{1}{6} \sum_{ijk} \hat{t}_i \hat{t}_j \hat{t}_k + \frac{1}{2} \sum_{ij} \hat{t}_{ij} + \frac{1}{8} \sum_{ijkl} \hat{t}_{ij} \hat{t}_{kl} \right. \\ \left. + \frac{1}{24} \sum_{ijkl} \hat{t}_i \hat{t}_j \hat{t}_k \hat{t}_l + \frac{1}{2} \sum_{ijk} \hat{t}_{ij} \hat{t}_k + \frac{1}{4} \sum_{ijkl} \hat{t}_{ij} \hat{t}_k \hat{t}_l \right) \Phi_0 \quad [26]$$

We may simplify this expression even further by defining the total one- and two-orbital cluster operators

$$\hat{T}_1 \equiv \sum_i \hat{t}_i = \sum_{ia} t_i^a a_a^\dagger a_i \quad [27]$$

and

$$\hat{T}_2 \equiv \frac{1}{2} \sum_{ij} \hat{t}_{ij} = \frac{1}{4} \sum_{ijab} t_{ij}^{ab} a_a^\dagger a_b^\dagger a_j a_i \quad [28]$$

respectively.<sup>d</sup> More generally, an  $n$ -orbital cluster operator may be defined as

$$\hat{T}_n = \left( \frac{1}{n!} \right)^2 \sum_{ij \dots ab \dots}^n t_{ij \dots ab \dots}^{ab \dots} a_a^\dagger a_b^\dagger \dots a_j a_i \quad [29]$$

---

<sup>c</sup>Note that commutation of cluster operators holds only when the occupied and virtual orbital spaces are disjoint, as is the case in spin-orbital or spin-restricted closed-shell theories. For spin-restricted open-shell approaches, where singly occupied orbitals contribute terms to both the occupied and virtual orbital subspaces, the commutation relations of cluster operators are significantly more complicated. See Ref. 36 for a discussion of this issue.

<sup>d</sup>The factors of  $1/2$  and  $1/4$  are included here to correct for the “double counting” resulting from the now unrestricted summations over  $i$ ,  $j$ ,  $a$ , and  $b$ .

This reduces the wavefunction expression to

$$\Psi = \left( 1 + \hat{T}_1 + \frac{1}{2!} \hat{T}_1^2 + \frac{1}{3!} \hat{T}_1^3 + \hat{T}_2 + \frac{1}{2!} \hat{T}_2^2 + \frac{1}{4!} \hat{T}_1^4 + \hat{T}_2 \hat{T}_1 + \frac{1}{2!} \hat{T}_2 \hat{T}_1^2 \right) \Phi_0 \quad [30]$$

Higher order terms (e.g.,  $\hat{T}_2^3$ ) do not appear, of course, because our example system contains only four electrons. If we remember that  $\hat{T}_1$  and  $\hat{T}_2$  commute, then *all* the terms from the equation above match those from the power series expansion of an exponential function! Thus, the general expression for Eq. [30] is

$$\Psi = e^{\hat{T}_1 + \hat{T}_2} \Phi_0 \equiv e^{\hat{T}} \Phi_0 \quad [31]$$

which is a rather convenient reduction from the original Eq. [12].

The “exponential ansatz” given in Eq. [31] is one of the central equations of coupled cluster theory. The exponentiated cluster operator,  $\hat{T}$ , when applied to the reference determinant, produces a new wavefunction containing cluster functions, each of which correlates the motion of electrons within specific orbitals. If  $\hat{T}$  includes contributions from all possible orbital groupings for the  $N$ -electron system (that is,  $\hat{T}_1, \hat{T}_2, \dots, \hat{T}_N$ ), then the exact wavefunction within the given one-electron basis may be obtained from the reference function. The cluster operators,  $\hat{T}_n$ , are frequently referred to as *excitation* operators, since the determinants they produce from  $\Phi_0$  resemble excited states in Hartree–Fock theory. Truncation of the cluster operator at specific substitution/excitation levels leads to a hierarchy of coupled cluster techniques (e.g.,  $\hat{T} \equiv \hat{T}_1 + \hat{T}_2 \rightarrow \text{CCSD}$ ;  $\hat{T} \equiv \hat{T}_1 + \hat{T}_2 + \hat{T}_3 \rightarrow \text{CCSDT}$ , etc., where “S,” “D,” and “T,” indicate that single, double, and triple excitations, respectively, are included in the wavefunction expansion).

### Wavefunction Separability and Size Consistency of the Energy

It is perhaps useful to compare the exponential ansatz of Eq. [31] with the analogous expansions of other wavefunctions. In the configuration interaction (CI) approach,<sup>85,86</sup> for example, a linear excitation operator is used instead of an exponential,

$$\Psi_{\text{CI}} = (1 + \hat{C}) \Phi_0 \quad [32]$$

where  $\hat{C}$  is a linear combination of cluster-like operators defined similarly to  $\hat{T}$ , namely,

$$\begin{aligned}\hat{C} &= \hat{C}_1 + \hat{C}_2 + \dots \\ &= \sum_{ia} c_i^a a_a^\dagger a_i + \frac{1}{4} \sum_{ijab} c_{ij}^{ab} a_a^\dagger a_b^\dagger a_j a_i + \dots\end{aligned}\quad [33]$$

Truncation of  $\hat{C}$  at the single- and double-excitation level (CISD) leads to a wavefunction with exactly the same number of amplitudes ( $c_i^a$  and  $c_{ij}^{ab}$ ) as that needed for the CCSD wavefunction ( $t_i^a$  and  $t_{ij}^{ab}$ ). However, the latter implicitly includes higher excitation levels (triples and quadruples) by the inclusion of  $\hat{T}$  products in the power series expansion of  $e^{\hat{T}}$ . Such products are commonly referred to in the literature as *disconnected* wavefunction contributions.<sup>e</sup> Both the CI and CC methods will produce exact wavefunctions if one does not truncate  $\hat{C}$  (full CI) or  $\hat{T}$  (full CC). In fact, in the limit of exact linear and exponential wavefunction expansions, a relationship between the CI and CC amplitudes may be developed<sup>5</sup> that reveals the factorization of each level of CI excitation into connected and disconnected components, for example,

$$\hat{C}_2 = \hat{T}_2 + \frac{1}{2} \hat{T}_1^2 \quad [34]$$

The two different forms of the excitation operator in CI and CC theory have significant consequences for both the energy and wavefunction as the number of electrons is increased or as the (molecular) system is separated into fragments.

Consider the structure of the coupled cluster and configuration interaction wavefunctions for a generic system involving two infinitely separated (and therefore noninteracting) components X and Y. If the molecular orbitals used to define the cluster functions  $\hat{T}$  and  $\hat{C}$  are localized on each of the two fragments—a choice that will not affect the energy associated with either the reference determinant,  $\Phi_0$ , or the correlated wavefunction,  $\Psi_{\text{CI}}$  or  $\Psi_{\text{CC}}$ —then the cluster operators may be separated into components involving intrafragment excitations only, that is,

$$\hat{T} = \hat{T}_X + \hat{T}_Y \quad \text{and} \quad \hat{C} = \hat{C}_X + \hat{C}_Y \quad [35]$$

For example, the amplitudes  $t_{ij}^{ab}$  or  $c_{ij}^{ab}$ , in which orbitals  $\phi_i$  and  $\phi_a$  are localized on fragment X and orbitals  $\phi_j$  and  $\phi_b$  are localized on fragment Y, will be zero. Thus, the total coupled cluster exponential operator may be written as a product of independent coupled cluster operators for each fragment, namely,<sup>87</sup>

$$\Psi_{\text{CC}} = e^{\hat{T}} \Phi_0 = e^{\hat{T}_X + \hat{T}_Y} \Phi_0 = e^{\hat{T}_X} e^{\hat{T}_Y} \Phi_0 \quad [36]$$

Since the reference determinant,  $\Phi_0$ , is factorizable into determinants isolated on each fragment (in the localized orbital description), the total coupled cluster

---

<sup>e</sup>This terminology should not be confused with so-called *disconnected* diagrammatic contributions, which are discussed later in the chapter.

wavefunction may be written as a product of coupled cluster wavefunctions for each of the separated fragments.<sup>f</sup> As a result, the sum of the coupled cluster energies computed for each fragment separately is the same as that computed for the “supermolecule” in which the fragments are included together in the calculation,

$$E_{\text{CC}} = E_{\text{CC}}^{\text{X}} + E_{\text{CC}}^{\text{Y}} \quad [37]$$

This property of the coupled cluster energy is commonly known as “size consistency.”<sup>89</sup>

For the configuration interaction wavefunction, however, multiplicative separability is not possible:

$$\Psi_{\text{CI}} = (1 + \hat{C})\Phi_0 = (1 + \hat{C}_{\text{X}} + \hat{C}_{\text{Y}})\Phi_0 \quad [38]$$

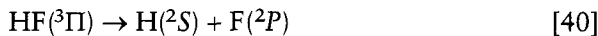
As a result, the CI energy is not size consistent, and the sum of the energies of the separated fragments differs from the CI energy of the supermolecule,

$$E_{\text{CI}} \neq E_{\text{CI}}^{\text{X}} + E_{\text{CI}}^{\text{Y}} \quad [39]$$

In the event that the CI cluster operator,  $\hat{C}$ , is not truncated, however, it is possible to write the resulting full CI wavefunction as a product of wavefunctions for each separated fragment, since the linear operator may be transformed into an exponential using a generalized form of Eq. [34].

Consider the classic example of an ensemble of hydrogen molecules. Both the CCSD and CISD wavefunctions are exact (within the given one-electron basis set) for a single  $\text{H}_2$  molecule, since there are only two electrons to be correlated. Because of the lack of multiplicative separability of the wavefunction, however, errors are introduced in the CI energy in the case of two (or more) noninteracting  $\text{H}_2$  units. The size-consistent CCSD method, on the other hand, produces the correct total energy, regardless of the number of noninteracting  $\text{H}_2$  monomers in the system, since the total coupled cluster wavefunction may be written as a product of separated wavefunctions, each of which is exact for the given hydrogen molecule.

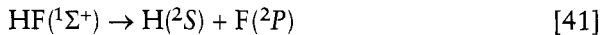
Some caution should be exercised in the application of the size consistency concept to open-shell fragments, however. As Taylor has pointed out,<sup>81</sup> a given method may be size consistent for some systems but not for others. For example, the spin-restricted Hartree–Fock (RHF) approach is size consistent for the dissociation of the hydrogen fluoride in its  ${}^3\Pi$  excited state into atoms,




---

<sup>f</sup>It should be noted that the localized orbital requirement is used here strictly for ease of analysis, and the property of multiplicative separability of the coupled cluster wavefunction does not strictly depend on this computational requirement, as discussed in Ref. 88.

since the single determinant wavefunction can correctly describe the high-spin electronic states in both the supermolecule and the separated fragments. The RHF method is not size consistent, however, when it describes the dissociation of the ground state of HF into these same atomic states,



This size inconsistency occurs because the two open-shell electrons on the atoms must be singlet-coupled to produce the correct dissociation limit, and a supermolecule, two-determinant approach is therefore required. This difficulty also applies to coupled cluster or perturbation-based wavefunctions that use the RHF determinant as a reference; these methods cannot be size consistent for a given molecular system unless the reference wavefunction is size consistent.

A more general property of the coupled cluster energy that is related to size consistency is “size extensivity.” This is a strictly mathematical characteristic of the wavefunction which relates to scaling of the computed energy with respect to the number of correlated electrons and the resulting energy dependence of the wavefunction amplitude equations. Size extensivity is not dependent on the system under study, and it applies to all regions of the potential energy surface—not just to the fragmentation limit. We will return to this topic later in the chapter after we have discussed the algebraic and diagrammatic techniques needed to derive working coupled cluster equations.

## FORMAL COUPLED CLUSTER THEORY

The exponential ansatz described above is essential to coupled cluster theory, but we do not yet have a recipe for determining the so-called cluster amplitudes ( $t_i^a$ ,  $t_{ij}^{ab}$ , etc.) that parameterize the power series expansion implicit in Eq. [31]. Naturally, the starting point for this analysis is the electronic Schrödinger equation,

$$\hat{H}|\Psi\rangle = E|\Psi\rangle \quad [42]$$

where the coupled cluster wavefunction,  $\Psi_{\text{CC}} \equiv e^{\hat{T}}\Phi_0$ , is used to approximate the exact solution,  $\Psi$ ,

$$\hat{H}e^{\hat{T}}|\Phi_0\rangle = E e^{\hat{T}}|\Phi_0\rangle \quad [43]$$

Using a “projective” technique, one may left-multiply this equation by the reference,  $\Phi_0$ , to obtain an expression for the energy,

$$\langle\Phi_0|\hat{H}e^{\hat{T}}|\Phi_0\rangle = E\langle\Phi_0|e^{\hat{T}}|\Phi_0\rangle = E \quad [44]$$

where intermediate normalization,  $\langle \Phi_0 | \Psi_{CC} \rangle = 1$ , is assumed. Additionally, one may obtain expressions for the cluster amplitudes by left-projecting the Schrödinger equation by the excited determinants produced by the action of the cluster operator,  $\hat{T}$ , on the reference,

$$\langle \Phi_{ij\cdots}^{ab\cdots} | \hat{H} e^{\hat{T}} | \Phi_0 \rangle = E \langle \Phi_{ij\cdots}^{ab\cdots} | e^{\hat{T}} | \Phi_0 \rangle \quad [45]$$

where  $|\Phi_{ij\cdots}^{ab\cdots}\rangle$  represents an excited determinant in which orbitals  $\phi_i$ ,  $\phi_j$ , etc. have been replaced with orbitals  $\phi_a$ ,  $\phi_b$ , etc.<sup>g</sup> Projection by the determinant  $|\Phi_{ij}^{ab}\rangle$ , for example, will produce an equation for the specific amplitude  $t_{ij}^{ab}$  (coupled to other amplitudes). These equations are nonlinear (owing to the presence of  $e^{\hat{T}}$ ) and energy dependent. Furthermore, they are formally exact; if the cluster operator,  $\hat{T}$ , is not truncated, the exact wavefunction within the space spanned by the set of orthogonal one-electron functions,  $\phi_p$ , may be obtained.

### Truncation of the Exponential Ansatz

Recall that the exponentiated operator may be expanded in a power series as

$$e^{\hat{T}} = 1 + \hat{T} + \frac{\hat{T}^2}{2!} + \frac{\hat{T}^3}{3!} + \dots \quad [46]$$

Inserting this into the energy expression Eq. [44] we obtain

$$\langle \Phi_0 | \hat{H} \left( 1 + \hat{T} + \frac{\hat{T}^2}{2!} + \frac{\hat{T}^3}{3!} + \dots \right) | \Phi_0 \rangle = E \quad [47]$$

which becomes, after distributing terms,

$$\langle \Phi_0 | \hat{H} | \Phi_0 \rangle + \langle \Phi_0 | \hat{H} \hat{T} | \Phi_0 \rangle + \left\langle \Phi_0 | \hat{H} \frac{\hat{T}^2}{2!} | \Phi_0 \right\rangle + \left\langle \Phi_0 | \hat{H} \frac{\hat{T}^3}{3!} | \Phi_0 \right\rangle + \dots = E \quad [48]$$

Note that  $\hat{H}$  is at most a two-particle operator and that  $\hat{T}$  is at least a one-particle excitation operator. Then, assuming that the reference wavefunction is a single determinant constructed from a set of one-electron functions, Slater's rules<sup>82</sup> state that matrix elements of the Hamiltonian between determinants that differ by more than two orbitals are zero. Thus, the fourth term on the left-hand side of Eq. [48] contains, at the least, threefold excitations, and, as a result, that matrix element (and *all* higher order elements) necessarily vanish. The energy equation then simplifies to

---

<sup>g</sup>In second-quantization terminology,  $|\Phi_{ij\cdots}^{ab\cdots}\rangle = a_a^\dagger a_b^\dagger \cdots a_i a_j |\Phi_0\rangle$ .

$$\langle \Phi_0 | \hat{H} | \Phi_0 \rangle + \langle \Phi_0 | \hat{H} \hat{T} | \Phi_0 \rangle + \left\langle \Phi_0 | \hat{H} \frac{\hat{T}^2}{2!} | \Phi_0 \right\rangle = E \quad [49]$$

This is the natural truncation of the coupled cluster energy equation; an analogous phenomenon occurs for the amplitude equation (Eq. [45]). This truncation depends *only* on the form of  $\hat{H}$  and not on that of  $\hat{T}$  or on the number of electrons. Equation [49] is correct even if  $\hat{T}$  is truncated to a particular excitation level.

## The Hausdorff Expansion

Although the energy and amplitude expressions (Eqs. [44] and [45], respectively) are useful for gaining a formal understanding of the coupled cluster method, they are not amenable to practical computer implementation.<sup>90</sup> One must first rewrite these expressions in terms of the one- and two-electron integrals arising from the electronic Hamiltonian as well as the cluster amplitudes, which, apart from the energy itself, are the only unknown quantities. To that end, it is convenient to exercise mathematical foresight and multiply the Schrödinger equation (Eq. [43]) by the inverse of the exponential operator,  $e^{\hat{T}}$ . Upon subsequent left-projection by the reference,  $\Phi_0$ , and the excited determinants,  $\Phi_{ij\dots}^{ab\dots}$ , one obtains modified energy and amplitude equations,

$$\langle \Phi_0 | e^{-\hat{T}} \hat{H} e^{\hat{T}} | \Phi_0 \rangle = E \quad [50]$$

and

$$\langle \Phi_{ij\dots}^{ab\dots} | e^{-\hat{T}} \hat{H} e^{\hat{T}} | \Phi_0 \rangle = 0 \quad [51]$$

respectively, which involve the similarity-transformed Hamiltonian,  $e^{-\hat{T}} \hat{H} e^{\hat{T}}$ . Equations [50] and [51] define the conventional coupled cluster method. It may be shown that these expressions are equivalent to Eqs. [44] and [45],<sup>5,80</sup> but with two advantages. First, the amplitude equations (Eq. [51]) are now decoupled from the energy equation (Eq. [50]). Second, a simplification via the so-called Campbell–Baker–Hausdorff formula<sup>91</sup> of  $e^{-\hat{T}} \hat{H} e^{\hat{T}}$  leads to a linear combination of nested commutators of  $\hat{H}$  with the cluster operator,  $\hat{T}$ , namely,

$$\begin{aligned} e^{-\hat{T}} \hat{H} e^{\hat{T}} &= \hat{H} + [\hat{H}, \hat{T}] + \frac{1}{2!} [[\hat{H}, \hat{T}], \hat{T}] + \frac{1}{3!} [[[[\hat{H}, \hat{T}], \hat{T}], \hat{T}]] \\ &\quad + \frac{1}{4!} [[[[[\hat{H}, \hat{T}], \hat{T}], \hat{T}], \hat{T}]] + \dots \end{aligned} \quad [52]$$

This expression is usually referred to simply as the Hausdorff expansion, and although it may not immediately appear to be a simplification of the coupled

cluster equations, the infinite series truncates naturally in a manner somewhat analogous to that described earlier for the operator,  $\hat{H}e^T$ .

As shown explicitly in Refs. 80, 84, and 92, the creation and annihilation operators described earlier may be used to represent dynamical operators such as the electronic Hamiltonian:

$$\hat{H} = \sum_{pq} h_{pq} a_p^\dagger a_q + \frac{1}{4} \sum_{pqrs} \langle pq||rs \rangle a_p^\dagger a_q^\dagger a_s a_r \quad [53]$$

In this expression,  $h_{pq} \equiv \langle \phi_p | \hat{h} | \phi_q \rangle$  represents a matrix element of the one-electron component of the Hamiltonian,  $\hat{h}$ , while  $\langle pq||rs \rangle \equiv \langle \phi_p \phi_q | \phi_r \phi_s \rangle - \langle \phi_p \phi_q | \phi_s \phi_r \rangle$  is its antisymmetrized two-electron counterpart. Equation [53] contains *general* annihilation and creation operators (e.g.,  $a_p^\dagger$  or  $a_q$ ) that may act on orbitals in either occupied or virtual subspaces. The cluster operators,  $\hat{T}_n$ , on the other hand, contain operators that are restricted to act in only one of these spaces (e.g.,  $a_b^\dagger$ , which may act only on the virtual orbitals). As pointed out earlier, the cluster operators therefore commute with one another, but not with the Hamiltonian,  $\hat{H}$ . For example, consider the commutator of the pair of general second-quantized operators from the one-electron component of the Hamiltonian in Eq. [53] with the single-excitation pair found in the cluster operator,  $\hat{T}_1$ :

$$[a_p^\dagger a_q, a_a^\dagger a_i] = a_p^\dagger a_q a_a^\dagger a_i - a_a^\dagger a_i a_p^\dagger a_q \quad [54]$$

The anticommutation relations of annihilation and creation operators given in Eqs. [19], [20], and [21] may be applied to the two terms on the right-hand side of this expression to give

$$[a_p^\dagger a_q, a_a^\dagger a_i] = a_p^\dagger \delta_{qa} a_i - a_a^\dagger \delta_{ip} a_q \quad [55]$$

The Kronecker delta functions,  $\delta_{qa}$  and  $\delta_{ip}$ , resulting from Eq. [21], cannot be simplified to 1 or 0 because the indices  $p$  and  $q$  may refer to either occupied or virtual orbitals. The important point here, however, is that the commutator has reduced the number of general-index second-quantized operators by one. Therefore, each nested commutator from the Hausdorff expansion of  $\hat{H}$  and  $\hat{T}$  serves to *eliminate* one of the electronic Hamiltonian's general-index annihilation or creation operators in favor of a simple delta function. Since  $\hat{H}$  contains at most *four* such operators (in its two-electron component), all creation or annihilation operators arising from  $\hat{H}$  will be eliminated beginning with the quadruply nested commutator in the Hausdorff expansion. All higher order terms will contain commutators of only the cluster operators,  $\hat{T}$ , and are therefore zero. Hence, Eq. [52] truncates itself naturally after the first five terms on the right-hand side.<sup>80</sup> This convenient property results entirely from the two-electron property of the Hamiltonian and from the fact that the cluster opera-

tors commute; it is not dependent on the number of electrons in the system, the level of substitution included in  $\hat{T}$ , or any consideration of the types of determinant upon which the operators act.

Using the truncated Hausdorff expansion, we may obtain analytic expressions for the commutators in Eq. [52] and insert these into the coupled cluster energy and amplitude equations (Eqs. [50] and [51], respectively). However, this is only the first step in obtaining expressions that may be efficiently implemented on the computer. We must next choose a truncation of  $\hat{T}$  and then derive expressions containing only one- and two-electron integrals and cluster amplitudes. This is a formidable task to which we will return in later sections.

## A Variational Coupled Cluster Theory?

The “projective” techniques described above for solving the coupled cluster equations represent a particularly convenient way of obtaining the amplitudes that define the coupled cluster wavefunction,  $e^{\hat{T}}\Phi_0$ . However, the asymmetric energy formula shown in Eq. [50] does not conform to any variational conditions in which the energy is determined from an expectation value equation. As a result, the computed energy will not be an upper bound to the exact energy in the event that the cluster operator,  $\hat{T}$ , is truncated. But the exponential ansatz does not *require* that we solve the coupled cluster equations in this manner. We could, instead, construct a variational solution by requiring that the amplitudes minimize the expression<sup>1,2</sup>

$$E_{\text{exact}} \leq E = \frac{\langle \Phi_0 | (e^{\hat{T}})^\dagger \hat{H} e^{\hat{T}} | \Phi_0 \rangle}{\langle \Phi_0 | (e^{\hat{T}})^\dagger e^{\hat{T}} | \Phi_0 \rangle} = \frac{\langle \Psi | \hat{H} | \Psi \rangle}{\langle \Psi | \Psi \rangle} \quad [56]$$

Unfortunately, this equation is considerably more complex than the projective energy expression given in Eq. [50], since there is no natural truncation of its power series expansion,

$$\langle \Phi_0 | (e^{\hat{T}})^\dagger \hat{H} e^{\hat{T}} | \Phi_0 \rangle = \langle \Phi_0 | (1 + \hat{T}^\dagger + \frac{1}{2}(\hat{T}^\dagger)^2 + \dots) \hat{H} (1 + \hat{T} + \frac{1}{2}(\hat{T})^2 + \dots) | \Phi_0 \rangle \quad [57]$$

For example, in the term  $\langle \Phi_0 | \hat{T}^\dagger \hat{H} \hat{T} | \Phi_0 \rangle$ , which is included in Eq. [57], as  $\hat{T}$  creates an excited determinant from  $|\Phi_0\rangle$  on the right,  $\hat{T}^\dagger$  creates an excited determinant from  $\langle\Phi_0|$  on the left. Thus, the Hamiltonian matrix elements will not vanish at some high excitation level, and the series will not terminate before the  $N$ -electron limit. Truncation of this expression for large numbers of terms appears to be arbitrary at best.

The ostensible impracticality of a variational coupled cluster theory raises an important question regarding the physical reality of the coupled cluster energy as computed using projective, asymmetric techniques. Quantum mechanics dictates that physical observables (such as the energy) are expectation

values of Hermitian operators. The coupled cluster energy expression contains the operator  $e^{-\hat{T}}\hat{H}e^{\hat{T}}$ , which is not Hermitian, regardless of the truncation of  $\hat{T}$ :<sup>b</sup>

$$(e^{-\hat{T}}\hat{H}e^{\hat{T}})^\dagger = (e^{\hat{T}})^\dagger \hat{H}(e^{-\hat{T}})^\dagger = e^{\hat{T}^\dagger}\hat{H}e^{-\hat{T}^\dagger} \neq e^{-\hat{T}}\hat{H}e^{\hat{T}} \quad [58]$$

However, if  $\hat{T}$  is not truncated, the similarity transformed operator has an energy eigenvalue spectrum that is *identical* to the original Hermitian operator,  $\hat{H}$ , thus justifying its formal use in quantum mechanical models. Practically speaking, the coupled cluster energy tends to closely approximate the expectation value result even when  $\hat{T}$  is truncated. Furthermore, one might speculate that some measure of the difference between the expectation value and asymmetric energies—perhaps as measured by the asymmetry of the coupled cluster reduced density<sup>65</sup>—might prove to be a useful diagnostic of the reliability of results obtained from the coupled cluster method for specific systems. This issue has been recently discussed by Kutzelnigg.<sup>93</sup>

Variational coupled cluster methods that make use of Eq. [57] have been studied by several researchers. The unitary coupled cluster (UCC) approach in which the cluster operator  $\hat{T}$  is replaced by  $\hat{T} - \hat{T}^\dagger$  (where  $\hat{T}^\dagger$  indicates a de-excitation operator that is the Hermitian adjoint of  $\hat{T}$ ) was pursued by Hoffmann and Simons.<sup>94,95</sup> The infinite series in this case is not truncated arbitrarily, but instead by identifying which terms are needed to complete the series through a particular order of perturbation theory. Bartlett and Noga have constructed an alternative theory, termed the expectation value coupled cluster (XCC) method,<sup>96</sup> in which the usual definition of  $\hat{T}$  is retained and Eq. [57] is used, but again the series truncation is based on perturbation theory arguments. Finally, we note the extended coupled cluster method (ECCM) of Arponen and Bishop,<sup>97,98</sup> which uses a modified energy functional including an additional exponentiated de-excitation operator analogous to  $e^{\hat{T}^\dagger}$ . These as well as other variational and semivariational approaches to the cluster expansion have been reviewed by Bartlett et al.<sup>99</sup> and by Szalay et al.<sup>100</sup>

---

<sup>b</sup>The inequality with the final term in this expression relies on the fact that the Hermitian adjoint of an excitation (cluster) operator,  $\hat{T}$ , is a de-excitation operator, as can be seen from the properties of its component annihilation and creation operators. For example, we note that

$$\hat{T}_1 = \sum_{ia} t_i^a a_a^\dagger a_i \neq \hat{T}_1^\dagger = \sum_{ia} (t_i^a)^* a_i^\dagger a_a$$

On the other hand, the inverse of the exponentiated excitation operator,  $e^{-\hat{T}}$ , is also an excitation operator, as can be seen from its power series expansion,

$$e^{-\hat{T}} = 1 - \hat{T} + \frac{1}{2!}\hat{T}^2 - \frac{1}{3!}\hat{T}^3 + \dots$$

## An Eigenvalue Approach to Coupled Cluster Theory

Up to this point, our discussion has focused on the expansion of the wavefunction using the exponential ansatz given in Eq. [31]. When the cluster operator,  $\hat{T}$ , is truncated, the resulting CC wavefunction may be viewed as an approximate eigenfunction of the exact electronic Hamiltonian. However, another equally valid perspective focuses instead on construction of the *exact* eigenvectors of an *approximate* Hamiltonian. In configuration interaction theory, for example, one conventionally represents the electronic Hamiltonian within a determinantal basis consisting of the reference ( $\Phi_0$ ), single excitations ( $\Phi_i^a$ ), double excitations ( $\Phi_{ij}^{ab}$ ), and so on. In the CISD approximation, the Hamiltonian is represented schematically as

$$\hat{H}_{\text{CISD}} = \begin{pmatrix} E_{\text{SCF}} & 0 & \hat{H}_{0D} \\ 0 & \hat{H}_{SS} & \hat{H}_{SD} \\ \hat{H}_{D0} & \hat{H}_{DS} & \hat{H}_{DD} \end{pmatrix} \quad [59]$$

where  $\hat{H}_{SD}$ , for example, represents the block of Hamiltonian matrix elements between singly and doubly excited determinants and  $E_{\text{SCF}} = \langle \Phi_0 | \hat{H} | \Phi_0 \rangle$ . We assume here that Brillouin's theorem<sup>82</sup> holds for the reference determinant, and therefore the matrix elements involving  $\Phi_0$  and singly excited determinants are zero. The CISD energy is the lowest eigenvalue of this Hermitian matrix, and the CISD wavefunction is the corresponding eigenvector, that is,

$$\hat{H}_{\text{CISD}} |\Psi_{\text{CISD}}\rangle = E_{\text{CISD}} |\Psi_{\text{CISD}}\rangle \quad [60]$$

The coupled cluster “Schrödinger equation,” which leads to the energy and amplitude expressions given in Eqs. [50] and [51], may be written as

$$e^{-\hat{T}} \hat{H} e^{\hat{T}} |\Phi_0\rangle = E |\Phi_0\rangle \quad [61]$$

Like Eq. [60], this equation represents an eigenvalue problem<sup>101</sup> in which the similarity-transformed Hamiltonian,  $\bar{H} \equiv e^{-\hat{T}} \hat{H} e^{\hat{T}}$ , is used in place of the bare electronic Hamiltonian,  $\hat{H}$ . The ground state eigenvector of  $\bar{H}$  is simply  $|\Phi_0\rangle$  with eigenvalue  $E$ . However,  $\bar{H}$  is not Hermitian, unlike the CI Hamiltonian, and its matrix representation is therefore nonsymmetric. In the CCSD approximation, for example,

$$\bar{H}_{\text{CCSD}} = \begin{pmatrix} E_{\text{CCSD}} & \bar{H}_{0S} & \bar{H}_{0D} \\ 0 & \bar{H}_{SS} & \bar{H}_{SD} \\ 0 & \bar{H}_{DS} & \bar{H}_{DD} \end{pmatrix} \quad [62]$$

where the CCSD energy is given by  $\langle \Phi_0 | \bar{H} | \Phi_0 \rangle$ , by Eq. [50] and  $\bar{H}_{DS} \neq \bar{H}_{SD}$ . The blocks of matrix elements  $\langle \Phi_i^a | \bar{H} | \Phi_0 \rangle$  and  $\langle \Phi_{ij}^{ab} | \bar{H} | \Phi_0 \rangle$  are both zero because the  $\hat{T}$  amplitudes that parameterize the similarity transformation of  $\bar{H}$  into  $\bar{H}$  satisfy the equations

$$0 = \langle \Phi_i^a | \bar{H} | \Phi_0 \rangle \quad [63]$$

and

$$0 = \langle \Phi_{ij}^{ab} | \bar{H} | \Phi_0 \rangle \quad [64]$$

which are simply specific cases of Eq. [51]. Furthermore, unlike the CI case,  $\bar{H}_{0S}$  is nonzero in spite of Brillouin's theorem because  $\bar{H}$  includes contributions from products of the bare Hamiltonian with the cluster operators,  $\hat{T}$ .

As a result of the asymmetry of  $\bar{H}$ , the right-hand eigenvalue problem given in Eq. [61] is different from the left-hand eigenvalue problem,

$$\langle \mathcal{L} | \bar{H} = \langle \mathcal{L} | E \quad [65]$$

The computed energy,  $E$ , however, is the same for both equations. In Eq. [65], the left eigenvector,  $\langle \mathcal{L} |$ , may be written in terms of a cluster operator,  $\hat{\mathcal{L}}$ , acting on the reference from the right, namely,

$$\langle \mathcal{L} | \equiv \langle \Phi_0 | \hat{\mathcal{L}} \quad [66]$$

The operator  $\hat{\mathcal{L}}$  may be defined in analogy to the cluster operator,  $\hat{T}$ , as a sum of cluster operators,

$$\hat{\mathcal{L}} = 1 + \hat{\mathcal{L}}_1 + \hat{\mathcal{L}}_2 + \dots \quad [67]$$

The leading term of 1, which does not appear in  $\hat{T}$  (cf. Eq. [29]), is required in order that the left- and right-hand eigenvectors have unit overlap with one another. Unlike the cluster operators,  $\hat{T}_n$ , the operators  $\hat{\mathcal{L}}_n$  act to the left on  $\langle \Phi_0 |$ . Therefore, it is convenient to define them as *de-excitation* operators (or, equivalently, as bra-state excitation operators),

$$\hat{\mathcal{L}}_n = \left( \frac{1}{n!} \right)^2 \sum_{ij\dots ab\dots}^n l_{ab\dots}^{ij\dots} a_i^\dagger a_j^\dagger \dots a_b a_a \quad [68]$$

The task of determining the left-hand ground state eigenvector of  $\bar{H}$  is thus reduced to determining the amplitudes  $l_{ab\dots}^{ij\dots}$ . The ground state coupled cluster energy may then be written as

$$E = \langle \Phi_0 | \hat{\mathcal{L}} \bar{H} | \Phi_0 \rangle \quad [69]$$

where the left and right wavefunctions are assumed to be normalized according to  $\langle \Phi_0 | \hat{\mathcal{L}} | \Phi_0 \rangle = 1$ . Equation [69] which is more general than Eq. [50], provides a particularly useful starting point for the derivation of coupled cluster analytic energy derivatives; the left-hand eigenvector,  $\langle \Phi_0 | \hat{\mathcal{L}}$ , is related to the  $\hat{\Lambda}$  operator that arises as a result of the response of the cluster amplitudes to an external perturbation parameter.<sup>49</sup>

The concept of the coupled cluster method as an eigenvalue problem may be easily generalized to include excited states (in this case, states that are not the lowest in energy within a given symmetry). We may write the more general right-hand problem as

$$\bar{H} \hat{\mathcal{R}}(m) | \Phi_0 \rangle = E_m \hat{\mathcal{R}}(m) | \Phi_0 \rangle \quad [70]$$

where

$$\hat{\mathcal{R}}(m) = \hat{\mathcal{R}}_0(m) + \hat{\mathcal{R}}_1(m) + \hat{\mathcal{R}}_2(m) + \dots \quad [71]$$

represents a cluster operator expansion for the  $m$ th excited state with energy  $E_m$ . For the ground state,  $\hat{\mathcal{R}}(0) = 1$ , as described above. Similarly, the left-hand eigenvalue problem becomes

$$\langle \Phi_0 | \hat{\mathcal{L}}(m) \bar{H} = \langle \Phi_0 | \hat{\mathcal{L}}(m) E_m \quad [72]$$

“Biorthonormality” of the left-hand and right-hand eigenvectors may be enforced such that

$$\langle \Phi_0 | \hat{\mathcal{L}}(m) \hat{\mathcal{R}}(n) | \Phi_0 \rangle = \delta_{mn} \quad [73]$$

which leads to the generalized coupled cluster energy expression

$$E_m = \langle \Phi_0 | \hat{\mathcal{L}}(m) \bar{H} \hat{\mathcal{R}}(m) | \Phi_0 \rangle \quad [74]$$

Note that the biorthonormality of the left- and right-hand states does not imply orthonormality of the left- or right-hand states among themselves, for example,

$$\langle \Phi_0 | \hat{\mathcal{R}}^\dagger(m) \hat{\mathcal{R}}(n) | \Phi_0 \rangle \neq \delta_{mn} \quad [75]$$

The eigenvalue perspective described above does not offer any computational convenience for the ground state problem because one must still use Eq. [51] to determine the cluster amplitudes that define the similarity transformation of the electronic Hamiltonian,  $\hat{H}$ , into the CC Hamiltonian,  $\bar{H}$ . However,

this perspective does provide a rather simple CI-like approach for determining excited state wavefunctions. Equation-of-motion coupled cluster theory (EOM-CC),<sup>5,60–63,65</sup> the name of which is based on early formulations involving response operators, has seen a considerable rise in popularity in recent years. The EOM-CCSD method,<sup>65,73</sup> for example, is defined as the diagonalization of the CCSD effective Hamiltonian,  $\bar{H}_{\text{CCSD}}$  (where the cluster amplitudes are taken from the corresponding CCSD ground state energy calculation) in the space of all singly and doubly excited determinants. It should be noted, however, that truncation of the cluster operator,  $\hat{T}$ , in the definition of  $\bar{H}$  does not introduce errors into the EOM-CC energy because the exact energy would still be obtained if the diagonalization basis were complete.

Much effort has been devoted recently to the development of a variety of excited state coupled cluster techniques that are related to EOM-CC. For example, the linear response coupled cluster (LR-CC) approach<sup>73</sup> originally described by Monkhorst<sup>5</sup> and implemented by several groups<sup>69,70,102–105</sup> can be used to obtain identical results to those given by conventional EOM-CC. In addition, the symmetry-adapted cluster (SAC-CI) method devised independently by Nakatsuji<sup>106–108</sup> in the late 1970s may be viewed as an approximation to EOM-CC and LR-CC. A relationship between EOM-CC and Fock-space multireference coupled cluster theory (FS-MRCC)<sup>64,109–112</sup> has been exploited in the construction of methods for describing classes of doublet electronic states that are accessible via either electron attachment (EOMEA-CC)<sup>88,113</sup> or ionization (EOMIP-CC)<sup>67,109–111</sup> from a given reference. Finally, we note the work by Nooijen and Bartlett on the similarity-transformed equation-of-motion coupled cluster (STEOM-CC) method,<sup>74,114</sup> in which the effective Hamiltonian described above is further transformed using a reduced cluster operator,  $\hat{S}$ , which serves to decouple singly excited determinants from doubly and triply excited determinants in  $\bar{H}$ .

---

## DERIVATION OF THE COUPLED CLUSTER EQUATIONS

It is the need to remove the “unlinked clusters” and the introduction of Feynman diagrams which make MBPT [and CC theory] appear unfamiliar to quantum chemists.<sup>115</sup>

—K. F. Freed

In this section we construct working equations for the coupled cluster singles and doubles (CCSD) method. Beginning from the approximation  $\hat{T} \equiv \hat{T}_1 + \hat{T}_2$ , we use algebraic and diagrammatic techniques to obtain programmable

equations for the cluster amplitudes,  $t_i^a$  and  $t_{ij}^{ab}$ , in terms of the one- and two-electron integrals of the electronic Hamiltonian. As a first step we must introduce a few important tools of second quantization such as normal ordering and Wick's theorem to make the mathematical analysis much less complicated. The approach described here may easily be extended to higher order cluster approximations (e.g., CCSDT and CCSDTQ, where the latter includes quadruple excitations), as well as to many-body perturbation theory expressions.

As indicated by Karl Freed in the quotation above, the general quantum chemistry community has been slow to accept diagrammatic analyses of many-body perturbation theory and coupled cluster methods, and, until recently, these techniques have been used by relatively few researchers in the field. One of the goals of this review is to explain in straightforward terms one diagrammatic approach commonly used for the construction of coupled cluster equations. While attempting to be somewhat rigorous in the algebraic derivation of the coupled cluster equations, we present the corresponding diagrams with only minimal justification. For readers with a strong mathematical background who are interested in more detail, an extensive analysis of a similar diagrammatic technique may be found in a text by Harris, Monkhorst, and Freeman.<sup>80</sup>

## Normal-Ordered Second-Quantized Operators

As stated in Merzbacher's text on quantum mechanics<sup>91</sup> (Chapter 21, Section 4), a normal-ordered string of second-quantization operators is one in which we find "all annihilation operators standing to the right of all creation operators." Normal ordering of such strings provides a bookkeeping system by which the nonzero matrix elements of second-quantized operators may be more easily identified. As an example, consider an arbitrary string of annihilation and creation operators,  $\hat{A} = a_p a_q^\dagger a_r a_s^\dagger$ . By application of the anticommutation relations given in Eqs. [19], [20], and [21], we may move the two annihilation operators to the right and therefore write the string in an equivalent form as

$$\begin{aligned}\hat{A} &= a_p a_q^\dagger a_r a_s^\dagger \\ &= \delta_{pq} a_r a_s^\dagger - a_q^\dagger a_p a_r a_s^\dagger \\ &= \delta_{pq} \delta_{rs} - \delta_{pq} a_s^\dagger a_r - \delta_{rs} a_q^\dagger a_p + a_q^\dagger a_p a_s^\dagger a_r \\ &= \delta_{pq} \delta_{rs} - \delta_{pq} a_s^\dagger a_r - \delta_{rs} a_q^\dagger a_p + \delta_{ps} a_q^\dagger a_r - a_q^\dagger a_s^\dagger a_p a_r\end{aligned}\quad [76]$$

Three of the five terms in the final rearrangement contain operator strings of reduced length, and the first term contains only Kronecker delta functions. Note also that all the operator strings on the right-hand side of the final equality are normal-ordered by Merzbacher's definition. If we now evaluate the quan-

tum mechanical expectation value of this operator in the true vacuum state,<sup>i</sup> | ⟩, we obtain

$$\begin{aligned}\langle \hat{A} \rangle &= \langle |\delta_{pq}\delta_{rs}| \rangle - \langle |\delta_{pq}a_s^\dagger a_r| \rangle - \langle |\delta_{rs}a_q^\dagger a_p| \rangle + \langle |\delta_{ps}a_q^\dagger a_r| \rangle - \langle |a_q^\dagger a_s^\dagger a_p a_r| \rangle \\ &= \delta_{pq}\delta_{rs}\end{aligned}\quad [77]$$

where we assume that the vacuum state is normalized. Hence, the only term of  $\hat{A}$  in Eq. [76] that produces a nonzero result is the one containing no second-quantized operators; all other terms involve application of an annihilation operator to | ⟩ on the right.

If, on the other hand, we wish to evaluate a matrix element of  $\hat{A}$  involving determinants other than | ⟩ on the left and right, normal ordering simplifies this analysis as well. For example, consider the matrix element of  $\hat{A}$  between the single-particle states  $\langle \phi_t |$  and  $| \phi_u \rangle$ :

$$\langle \phi_t | \hat{A} | \phi_u \rangle = \langle | a_t \hat{A} a_u^\dagger | \rangle \quad [78]$$

Since the left- and right-hand states may be written simply as single annihilation and creation operators acting on the vacuum, the desired matrix element of  $\hat{A}$  may be rewritten as the vacuum expectation value of a new operator,  $\hat{B} \equiv a_t \hat{A} a_u^\dagger$ . Therefore, we need only rewrite  $\hat{B}$  in normal order and select only the terms that contain no annihilation or creation operators, as we did in Eq. [77]. After much algebraic manipulation, which we shall omit here, it can be shown that

$$\langle \phi_t | \hat{A} | \phi_u \rangle = \langle | \hat{B} | \rangle = \delta_{tu}\delta_{pq}\delta_{rs} + \delta_{tq}\delta_{ps}\delta_{ru} - \delta_{tq}\delta_{pu}\delta_{rs} - \delta_{ts}\delta_{pq}\delta_{ru} \quad [79]$$

By rearranging a given string of annihilation and creation operators into a normal-ordered form, matrix elements of such operators between determinantal wavefunctions may be evaluated in a relatively algorithmic manner. However, such an approach based on the direct application of the anticommutation relations can be quite tedious even for relatively short operator strings, and many opportunities for error may arise.

### Wick's Theorem for the Evaluation of Matrix Elements

Using the anticommutation relations of Eqs. [19], [20], and [21], an arbitrary string of annihilation and creation operators can be written as a linear combination of normal-ordered strings (most of which contain reduced num-

---

<sup>i</sup>The vacuum, | ⟩, is a state containing no electrons.

bers of operators) multiplied by Kronecker delta functions. These reduced terms may be viewed as arising from so-called contractions between operator pairs. A *contraction* between two arbitrary annihilation/creation operators,  $A$  and  $B$ , is defined as

$$\bar{AB} \equiv AB - \{AB\}_v \quad [80]$$

where the notation  $\{AB\}_v$  indicates the normal-ordered form of the pair (the subscript  $v$  for vacuum will be explained shortly). The contraction between the operators is simply the original ordering of the pair minus the normal-ordered pair. For example, if both operators are annihilation or creation operators, the contraction is zero because such pairs are already normal-ordered:

$$\bar{a_p^\dagger a_q} = a_p^\dagger a_q - \{a_p^\dagger a_q\}_v = a_p^\dagger a_q - a_p^\dagger a_q = 0 \quad [81]$$

and

$$\bar{a_p^\dagger a_q^\dagger} = a_p^\dagger a_q^\dagger - \{a_p^\dagger a_q^\dagger\}_v = a_p^\dagger a_q^\dagger - a_p^\dagger a_q^\dagger = 0 \quad [82]$$

In addition, a third combination in which  $A$  is a creation operator and  $B$  is an annihilation operator is also zero, since the string is again already normal-ordered:

$$\bar{a_p^\dagger a_q} = a_p^\dagger a_q - \{a_p^\dagger a_q\}_v = a_p^\dagger a_q - a_p^\dagger a_q = 0 \quad [83]$$

The final combination, in which  $A$  is an annihilation operator and  $B$  is a creation operator, is not zero, however, owing to the anticommutation relations in Eq. [21].<sup>j</sup> Thus we write

$$\bar{a_p^\dagger a_q^\dagger} = a_p^\dagger a_q^\dagger - \{a_p^\dagger a_q^\dagger\}_v = a_p^\dagger a_q^\dagger + a_q^\dagger a_p^\dagger = \delta_{pq} \quad [84]$$

Note that we must maintain the correct sign when the operators in the braces,  $\{\ }_v$ , are reordered.

Wick's theorem<sup>116</sup> provides a recipe by which an arbitrary string of annihilation and creation operators,  $ABC \cdots XYZ$ , may be written as a linear combination of normal-ordered strings. Schematically, Wick's theorem is

---

<sup>j</sup>Note that the use of the braces,  $\{\ }_v$ , around a string implies that the operators contained therein, except for any pair being contracted, exactly anticommute. Hence, a general term such as  $\{ABC \cdots XYZ\}_v$  may be written *exactly* as  $-\{BAC \cdots XYZ\}_v$ , without concern for the anticommutation relations.

$$\begin{aligned}
 ABC \cdots XYZ &= \{ABC \cdots XYZ\}_v \\
 &+ \sum_{singles} \{\overline{AB} \cdots XYZ\}_v \\
 &+ \sum_{doubles} \{\overline{\overline{ABC}} \cdots XYZ\}_v \\
 &+ \dots
 \end{aligned} \tag{85}$$

where the limits (“singles,” “doubles,” etc.) refer to the number of pairwise contractions included in the summation. The notation  $\{ \}_v$  has again been used to indicate the normal-ordered form of the given string. If we apply this theorem to the operator from the last section,  $\hat{A}$ , we obtain

$$\hat{A} = \{a_p a_q^\dagger a_r a_s^\dagger\}_v + \{\overline{a_p} a_q^\dagger a_r a_s^\dagger\}_v + \{\overline{a_p} \overline{a_q}^\dagger a_r a_s^\dagger\}_v + \{a_p a_q^\dagger \overline{a_r} a_s^\dagger\}_v + \{\overline{a_p} \overline{a_q}^\dagger \overline{a_r} a_s^\dagger\}_v \tag{86}$$

where only the nonzero contractions have been included (cf. Eqs. [81]–[84]). The evaluation of the pairwise contractions may introduce sign changes because the string of operators must be permuted to bring the pair together before the contraction may be evaluated. If the number of permutations is odd, the sign is negative; if the number is even, the sign is positive. For example, a contraction of the form

$$\{\overline{\overline{ABCD}}\}_v = \{\overline{AB} \overline{CD}\}_v \tag{87}$$

would have a positive sign because two permutations are necessary to bring operators  $A$  and  $D$  into adjacency; but a contraction of the form

$$\{\overline{AB} \overline{CD}\}_v = - \{\overline{AC} \overline{BD}\}_v \tag{88}$$

would have a negative sign, since only one permutation is necessary to bring operators  $A$  and  $C$  together. Thus, the contraction introduces the sign  $(-1)^P$ , where  $P$  is the number of permutations required to bring the operators into adjacency. Evaluating the contractions above for  $\hat{A}$  gives

$$\begin{aligned}
 \hat{A} &= \{a_p a_q^\dagger a_r a_s^\dagger\}_v + \delta_{pq} \{a_r a_s^\dagger\}_v + \delta_{ps} \{a_q^\dagger a_r\}_v + \delta_{rs} \{a_p a_q^\dagger\}_v + \delta_{pq} \delta_{rs} \\
 &= a_q^\dagger a_s^\dagger a_p a_r - \delta_{pq} a_s^\dagger a_r + \delta_{ps} a_q^\dagger a_r - \delta_{rs} a_q^\dagger a_p + \delta_{pq} \delta_{rs}
 \end{aligned} \tag{89}$$

This result is identical to that obtained using the anticommutation relations and given in Eq. [76].

How does Wick’s theorem help us in evaluating matrix elements of second-quantized operators? Recall that any matrix element of an operator may be written as a vacuum expectation value by simply writing its left- and right-hand determinants as operator strings acting on the vacuum state,  $| \rangle$ . The

composite string of annihilation and creation operators may then be rewritten using Wick's theorem as an expansion of normal-ordered strings. *However, the only terms that need to be retained in this expansion are those that are "fully contracted."* All other terms will give a zero result, by construction. For example, for the operator  $\hat{B}$  from the last section, Wick's theorem gives the following fully contracted terms:

$$\{\overbrace{a_t a_p a_q^+ a_r a_s^+ a_u^+}\}_{\text{v}} + \{\overbrace{a_t a_p a_q^+ a_r a_s^+ a_u^+}\}_{\text{v}} + \{\overbrace{a_t a_p a_q^+ a_r a_s^+ a_u^+}\}_{\text{v}} + \{\overbrace{a_t a_p a_q^+ a_r a_s^+ a_u^+}\}_{\text{v}} \quad [90]$$

which, when the contractions are evaluated, will give exactly the result given in Eq. [79]. The large number of contractions in Eq. [90] also suggests a useful rule of thumb for determining the sign of a fully contracted term: if the number of crossings in the contraction lines is odd, the sign on the term is negative; if the number of crossings is even, the sign is positive. For example, the sign on the second term in Eq. [90] is positive, since there are two crossings, whereas the sign on the third term is negative, since there is only one crossing.<sup>k</sup>

A somewhat more general version of Wick's theorem may be developed which involves products of operator strings, some or all of which may be normal-ordered.<sup>117</sup> The original form of Wick's theorem is only slightly modified in that the contractions need be evaluated only between normal-ordered strings and not within them. For example, for a product of two normal-ordered strings, the generalized Wick's theorem says that

$$\begin{aligned} \{ABC \dots\}_{\text{v}} \{XYZ \dots\}_{\text{v}} &= \{ABC \dots XYZ \dots\}_{\text{v}} + \sum_{\text{singles}} \{\overbrace{ABC \dots XYZ \dots}\}_{\text{v}} \\ &\quad + \sum_{\text{doubles}} \{\overbrace{ABC \dots XYZ \dots}\}_{\text{v}} + \dots \end{aligned} \quad [91]$$

This equation easily extends to products of several strings.

Another approach to the problem of matrix element evaluation and operator algebra is presented in the text by Harris, Monkhorst, and Freeman,<sup>80</sup> who describe the so-called contraction theorem. While Wick's theorem serves as a convenient approach to the conversion of a general string of construction operators (or products of strings) into sums of reduced normal-ordered strings, the contraction theorem avoids all use of normal ordering and deals strictly with commutators and anticommutators of general strings. This latter approach will give identical results to the application of Wick's theorem and has a few subtle differences, including an altered sign rule. Note also that one rarely (if ever) finds a proof of Wick's theorem in the modern literature, but Harris, Monkhorst, and Freeman give an explicit proof of their contraction theorem.

---

<sup>k</sup>This sign rule applies only to fully contracted terms and assumes that one places all the contraction lines above the expression.

## The Fermi Vacuum and the Particle–Hole Formalism

In many-electron theories such as configuration interaction or coupled cluster theory, it is more convenient to deal with the  $n$ -electron reference determinant,  $|\Phi_0\rangle$ , rather than the true vacuum state,  $| \rangle$ . In the evaluation of matrix elements using Wick's theorem as described above, even the use of normal-ordered strings would be tremendously tedious if one had to include the complete set of operators required to generate  $|\Phi_0\rangle$  from the true vacuum (i.e.,  $|\Phi_0\rangle = a_1^\dagger a_2^\dagger a_3^\dagger \cdots | \rangle$ ).

We will therefore alter the definition of normal ordering from one given relative to the true vacuum to one given relative to the reference state  $|\Phi_0\rangle$  (which is sometimes called the “Fermi vacuum”). The one-electron states occupied in  $|\Phi_0\rangle$  are referred to as *hole states*, and those unoccupied in  $|\Phi_0\rangle$  are referred to as *particle states*. This perhaps nonintuitive nomenclature is based upon the determinant produced when annihilation–creation operator strings act on the Fermi vacuum. That is, a “hole” is created when an originally occupied state is acted upon by an annihilation operator such as  $a_i$ , whereas a “particle” is created when an originally unoccupied state is acted upon by a creation operator such as  $a_i^\dagger$ . Therefore, we will refer to operators that create or destroy holes and particles as *quasiparticle* (or just *q-particle*) construction operators. That is, *q*-annihilation operators are those that annihilate holes and particles (e.g.,  $a_i^\dagger$  and  $a_i$ ), and *q*-creation operators are those that create holes and particles (e.g.,  $a_i$  and  $a_i^\dagger$ ).<sup>1</sup> Therefore, a string of second-quantized operators is normal-ordered relative to the Fermi vacuum if all *q*-annihilation operators lie to the right of all *q*-creation operators. We will use  $\{ \}$  to denote such normal-ordered strings (note the lack of the subscript v, which we implicitly used earlier to indicate normal ordering relative to the true vacuum).

This new definition of normal ordering changes our analysis of the Wick's theorem contractions only slightly. Whereas before, the only nonzero pairwise contraction required the annihilation operator to be to the left of the creation operator (cf. Eq. [84]), now the only nonzero contractions place the *q*-particle operator to the left of the *q*-particle creation operator. There are only two ways this can occur, namely,

$$\overline{a_i^\dagger a_j} = a_i^\dagger a_j - \{a_i^\dagger a_j\} = a_i^\dagger a_j + a_j a_i^\dagger = \delta_{ij} \quad [92]$$

and

$$\overline{a_a^\dagger a_b^\dagger} = a_a^\dagger a_b^\dagger - \{a_a^\dagger a_b^\dagger\} = a_a^\dagger a_b^\dagger + a_b^\dagger a_a^\dagger = \delta_{ab} \quad [93]$$

---

<sup>1</sup>Note that this *q*-particle definition of annihilation and creation simply reverses the roles of second-quantized operators acting in the occupied (hole) space, but leaves those acting in the unoccupied (particle) space untouched.

The analogous contractions that place the  $q$ -particle annihilation operator to the right of the  $q$ -particle creation operators are zero:

$$\overline{a_a^\dagger a_b} = \overline{a_i^\dagger a_j^\dagger} = 0 \quad [94]$$

All other combinations necessarily involve mixed hole and particle indices for which the Kronecker delta functions will give zero.

## The Normal-Ordered Electronic Hamiltonian

The second-quantized form of the electronic Hamiltonian<sup>80,84,92</sup>

$$\hat{H} = \sum_{pq} \langle p|\hat{h}|q\rangle a_p^\dagger a_q + \frac{1}{4} \sum_{pqrs} \langle pq||rs\rangle a_p^\dagger a_q^\dagger a_s a_r \quad [95]$$

may be cast into normal-ordered form using Wick's theorem. We may begin by rewriting the pair of operators in the one-electron part of the Hamiltonian as

$$a_p^\dagger a_q = \{a_p^\dagger a_q\} + \{\overline{a_p^\dagger a_q}\} \quad [96]$$

The contraction rules we examined earlier (cf. Eqs. [92] and [93]) state that since the creation operator is on the left, the contraction is zero unless  $a_p^\dagger$  and  $a_q$  both act in the hole space and give  $\delta_{pq}$ . This simplifies the one-electron part of the equation to

$$\sum_{pq} \langle p|\hat{h}|q\rangle \{a_p^\dagger a_q\} + \sum_i \langle i|h|i\rangle \quad [97]$$

Now we rewrite the string of annihilation and creation operators from the two-electron part of  $\hat{H}$  as

$$\begin{aligned} a_p^\dagger a_q^\dagger a_s a_r &= \{a_p^\dagger a_q^\dagger a_s a_r\} + \{\overline{a_p^\dagger a_q^\dagger a_s a_r}\} + \{a_p^\dagger \overline{a_q^\dagger a_s a_r}\} + \{\overline{a_p^\dagger a_q^\dagger a_s a_r}\} \\ &\quad + \{a_p^\dagger \overline{a_q^\dagger a_s a_r}\} + \{\overline{a_p^\dagger a_q^\dagger a_s a_r}\} + \{\overline{a_p^\dagger a_q^\dagger a_s a_r}\} \end{aligned} \quad [98]$$

Again, all these contractions are zero unless the leftmost operator of the contraction acts in the hole space. This leads to the simplified form

$$\begin{aligned} a_p^\dagger a_q^\dagger a_s a_r &= \{a_p^\dagger a_q^\dagger a_s a_r\} - \delta_{p \in i} \delta_{ps} \{a_q^\dagger a_r\} + \delta_{q \in i} \delta_{qs} \{a_p^\dagger a_r\} + \delta_{p \in i} \delta_{pr} \{a_q^\dagger a_s\} \\ &\quad - \delta_{q \in i} \delta_{qr} \{a_p^\dagger a_s\} - \delta_{p \in i} \delta_{ps} \delta_{q \in i} \delta_{qr} + \delta_{p \in i} \delta_{pr} \delta_{q \in j} \delta_{qs} \end{aligned} \quad [99]$$

where the notation  $p \in i$  means that  $p$  must be contained in the set of occupied orbitals and the Kronecker delta indicates that  $p$  must be equal to  $i$ . Note that the signs on each of the terms are derived from the contraction rules discussed earlier. Inserting this expression back into the equation for the two-electron part of the Hamiltonian, we obtain

$$\begin{aligned} & \frac{1}{4} \sum_{pqrs} \langle pq||rs \rangle \{a_p^\dagger a_q^\dagger a_s a_r\} - \frac{1}{4} \sum_{qri} \langle iq||ri \rangle \{a_q^\dagger a_r\} + \frac{1}{4} \sum_{pri} \langle pi||ri \rangle \{a_p^\dagger a_r\} \\ & + \frac{1}{4} \sum_{qsi} \langle iq||is \rangle \{a_q^\dagger a_s\} - \frac{1}{4} \sum_{psi} \langle pi||is \rangle \{a_p^\dagger a_s\} - \frac{1}{4} \sum_{ij} \langle ij||ji \rangle + \frac{1}{4} \sum_{ij} \langle ij||ij \rangle \end{aligned} \quad [100]$$

Remembering that for antisymmetrized two-electron integrals in Dirac's notation,  $\langle pq||rs \rangle = -\langle pq||sr \rangle = -\langle qp||rs \rangle = \langle qp||sr \rangle$ , we may re-index sums and combine terms where appropriate to obtain

$$\frac{1}{4} \sum_{pqrs} \langle pq||rs \rangle \{a_p^\dagger a_q^\dagger a_s a_r\} + \sum_{pri} \langle pi||ri \rangle \{a_p^\dagger a_r\} + \frac{1}{2} \sum_{ij} \langle ij||ij \rangle \quad [101]$$

The complete Hamiltonian is therefore

$$\begin{aligned} \hat{H} = & \sum_{pq} \langle p|b|q \rangle \{a_p^\dagger a_q\} + \sum_{pri} \langle pi||ri \rangle \{a_p^\dagger a_r\} + \frac{1}{4} \sum_{pqrs} \langle pq||rs \rangle \{a_p^\dagger a_q^\dagger a_s a_r\} \\ & + \sum_i \langle i|b|i \rangle + \frac{1}{2} \sum_{ij} \langle ij||ij \rangle \end{aligned} \quad [102]$$

Note that the first and second terms on the right-hand side of this equation are simply the spin-orbital Fock operator (in normal-ordered form), and the last two terms are the Hartree–Fock energy (i.e., the Fermi vacuum expectation value of the Hamiltonian). Thus, we may write

$$\hat{H} = \sum_{pq} f_{pq} \{a_p^\dagger a_q\} + \frac{1}{4} \sum_{pqrs} \langle pq||rs \rangle \{a_p^\dagger a_q^\dagger a_s a_r\} + \langle \Phi_0 | \hat{H} | \Phi_0 \rangle \quad [103]$$

or

$$\hat{H} = \hat{F}_N + \hat{V}_N + \langle \Phi_0 | \hat{H} | \Phi_0 \rangle \quad [104]$$

where the subscript N indicates normal ordering of all the component operator strings. Therefore, the normal-ordered Hamiltonian is simply

$$\hat{H}_N \equiv \hat{F}_N + \hat{V}_N = \hat{H} - \langle \Phi_0 | \hat{H} | \Phi_0 \rangle \quad [105]$$

This result is easily generalized: the normal-ordered form of an operator is simply the operator itself minus its reference expectation value. For the Hamiltonian example, above, the normal-ordered Hamiltonian is just the Hamiltonian minus the SCF energy (i.e.,  $\hat{H}_N$  may be considered to be a *correlation* operator). Owing to its considerable convenience for coupled cluster and many-body perturbation theory analyses, this conventional form of  $\hat{H}$  given in Eq. [105] is adopted for the remainder of this chapter.

## Simplification of the Coupled Cluster Hamiltonian

The concepts of normal ordering and Wick's theorem provide the mathematical tools needed to derive programmable coupled cluster equations from the more formal expressions given in Eqs. [50] and [51]. If we truncate the cluster operator such that  $\hat{T} \equiv \hat{T}_1 + \hat{T}_2$  and insert it into the similarity-transformed normal-ordered Hamiltonian,  $\bar{H} \equiv e^{-\hat{T}} \hat{H}_N e^{\hat{T}}$ , we obtain

$$\begin{aligned}\bar{H} = & \hat{H}_N + [\hat{H}_N, \hat{T}_1] + [\hat{H}_N, \hat{T}_2] + \frac{1}{2}[[\hat{H}_N, \hat{T}_1], \hat{T}_1] \\ & + \frac{1}{2}[[\hat{H}_N, \hat{T}_2], \hat{T}_2] + [[\hat{H}_N, \hat{T}_1], \hat{T}_2] + \dots\end{aligned}\quad [106]$$

where the Hausdorff expansion above terminates naturally at quadruply nested commutators as described earlier.<sup>79</sup> Our task in constructing the CCSD equations is to obtain second-quantized expressions for each term of  $\bar{H}$  above, insert these into Eqs. [50] and [51], and finally evaluate the resulting matrix elements.

The first commutator of Eq. [106] expands to give

$$[\hat{H}_N, \hat{T}_1] = [\hat{F}_N, \hat{T}_1] + [\hat{V}_N, \hat{T}_1] = \hat{F}_N \hat{T}_1 - \hat{T}_1 \hat{F}_N + \hat{V}_N \hat{T}_1 - \hat{T}_1 \hat{V}_N \quad [107]$$

using the definition of  $\hat{H}_N$  given in Eq. [105]. The second-quantized definition of  $\hat{T}_1$  is simply

$$\hat{T}_1 = \sum_{ia} t_i^a \{a_a^\dagger a_i\} \quad [108]$$

where the braces indicate that the operator string is already normal-ordered (i.e., this is the only nonzero term resulting from application of Wick's theorem

<sup>79</sup>Since the cluster operators commute, we have

$$[[\hat{H}_N, \hat{T}_1], \hat{T}_2] = \frac{1}{2}[[\hat{H}_N, \hat{T}_1], \hat{T}_2] + \frac{1}{2}[[\hat{H}_N, \hat{T}_2], \hat{T}_1]$$

Therefore, a factor of  $1/2$  does not appear in front of this term in the expansion above.

to Eq. [27]). Given the second-quantized form of  $\hat{F}_N$  from the preceding section, the first term of the commutator may be written as

$$\hat{F}_N \hat{T}_1 = \sum_{pq} \sum_{ia} f_{pq} t_i^a \{a_p^\dagger a_q\} \{a_a^\dagger a_i\} \quad [109]$$

The generalized form of Wick's theorem (see Eq. [91]) says that this product of normal-ordered operator strings may be written using only contractions between the two strings. That is,

$$\begin{aligned} \{a_p^\dagger a_q\} \{a_a^\dagger a_i\} &= \{a_p^\dagger a_q a_a^\dagger a_i\} + \{\overline{a_p^\dagger a_q} \overline{a_a^\dagger a_i}\} + \{a_p^\dagger \overline{a_q} a_a^\dagger a_i\} + \{\overline{a_p^\dagger a_q} \overline{a_a^\dagger a_i}\} \\ &= \{a_p^\dagger a_q a_a^\dagger a_i\} + \delta_{pi} \{a_q a_a^\dagger\} + \delta_{qa} \{a_p^\dagger a_i\} + \delta_{pi} \delta_{qa} \end{aligned} \quad [110]$$

For the second term of the expanded commutator,  $\hat{T}_1 \hat{F}_N$ , where the operator strings from  $\hat{F}_N$  and  $\hat{T}_1$  are simply reversed in order, Wick's theorem gives only one term, namely,

$$\{a_a^\dagger a_i\} \{a_p^\dagger a_q\} = \{a_a^\dagger a_i a_p^\dagger a_q\} = \{a_p^\dagger a_q a_a^\dagger a_i\} \quad [111]$$

All other contractions, which involve  $a_a^\dagger$  and  $a_i$  on the left, are zero by Eq. [94]. The final equality in this expression arises from the fact that, by construction, all operators within the braces anticommute. Therefore, using Eqs. [110] and [111], we may write

$$\begin{aligned} \hat{F}_N \hat{T}_1 - \hat{T}_1 \hat{F}_N &= \sum_{pq} \sum_{ia} f_{pq} t_i^a (\delta_{pi} \{a_q a_a^\dagger\} + \delta_{qa} \{a_p^\dagger a_i\} + \delta_{pi} \delta_{qa}) \\ &= \sum_{qia} f_{iq} t_i^a \{a_q a_a^\dagger\} + \sum_{pia} f_{pa} t_i^a \{a_p^\dagger a_i\} + \sum_{ia} f_{ia} t_i^a \end{aligned} \quad [112]$$

This example illustrates how the commutator allows only those terms involving contractions between the operators to survive; the “uncontracted” terms are eliminated. Note that the final term on the right-hand side involves components of the Fock operator in the occupied-virtual block; if Brillouin's theorem<sup>82</sup> holds for the set of molecular orbitals used to construct  $\Phi_0$ , then this term is zero.

Now consider the first doubly nested commutator from Eq. [106]. The term involving the Fock operator expands to give

$$\frac{1}{2} [[\hat{F}_N, \hat{T}_1], \hat{T}_1] = \frac{1}{2} \hat{F}_N \hat{T}_1^2 - \hat{T}_1 \hat{F}_N \hat{T}_1 + \frac{1}{2} \hat{T}_1^2 \hat{F}_N \quad [113]$$

Applying Wick's theorem to the operator strings in the first term on the right-hand side of this equation gives

$$\begin{aligned} \frac{1}{2}\hat{F}_N\hat{T}_1^2 = & \frac{1}{2}\sum_{pq}\sum_{ia}\sum_{jb}f_{pq}t_i^at_j^b(\{a_p^\dagger a_q a_a^\dagger a_i a_b^\dagger a_j\} + \{\overline{a_p^\dagger a_q a_a^\dagger a_i} \overline{a_b^\dagger a_j}\} + \{\overline{a_p^\dagger a_q a_a^\dagger a_i} \overline{a_b^\dagger a_j}\}) \\ & + \{a_p^\dagger a_q \overline{a_a^\dagger a_i} a_b^\dagger a_j\} + \{a_p^\dagger a_q \overline{a_a^\dagger a_i} \overline{a_b^\dagger a_j}\} + \{a_p^\dagger a_q \overline{a_a^\dagger a_i} a_b^\dagger a_j\} \\ & + \{a_p^\dagger a_q \overline{a_a^\dagger a_i} a_b^\dagger a_j\} + \{a_p^\dagger a_q \overline{a_a^\dagger a_i} \overline{a_b^\dagger a_j}\} + \{a_p^\dagger a_q \overline{a_a^\dagger a_i} a_b^\dagger a_j\} \end{aligned} \quad [114]$$

Evaluating the contractions leads to

$$\begin{aligned} \frac{1}{2}\hat{F}_N\hat{T}_1^2 = & \frac{1}{2}\sum_{aibj}t_i^at_j^b\left(\sum_{pq}f_{pq}\{a_p^\dagger a_q a_a^\dagger a_i a_b^\dagger a_j\} + \sum_qf_{iq}\{a_q a_a^\dagger a_b^\dagger a_j\}\right. \\ & + \sum_qf_{iq}\{a_q a_a^\dagger a_i a_b^\dagger\} + \sum_pf_{pa}\{a_p^\dagger a_i a_b^\dagger a_j\} \\ & + \sum_pf_{pb}\{a_p^\dagger a_a^\dagger a_i a_j\} + f_{ia}\{a_b^\dagger a_j\} + f_{ja}\{a_i a_b^\dagger\} \\ & \left.- f_{ib}\{a_a^\dagger a_j\} + f_{jb}\{a_a^\dagger a_i\}\right) \end{aligned} \quad [115]$$

This expression may be simplified significantly by recognizing that because of the summation outside the parentheses,  $i$ ,  $j$ ,  $a$ , and  $b$  are dummy indices and may be exchanged. For example, the second and third terms on the right-hand side are identical:

$$\sum_{aibj}t_i^at_j^b\left(\sum_qf_{iq}\{a_q a_a^\dagger a_b^\dagger a_j\} + \sum_qf_{jq}\{a_q a_a^\dagger a_i a_b^\dagger\}\right) \quad [116]$$

$$= \sum_{aibj}\sum_q(f_{jq}t_i^at_j^b\{a_q a_a^\dagger a_i a_b^\dagger\} + f_{iq}t_i^at_j^b\{a_q a_a^\dagger a_i a_b^\dagger\}) \quad [117]$$

The first step in this analysis results from simply swapping index  $i$  with  $j$  and index  $a$  with  $b$ . Similarly, one may show equivalence of terms four and five, six and nine, and seven and eight (with appropriate sign changes). The final, simplified expression is thus

$$\begin{aligned} \frac{1}{2}\hat{F}_N\hat{T}_1^2 = & \frac{1}{2}\sum_{aibj}t_i^at_j^b\left(\sum_{pq}f_{pq}\{a_p^\dagger a_q a_a^\dagger a_i a_b^\dagger a_j\} + 2\sum_qf_{iq}\{a_q a_a^\dagger a_i a_b^\dagger\}\right. \\ & \left.+ 2\sum_pf_{pb}\{a_p^\dagger a_a^\dagger a_i a_j\} + 2f_{jb}\{a_a^\dagger a_i\} + 2f_{ja}\{a_i a_b^\dagger\}\right) \end{aligned} \quad [118]$$

A similar analysis for the remaining two terms of the doubly nested commutator gives

$$\begin{aligned} \hat{T}_1 \hat{F}_N \hat{T}_1 &= \sum_{aibj} t_i^a t_j^b \left( \sum_{pq} f_{pq} \{a_a^\dagger a_i a_p^\dagger a_q a_b^\dagger a_j\} + \sum_q f_{jq} \{a_a^\dagger a_i a_q a_b^\dagger\} \right. \\ &\quad \left. + \sum_p f_{pb} \{a_a^\dagger a_i a_p^\dagger a_j\} + f_{jb} \{a_a^\dagger a_i\} \right) \end{aligned} \quad [119]$$

and

$$\frac{1}{2} \hat{T}_1^2 \hat{F}_N = \frac{1}{2} \sum_{aibj} \sum_{pq} f_{pq} t_i^a t_j^b \{a_a^\dagger a_i a_b^\dagger a_j a_p^\dagger a_q\} \quad [120]$$

Inserting these expressions into Eq. [113] and canceling terms gives the rather simple result

$$\frac{1}{2} [[\hat{F}_N, \hat{T}_1], \hat{T}_1] = \sum_{aibj} f_{ja} t_i^a t_j^b \{a_i a_b^\dagger\} \quad [121]$$

The two examples given so far,  $[\hat{F}_N, \hat{T}_1]$  and  $\frac{1}{2} [[\hat{F}_N, \hat{T}_1], \hat{T}_1]$ , allow us to make an important generalization when Wick's theorem is applied to the commutators in Eq. [106]:

The only nonzero terms in the Hausdorff expansion are those in which the Hamiltonian,  $\hat{H}_N$ , has at least one contraction with every cluster operator,  $\hat{T}_n$ , on its right.

That is, the Hamiltonian must share at least one index with every cluster operator component in the final expression. We may therefore rewrite Eq. [106] in a simpler form:

$$\begin{aligned} \bar{H} &= (\hat{H}_N + \hat{H}_N \hat{T}_1 + \hat{H}_N \hat{T}_2 + \frac{1}{2} \hat{H}_N \hat{T}_1^2 + \frac{1}{2} \hat{H}_N \hat{T}_2^2 + \hat{H}_N \hat{T}_1 \hat{T}_2 \\ &\quad + \frac{1}{6} \hat{H}_N \hat{T}_1^3 + \frac{1}{2} \hat{H}_N \hat{T}_1^2 \hat{T}_2 + \frac{1}{2} \hat{H}_N \hat{T}_1 \hat{T}_2^2 + \frac{1}{6} \hat{H}_N \hat{T}_2^3 \\ &\quad + \frac{1}{24} \hat{H}_N \hat{T}_1^4 + \frac{1}{6} \hat{H}_N \hat{T}_1^3 \hat{T}_2 + \frac{1}{4} \hat{H}_N \hat{T}_1^2 \hat{T}_2^2 + \frac{1}{6} \hat{H}_N \hat{T}_1 \hat{T}_2^3 + \frac{1}{24} \hat{H}_N \hat{T}_2^4)_c \end{aligned} \quad [122]$$

where we have now written every term in the CCSD Hausdorff expansion explicitly and the subscript c indicates that only those terms in which the Hamiltonian is connected (in the Wick's theorem sense) to every cluster operator on its right should be included in the algebraic interpretation of the operator.

This is often referred to as the “connected cluster” form of the similarity-transformed Hamiltonian.<sup>2</sup> This expression makes the truncation of the Hausdorff expansion even clearer; since the Hamiltonian contains at most four annihilation and creation operators (in  $\hat{V}_N$ ),  $\hat{H}_N$  can connect to at most four cluster operators at once. Therefore, the Hausdorff expansion must truncate at the quartic terms.

## The CCSD Energy Equation

Using the connected cluster form of  $\bar{H}$  defined above, as well as the techniques of Wick’s theorem and normal ordering, we may derive a programmable form of the energy expression in the CCSD approximation. In accord with Eq. [50] and the normal-ordered Hamiltonian, the energy is given by

$$E_{\text{CCSD}} - E_0 = \langle \Phi_0 | \bar{H} | \Phi_0 \rangle \quad [123]$$

where the CCSD effective Hamiltonian of Eq. [122] is inserted for  $\bar{H}$  and  $E_0$  is the SCF energy,  $\langle \Phi_0 | \hat{H} | \Phi_0 \rangle$ . The leading term in this expression is the reference expectation value of the normal-ordered Hamiltonian, which is zero by construction:

$$\langle \Phi_0 | \hat{H}_N | \Phi_0 \rangle = 0 \quad [124]$$

For all other terms, we may use the advantage of normal-ordering of the operators to determine all the fully contracted terms of the operator product. For example, for the second term on the right-hand side of Eq. [122], insertion of the definition of the normal-ordered Hamiltonian gives

$$(\hat{H}_N \hat{T}_1)_c = (\hat{F}_N \hat{T}_1)_c + (\hat{V}_N \hat{T}_1)_c \quad [125]$$

where the subscript c has the same meaning as in Eq. [122]. We have already evaluated the first component of this pair, and the result is given in Eq. [112], which contains only one fully contracted term, that is,

$$\langle \Phi_0 | (\hat{F}_N \hat{T}_1)_c | \Phi_0 \rangle = \sum_{ia} f_{ia} t_i^a \quad [126]$$

The two-electron component, on the other hand, contributes nothing to the energy expression because no fully contracted terms can be generated from it:

$$\begin{aligned}
(\hat{V}_N \hat{T}_1)_c &= \frac{1}{4} \sum_{pqrs} \sum_{ia} \langle pq || rs \rangle t_i^a \{a_p^\dagger a_q^\dagger a_s a_r\} \{a_a^\dagger a_i\} \\
&= \frac{1}{4} \sum_{pqrs} \sum_{ia} \langle pq || rs \rangle t_i^a (\{a_p^\dagger a_q^\dagger a_s a_r a_a^\dagger a_i\} + \{a_p^\dagger a_q^\dagger a_s a_r a_a^\dagger a_i\} \\
&\quad + \{a_p^\dagger a_q^\dagger \overline{a_s a_r a_a^\dagger a_i}\} + \{a_p^\dagger a_q^\dagger \overline{a_s a_r a_a^\dagger a_i}\} + \{a_p^\dagger a_q^\dagger \overline{a_s a_r a_a^\dagger a_i}\} \\
&\quad + \{a_p^\dagger a_q^\dagger \overline{a_s a_r a_a^\dagger a_i}\} + \{a_p^\dagger a_q^\dagger \overline{a_s a_r a_a^\dagger a_i}\} + \{a_p^\dagger a_q^\dagger \overline{a_s a_r a_a^\dagger a_i}\} \\
&\quad + \{a_p^\dagger a_q^\dagger \overline{a_s a_r a_a^\dagger a_i}\})
\end{aligned} \tag{127}$$

Therefore, the energy contribution from the linear  $\hat{T}_1$  operator is

$$E_{CCSD} \leftarrow \langle \Phi_0 | (\hat{H}_N \hat{T}_1)_c | \Phi_0 \rangle = \sum_{ia} f_{ia} t_i^a \tag{128}$$

(The left arrow indicates that this is only one of several terms contributing to the energy on the left-hand side.) However, this term will be zero if Brillouin's theorem holds for the molecular orbitals in which the Fock matrix is represented.<sup>82</sup>

Next consider the contribution to the energy from the linear  $\hat{T}_2$  term in Eq. [123],

$$\langle \Phi_0 | (\hat{H}_N \hat{T}_2)_c | \Phi_0 \rangle = \langle \Phi_0 | \left[ (\hat{F}_N \hat{T}_2)_c + (\hat{V}_N \hat{T}_2)_c \right] | \Phi_0 \rangle \tag{129}$$

The normal-ordered form of  $\hat{T}_2$  may be derived from Eq. [28] to obtain

$$\hat{T}_2 = \frac{1}{4} \sum_{aibj} t_{ij}^{ab} \{a_a^\dagger a_b^\dagger a_j a_i\} \tag{130}$$

The reference expectation value of the first term on the right-hand side of Eq. [129] is zero because it cannot produce any fully contracted components:

$$\begin{aligned}
(\hat{F}_N \hat{T}_2)_c &= \frac{1}{4} \sum_{pq} \sum_{aibj} f_{pq} t_{ij}^{ab} \{a_p^\dagger a_q\} \{a_a^\dagger a_b^\dagger a_j a_i\} \\
&= \frac{1}{4} \sum_{pq} \sum_{aibj} f_{pq} t_{ij}^{ab} (\{a_p^\dagger a_q a_a^\dagger a_b^\dagger a_j a_i\} + \{a_p^\dagger a_q a_a^\dagger a_b^\dagger a_j a_i\} \\
&\quad + \{a_p^\dagger a_q \overline{a_a^\dagger a_b^\dagger a_j a_i}\} + \{a_p^\dagger a_q \overline{a_a^\dagger a_b^\dagger a_j a_i}\} + \{a_p^\dagger a_q \overline{a_a^\dagger a_b^\dagger a_j a_i}\} \\
&\quad + \{a_p^\dagger a_q \overline{a_a^\dagger a_b^\dagger a_j a_i}\} + \{a_p^\dagger a_q \overline{a_a^\dagger a_b^\dagger a_j a_i}\} + \{a_p^\dagger a_q \overline{a_a^\dagger a_b^\dagger a_j a_i}\} \\
&\quad + \{a_p^\dagger a_q \overline{a_a^\dagger a_b^\dagger a_j a_i}\})
\end{aligned} \tag{131}$$

The two-electron component, however, produces four equivalent fully contracted terms, and therefore contributes to the coupled cluster energy:

$$\begin{aligned}
 \langle \Phi_0 | (\hat{V}_N \hat{T}_2)_c | \Phi_0 \rangle &= \frac{1}{16} \sum_{pqrs} \sum_{aibj} \langle pq || rs \rangle t_{ij}^{ab} \langle \Phi_0 | \{a_p^\dagger a_q^\dagger a_s a_r\} \{a_a^\dagger a_b^\dagger a_j a_i\} | \Phi_0 \rangle \\
 &= \frac{1}{16} \sum_{pqrs} \sum_{aibj} \langle pq || rs \rangle t_{ij}^{ab} \left( \{a_p^\dagger a_q^\dagger a_s a_r a_a^\dagger a_b^\dagger a_j a_i\} + \{a_p^\dagger a_q^\dagger a_s a_r a_a^\dagger a_b^\dagger a_j a_i\} \right. \\
 &\quad \left. + \{a_p^\dagger a_q^\dagger a_s a_r a_a^\dagger a_b^\dagger a_j a_i\} + \{a_p^\dagger a_q^\dagger a_s a_r a_a^\dagger a_b^\dagger a_j a_i\} \right) \\
 &= \frac{1}{16} \sum_{pqrs} \sum_{aibj} \langle pq || rs \rangle t_{ij}^{ab} (\delta_{pi} \delta_{qj} \delta_{ra} \delta_{sb} + \delta_{pj} \delta_{qi} \delta_{rb} \delta_{sa} - \delta_{pj} \delta_{qi} \delta_{ra} \delta_{sb} - \delta_{pi} \delta_{qj} \delta_{rb} \delta_{sa}) \\
 &= \frac{1}{4} \sum_{aibj} \langle ij || ab \rangle t_{ij}^{ab}
 \end{aligned} \tag{132}$$

The factor of  $\frac{1}{16}$  appearing in the first three equalities arises simply from the product of the factors of  $\frac{1}{4}$  that appear in the definitions of  $\hat{V}_N$  (Eq. [104]) and  $\hat{T}_2$  (Eq. [130]), and the final factor of  $\frac{1}{4}$  results from the collection of the last four terms together.

Next we consider the first quadratic term from Eq. [123], which involves two  $\hat{T}_1$  cluster operators. The reference expectation value of the one-electron component,  $\frac{1}{2}(\hat{F}_N \hat{T}_1^2)_c$ , is zero because the single construction operator pair in the Fock operator cannot produce fully contracted terms with the two construction operator pairs in  $\hat{T}_1^2$ . The two-electron component, on the other hand, does produce fully contracted terms, namely,

$$\begin{aligned}
 \frac{1}{2} \langle \Phi_0 | (\hat{V}_N \hat{T}_1^2)_c | \Phi_0 \rangle &= \frac{1}{8} \sum_{pqrs} \sum_{ai} \sum_{bj} \langle pq || rs \rangle t_i^a t_j^b \langle \Phi_0 | \{a_p^\dagger a_q^\dagger a_s a_r\} \{a_a^\dagger a_i\} \{a_b^\dagger a_j\} | \Phi_0 \rangle \\
 &= \frac{1}{8} \sum_{pqrs} \sum_{aibj} \langle pq || rs \rangle t_i^a t_j^b \left( \{a_p^\dagger a_q^\dagger a_s a_r a_a^\dagger a_i a_b^\dagger a_j\} + \{a_p^\dagger a_q^\dagger a_s a_r a_a^\dagger a_i a_b^\dagger a_j\} \right. \\
 &\quad \left. + \{a_p^\dagger a_q^\dagger a_s a_r a_a^\dagger a_b^\dagger a_i a_j\} + \{a_p^\dagger a_q^\dagger a_s a_r a_a^\dagger a_i a_b^\dagger a_j\} \right) \\
 &= \frac{1}{8} \sum_{pqrs} \sum_{aibj} \langle pq || rs \rangle t_i^a t_j^b (-\delta_{pj} \delta_{qi} \delta_{ra} \delta_{sb} + \delta_{pj} \delta_{qi} \delta_{rb} \delta_{sa} + \delta_{pi} \delta_{qj} \delta_{ra} \delta_{sb} - \delta_{pi} \delta_{qj} \delta_{rb} \delta_{sa}) \\
 &= \frac{1}{2} \sum_{aibj} \langle ij || ab \rangle t_i^a t_j^b
 \end{aligned} \tag{133}$$

The factor of  $\frac{1}{8}$  appearing in the first three equalities arises from product of the factor of  $\frac{1}{2}$  from the Hausdorff expansion and the  $\frac{1}{4}$  from the definition of  $\hat{V}_N$  (Eq. [104]).

In all the remaining terms in the energy expression in Eq. [123], the cluster operators contribute more construction operator pairs than the Hamiltonian

components. For example, the “mixed” term,  $(\hat{H}_N \hat{T}_1 \hat{T}_2)_{\epsilon}$ , involves three pairs from the cluster operators (one from  $\hat{T}_1$  and two from  $\hat{T}_2$ ) but only two from the two-electron component of the Hamiltonian. Therefore, none of these terms can produce fully contracted products, and their reference expectation values are zero. The absence of these “higher order” components might also be rationalized in terms of Slater’s rules: since the Hamiltonian is a two-electron operator, the  $\hat{T}_1 \hat{T}_2$  product produces on the right a triply excited determinant that cannot couple to the reference  $\Phi_0$  through the Hamiltonian. However, as we will see in the next section, this interpretation is inadequate because it fails to explain why certain terms are missing from the amplitude equations for higher excitations (e.g., the CCSDT  $\hat{T}_3$  amplitude equation).

We have now derived all the contributions to the CCSD energy. Summing Eqs. [126], [132], and [133], we obtain the final expression

$$E_{\text{CCSD}} - E_0 = \sum_{ia} f_{ia} t_i^a + \frac{1}{4} \sum_{aibj} \langle ij || ab \rangle t_{ij}^{ab} + \frac{1}{2} \sum_{aibj} \langle ij || ab \rangle t_i^a t_j^b \quad [134]$$

This equation is not restricted to the CCSD approximation, however. Since higher excitation cluster operators such as  $\hat{T}_3$  and  $\hat{T}_4$  cannot produce fully contracted terms with the Hamiltonian, their contribution to the coupled cluster energy expression is zero. Therefore, Eq. [134] also holds for more complicated methods such as CCSDT and CCSDTQ. Higher excitation cluster operators can contribute to the energy indirectly, however, through the equations used to determine the amplitudes,  $t_i^a$  and  $t_{ij}^{ab}$ , which are needed in the energy equation above.

## The CCSD Amplitude Equations

As discussed earlier, the cluster amplitudes that parameterize the coupled cluster wavefunction may be determined from the “projective” Schrödinger equation given in Eq. [51]. In the CCSD approximation, the single-excitation amplitudes,  $t_i^a$ , may be determined from

$$0 = \langle \Phi_i^a | \bar{H} | \Phi_0 \rangle \quad [135]$$

and the double-excitation amplitudes,  $t_{ij}^{ab}$ , from

$$0 = \langle \Phi_{ij}^{ab} | \bar{H} | \Phi_0 \rangle \quad [136]$$

where  $\bar{H}$  is given by Eq. [122]. For reasons we describe in detail later in the section entitled Computer Implementation of Coupled Cluster Theory, Eq. [135] is commonly referred to as the  $\hat{T}_1$  amplitude equation and Eq. [136] as the  $\hat{T}_2$  amplitude equation. Rather than dealing with all 15 terms arising from the insertion of Eq. [122] into Eqs. [135] and [136], we will focus on only a few representative examples.

The construction of the coupled cluster amplitude equations is somewhat more complicated than the energy equation in that the latter requires only reference expectation values of the second-quantized operators. For the amplitude equations, we now require matrix elements between the reference,  $\Phi_0$ , on the right and specific excited determinants on the left. We must therefore convert these into reference expectation value expressions by writing the excited determinants as excitation operator strings acting on  $\Phi_0$ . For example, a doubly excited bra determinant may be written as

$$\langle \Phi_{ij}^{ab} | = \langle \Phi | \{a_i^\dagger a_j^\dagger a_b a_a\} \quad [137]$$

The final matrix element therefore requires that we obtain all fully contracted Wick's theorem terms from the product of the operator string above and the elements of  $\bar{H}$ .

The leading term of  $\bar{H}$  in Eq. [122] is simply the electronic Hamiltonian itself. For its contribution to the  $\hat{T}_1$  amplitude equation, we must therefore evaluate matrix elements of  $\hat{H}_N$  between singly excited determinants and  $\Phi_0$ ,

$$\begin{aligned} \langle \Phi_i^a | (\hat{F}_N + \hat{V}_N) | \Phi_0 \rangle &= \sum_{pq} f_{pq} \langle \Phi_0 | \{a_i^\dagger a_a\} \{a_p^\dagger a_q\} | \Phi_0 \rangle \\ &\quad + \frac{1}{4} \sum_{pqrs} \langle pq || rs \rangle \langle \Phi_0 | \{a_i^\dagger a_a\} \{a_p^\dagger a_q^\dagger a_s a_r\} | \Phi_0 \rangle \end{aligned} \quad [138]$$

The two-electron component of this equation cannot produce full contractions and is therefore zero. The one-electron term, however, simplifies to a single Fock matrix element:

$$\begin{aligned} \langle \Phi_i^a | \hat{F}_N | \Phi_0 \rangle &= \sum_{pq} f_{pq} \langle \Phi_0 | \{a_i^\dagger a_a\} \{a_p^\dagger a_q\} | \Phi_0 \rangle \\ &= \sum_{pq} f_{pq} \{a_i^\dagger \overline{a_a} \overline{a_p^\dagger} a_q^\dagger\} \\ &= \sum_{pq} f_{pq} \delta_{iq} \delta_{ap} \\ &= f_{ai} \end{aligned} \quad [139]$$

For the contribution of  $\hat{H}_N$  to the  $\hat{T}_2$  amplitude equation, on the other hand, we must evaluate the matrix elements of the normal-ordered Hamiltonian between doubly excited determinants and  $\Phi_0$ , namely,

$$\begin{aligned} \langle \Phi_{ij}^{ab} | (\hat{F}_N + \hat{V}_N) | \Phi_0 \rangle &= \sum_{pq} f_{pq} \langle \Phi_0 | \{a_i^\dagger a_j^\dagger a_b a_a\} \{a_p^\dagger a_q\} | \Phi_0 \rangle \\ &\quad + \frac{1}{4} \sum_{pqrs} \langle pq || rs \rangle \langle \Phi_0 | \{a_i^\dagger a_j^\dagger a_b a_a\} \{a_p^\dagger a_q^\dagger a_s a_r\} | \Phi_0 \rangle \end{aligned} \quad [140]$$

In this case, it is the one-electron component that cannot produce full contractions, whereas the two-electron component contributes only a single integral:

$$\begin{aligned}
 \langle \Phi_{ij}^{ab} | \hat{V}_N | \Phi_0 \rangle &= \frac{1}{4} \sum_{pqrs} \langle pq || rs \rangle \langle \Phi_0 | \{a_i^\dagger a_j^\dagger a_b a_a\} \{a_p^\dagger a_q^\dagger a_s a_r\} | \Phi_0 \rangle \\
 &= \frac{1}{4} \sum_{pqrs} \langle pq || rs \rangle \left( \{a_i^\dagger a_j^\dagger a_b a_a \overbrace{a_p^\dagger a_q^\dagger a_s a_r} + \{a_i^\dagger a_j^\dagger a_b a_a \overbrace{a_p^\dagger a_q^\dagger a_s a_r} \right. \\
 &\quad \left. + \{a_i^\dagger a_j^\dagger a_b a_a \overbrace{a_p^\dagger a_q^\dagger a_s a_r} + \{a_i^\dagger a_j^\dagger a_b a_a \overbrace{a_p^\dagger a_q^\dagger a_s a_r} \right) \\
 &= \frac{1}{4} \sum_{pqrs} \langle pq || rs \rangle (\delta_{pa} \delta_{qb} \delta_{ri} \delta_{sj} - \delta_{pb} \delta_{qa} \delta_{ri} \delta_{sj} - \delta_{pa} \delta_{qb} \delta_{rj} \delta_{si} + \delta_{pb} \delta_{qa} \delta_{rj} \delta_{si}) \\
 &= \langle ab || ij \rangle
 \end{aligned} \tag{141}$$

The second term of Eq. [122], which is linear in  $\hat{T}_1$ , provides a more interesting example than  $\hat{H}_N$  alone. Its contribution to the  $\hat{T}_1$  amplitude equation involves the matrix elements

$$\begin{aligned}
 \langle \Phi_i^a | ([\hat{F}_N + \hat{V}_N] \hat{T}_1)_c | \Phi_0 \rangle &= \sum_{pq} \sum_{jb} f_{pq} t_j^b \langle \Phi_0 | \{a_i^\dagger a_a\} (\{a_p^\dagger a_q^\dagger\} \{a_b^\dagger a_j\})_c | \Phi_0 \rangle \\
 &\quad + \frac{1}{4} \sum_{pqrs} \sum_{jb} \langle pq || rs \rangle t_j^b \langle \Phi_0 | \{a_i^\dagger a_a\} (\{a_p^\dagger a_q^\dagger a_s a_r\} \{a_b^\dagger a_j\})_c | \Phi_0 \rangle
 \end{aligned} \tag{142}$$

where the subscript c reminds us that we must retain at least one contraction between the Hamiltonian fragment and the cluster operator on its right. For the two-electron term, Wick's theorem gives

$$\begin{aligned}
 \langle \Phi_i^a | (\hat{V}_N \hat{T}_1)_c | \Phi_0 \rangle &= \frac{1}{4} \sum_{pqrs} \sum_{jb} \langle pq || rs \rangle t_j^b \langle \Phi_0 | \{a_i^\dagger a_a\} (\{a_p^\dagger a_q^\dagger a_s a_r\} \{a_b^\dagger a_j\})_c | \Phi_0 \rangle \\
 &= \frac{1}{4} \sum_{pqrs} \sum_{jb} \langle pq || rs \rangle t_j^b \left( \{a_i^\dagger a_a \overbrace{a_p^\dagger a_q^\dagger a_s a_r} a_b a_j\} + \{a_i^\dagger a_a \overbrace{a_p^\dagger a_q^\dagger a_s a_r} a_b a_j^\dagger\} \right. \\
 &\quad \left. + \{a_i^\dagger a_a \overbrace{a_p^\dagger a_q^\dagger a_s a_r} a_b^\dagger a_j\} + \{a_i^\dagger a_a \overbrace{a_p^\dagger a_q^\dagger a_s a_r} a_b a_j^\dagger\} \right) \\
 &= \frac{1}{4} \sum_{pqrs} \sum_{jb} \langle pq || rs \rangle t_j^b (-\delta_{pa} \delta_{qj} \delta_{rb} \delta_{si} + \delta_{pj} \delta_{qa} \delta_{rb} \delta_{si} + \delta_{pa} \delta_{qj} \delta_{ri} \delta_{sb} - \delta_{pj} \delta_{qa} \delta_{ri} \delta_{sb}) \\
 &= \sum_{bj} \langle ja || bi \rangle t_j^b
 \end{aligned} \tag{143}$$

The contribution of  $(\hat{H}_N \hat{T}_1)_c$  to the  $\hat{T}_2$  equation involves the matrix elements

$$\begin{aligned} \langle \Phi_{ij}^{ab} | (\hat{F}_N + \hat{V}_N) \hat{T}_1 \rangle_c |\Phi_0\rangle &= \sum_{pq} \sum_{kc} f_{pq} t_k^c \langle \Phi_0 | \{a_i^\dagger a_j^\dagger a_b a_a\} (\{a_p^\dagger a_q^\dagger\} \{a_c^\dagger a_k^\dagger\})_c |\Phi_0\rangle \\ &\quad + \frac{1}{4} \sum_{pqrs} \sum_{kc} \langle pq || rs \rangle t_k^c \langle \Phi_0 | \{a_i^\dagger a_j^\dagger a_b a_a\} (\{a_p^\dagger a_q^\dagger a_s a_r\} \{a_c^\dagger a_k^\dagger\})_c |\Phi_0\rangle \end{aligned} \quad [144]$$

In this case, the two-electron term simplifies to four contributions after some rather complicated manipulation:

$$\begin{aligned} \langle \Phi_{ij}^{ab} | (\hat{V}_N \hat{T}_1)_c |\Phi_0\rangle &= \frac{1}{4} \sum_{pqrs} \sum_{kc} \langle pq || rs \rangle t_k^c \langle \Phi_0 | \{a_i^\dagger a_j^\dagger a_b a_a\} (\{a_p^\dagger a_q^\dagger a_s a_r\} \{a_c^\dagger a_k^\dagger\})_c |\Phi_0\rangle \\ &= \frac{1}{4} \sum_{pqrs} \sum_{kc} \langle pq || rs \rangle t_k^c \left( \{a_i^\dagger a_j^\dagger a_b a_a a_p^\dagger a_q^\dagger a_s a_r a_c^\dagger a_k\} + \{a_i^\dagger a_j^\dagger a_b a_a a_p^\dagger a_q^\dagger a_s a_r a_c^\dagger a_k\} \right. \\ &\quad + \{a_i^\dagger a_j^\dagger a_b a_a a_p^\dagger a_q^\dagger a_s a_r a_c^\dagger a_k\} + \{a_i^\dagger a_j^\dagger a_b a_a a_p^\dagger a_q^\dagger a_s a_r a_c^\dagger a_k\} \\ &\quad + \{a_i^\dagger a_j^\dagger a_b a_a a_p^\dagger a_q^\dagger a_s a_r a_c^\dagger a_k\} + \{a_i^\dagger a_j^\dagger a_b a_a a_p^\dagger a_q^\dagger a_s a_r a_c^\dagger a_k\} \\ &\quad + \{a_i^\dagger a_j^\dagger a_b a_a a_p^\dagger a_q^\dagger a_s a_r a_c^\dagger a_k\} + \{a_i^\dagger a_j^\dagger a_b a_a a_p^\dagger a_q^\dagger a_s a_r a_c^\dagger a_k\} \\ &\quad + \{a_i^\dagger a_j^\dagger a_b a_a a_p^\dagger a_q^\dagger a_s a_r a_c^\dagger a_k\} + \{a_i^\dagger a_j^\dagger a_b a_a a_p^\dagger a_q^\dagger a_s a_r a_c^\dagger a_k\} \\ &\quad + \{a_i^\dagger a_j^\dagger a_b a_a a_p^\dagger a_q^\dagger a_s a_r a_c^\dagger a_k\} + \{a_i^\dagger a_j^\dagger a_b a_a a_p^\dagger a_q^\dagger a_s a_r a_c^\dagger a_k\} \\ &\quad + \{a_i^\dagger a_j^\dagger a_b a_a a_p^\dagger a_q^\dagger a_s a_r a_c^\dagger a_k\} + \{a_i^\dagger a_j^\dagger a_b a_a a_p^\dagger a_q^\dagger a_s a_r a_c^\dagger a_k\} \\ &\quad + \{a_i^\dagger a_j^\dagger a_b a_a a_p^\dagger a_q^\dagger a_s a_r a_c^\dagger a_k\} + \{a_i^\dagger a_j^\dagger a_b a_a a_p^\dagger a_q^\dagger a_s a_r a_c^\dagger a_k\} \\ &\quad + \{a_i^\dagger a_j^\dagger a_b a_a a_p^\dagger a_q^\dagger a_s a_r a_c^\dagger a_k\} + \{a_i^\dagger a_j^\dagger a_b a_a a_p^\dagger a_q^\dagger a_s a_r a_c^\dagger a_k\} \\ &\quad + \{a_i^\dagger a_j^\dagger a_b a_a a_p^\dagger a_q^\dagger a_s a_r a_c^\dagger a_k\} + \{a_i^\dagger a_j^\dagger a_b a_a a_p^\dagger a_q^\dagger a_s a_r a_c^\dagger a_k\} \Big) \\ &= \frac{1}{4} \sum_{pqrs} \sum_{kc} \langle pq || rs \rangle t_k^c \times (\delta_{pa} \delta_{qb} \delta_{rc} \delta_{si} \delta_{ik} - \delta_{pb} \delta_{qa} \delta_{rc} \delta_{sj} \delta_{ik} - \delta_{pa} \delta_{qb} \delta_{rc} \delta_{si} \delta_{jk} \\ &\quad + \delta_{pb} \delta_{qa} \delta_{rc} \delta_{si} \delta_{jk} - \delta_{pa} \delta_{qb} \delta_{ri} \delta_{sc} \delta_{ik} + \delta_{pb} \delta_{qa} \delta_{ri} \delta_{sc} \delta_{ik} + \delta_{pa} \delta_{qb} \delta_{ri} \delta_{sc} \delta_{jk} \\ &\quad - \delta_{pb} \delta_{qa} \delta_{ri} \delta_{sc} \delta_{jk} - \delta_{pa} \delta_{qk} \delta_{ri} \delta_{sj} \delta_{bc} + \delta_{pb} \delta_{qk} \delta_{ri} \delta_{sj} \delta_{ac} - \delta_{pb} \delta_{qk} \delta_{rj} \delta_{si} \delta_{ac} \\ &\quad + \delta_{pa} \delta_{qk} \delta_{rj} \delta_{si} \delta_{bc} + \delta_{pk} \delta_{qa} \delta_{ri} \delta_{sj} \delta_{bc} - \delta_{pk} \delta_{qb} \delta_{ri} \delta_{sj} \delta_{ac} - \delta_{pk} \delta_{qa} \delta_{rj} \delta_{si} \delta_{bc} \\ &\quad + \delta_{pk} \delta_{qb} \delta_{rj} \delta_{si} \delta_{ac}) \\ &= \sum_c (\langle ab || cj \rangle t_i^c - \langle ab || ci \rangle t_j^c) + \sum_k (\langle ij || bk \rangle t_k^a - \langle ij || ak \rangle t_k^b) \end{aligned} \quad [145]$$

As our third example, we consider the contribution of the one-electron component of the fourth term of Eq. [122] to the  $\hat{T}_1$  amplitude equation. The matrix element of interest in this case is

$$\frac{1}{2} \langle \Phi_i^\alpha | (\hat{F}_N \hat{T}_1^2)_c | \Phi_0 \rangle = \frac{1}{2} \sum_{pq} \sum_{jb} \sum_{kc} f_{pq} t_j^b t_k^c \langle \Phi_0 | \{a_i^\dagger a_a\} \{a_p^\dagger a_q\} \{a_b^\dagger a_j\} \{a_c^\dagger a_k\})_c | \Phi_0 \rangle$$

[146]

When applied to the operator strings in this expression, Wick's theorem gives only two nonzero contractions, in spite of the relatively large number of construction operators:

$$\begin{aligned} \langle \Phi_0 | \{a_i^\dagger a_a\} \{a_p^\dagger a_q\} \{a_b^\dagger a_j\} \{a_c^\dagger a_k\})_c | \Phi_0 \rangle &= \overbrace{\{a_i^\dagger a_a a_p^\dagger a_q a_b^\dagger a_j a_c^\dagger a_k\}} + \overbrace{\{a_i^\dagger a_a a_p^\dagger a_q a_b^\dagger a_j a_c^\dagger a_k\}} \\ &= -\delta_{pk} \delta_{qb} \delta_{ij} \delta_{ac} - \delta_{pj} \delta_{qc} \delta_{ik} \delta_{ac} \end{aligned}$$

[147]

When the Kronecker delta strings are inserted back into the matrix element expression, we obtain

$$\frac{1}{2} \langle \Phi_i^\alpha | (\hat{F}_N \hat{T}_1^2)_c | \Phi_0 \rangle = - \sum_{kc} f_{kc} t_i^c t_k^\alpha$$

[148]

Additional contractions such as

$$\overbrace{\{a_i^\dagger a_a a_p^\dagger a_q a_b^\dagger a_j a_c^\dagger a_k\}} \quad \text{and} \quad \overbrace{\{a_i^\dagger a_a a_p^\dagger a_q a_b^\dagger a_j a_c^\dagger a_k\}}$$

[149]

are not included even though they are nonzero because, as our earlier analysis of the commutators of the Hausdorff expansion indicated, the Hamiltonian fragment must be connected at least once to every cluster operator on the right. Similar analyses apply to other contributions such as  $(\hat{V}_N \hat{T}_2^2)_c$ ,  $(\hat{V}_N \hat{T}_1 \hat{T}_2)_c$ , and so on.

This last point also has interesting consequences for the higher excitation amplitude equations such as that for  $\hat{T}_3$ . For example, one term that arises in the general Hausdorff expansion is  $\frac{1}{5!} (\hat{V}_N \hat{T}_1^5)_c$ . This term does not contribute to the  $\hat{T}_3$  amplitude equation

$$0 = \frac{1}{5!} \langle \Phi_{ijk}^{abc} | (\hat{V}_N \hat{T}_1^5)_c | \Phi_0 \rangle$$

[150]

From a configuration interaction perspective, such a matrix element of the Hamiltonian between the quintuply excited determinant generated by the oper-

ator  $\hat{T}_1^5$  on the right and the triply excited determinant on the left is nonzero according to Slater's rules. However, because the two-electron fragment of the Hamiltonian cannot connect to more than four cluster operators on its right, such a matrix element cannot contribute to the amplitude equation by the connected cluster properties of the Hausdorff expansion. Similarly, the  $(\hat{F}_N \hat{T}_2)_c$  contribution to  $\hat{T}_3$  is also zero because any connection between  $\hat{F}_N$  and  $\hat{T}_2$  does not leave enough construction operator pairs to completely connect to the triply excited determinant on the left.

The final example of this section is the contribution of the  $\frac{1}{2}(\hat{V}_N \hat{T}_1^2 \hat{T}_2)_c$  term of Eq. [122] to the  $\hat{T}_2$  amplitude equation. The matrix elements of interest in this case involve only the two-electron component of  $\hat{H}_N$ , because the one-electron component cannot connect to more than two cluster operators:

$$\begin{aligned} \frac{1}{2} \langle \Phi_{ij}^{ab} | (\hat{V}_N \hat{T}_1^2 \hat{T}_2)_c | \Phi_0 \rangle = & \frac{1}{32} \sum_{pqrs} \sum_{kc} \sum_{ld} \sum_{mnef} \langle pq || rs \rangle t_k^c t_l^d t_{mn}^{ef} \\ & \times \langle \Phi_0 | \{a_i^\dagger a_j^\dagger a_b a_a\} \{a_p^\dagger a_q^\dagger a_s a_r\} \{a_c^\dagger a_k\} \{a_d^\dagger a_l\} \{a_e^\dagger a_f^\dagger a_n a_m\} \}_c | \Phi_0 \rangle \end{aligned} \quad [151]$$

The factor of  $\frac{1}{32}$  appearing here arises as the product of the factor of  $\frac{1}{2}$  from the Hausdorff expansion and the two factors of  $\frac{1}{4}$  from the definitions of  $\hat{V}_N$  (Eq. [104]) and  $\hat{T}_2$  (Eq. [130]). To derive from this matrix element an expression involving only two-electron integrals and cluster amplitudes, we must apply Wick's theorem to the string of 16 annihilation and creation operators above. Although this might be a useful exercise for those readers who wish to test their own stamina and patience, we will avoid it here. We note that this task is tedious at best and recognize that Wick's theorem has not eliminated all the opportunities for error when one is dealing with complicated second-quantized equations.

Once all the contributions of Eq. [122] to Eqs. [135] and [136] have been determined in the manner described above, they are summed to give the amplitude equations. For  $\hat{T}_1$ , the resulting equation is

$$\begin{aligned} 0 = & f_{ai} + \sum_c f_{ac} t_i^c - \sum_k f_{ki} t_k^a + \sum_{kc} \langle ka || ci \rangle t_k^c + \sum_{kc} f_{kc} t_{ik}^{ac} + \frac{1}{2} \sum_{kcd} \langle ka || cd \rangle t_{ki}^{cd} \\ & - \frac{1}{2} \sum_{klc} \langle kl || ci \rangle t_{kl}^{ca} - \sum_{kc} f_{kc} t_i^c t_k^a - \sum_{klc} \langle kl || ci \rangle t_k^c t_l^a - \sum_{kcd} \langle ka || cd \rangle t_k^c t_i^d \\ & - \sum_{klcd} \langle kl || cd \rangle t_k^c t_i^d t_l^a + \sum_{klcd} \langle kl || cd \rangle t_k^c t_l^d - \frac{1}{2} \sum_{klcd} \langle kl || cd \rangle t_{ki}^{cd} t_l^a - \frac{1}{2} \sum_{klcd} \langle kl || cd \rangle t_{kl}^{cad} t_i^d \end{aligned} \quad [152]$$

whereas for  $\hat{T}_2$ , the resulting equation is

$$\begin{aligned}
0 = & \langle ab||ij\rangle + \sum_c (f_{bc} t_{ij}^{ac} - f_{ac} t_{ij}^{bc}) - \sum_k (f_{ki} t_{ik}^{ab} - f_{ki} t_{jk}^{ab}) + \frac{1}{2} \sum_{kl} \langle kl||ij\rangle t_{kl}^{ab} \\
& + \frac{1}{2} \sum_{cd} \langle ab||cd\rangle t_{ij}^{cd} + P(ij)P(ab) \sum_{kc} \langle kb||cj\rangle t_{ik}^{ac} + P(ij) \sum_c \langle ab||cj\rangle t_i^c \\
& - P(ab) \sum_k \langle kb||ij\rangle t_k^a + \frac{1}{2} P(ij)P(ab) \sum_{klcd} \langle kl||cd\rangle t_{ik}^{act} t_{lj}^{db} + \frac{1}{4} \sum_{klcd} \langle kl||cd\rangle t_{ij}^{ecd} t_{kl}^{ab} \\
& - P(ab) \frac{1}{2} \sum_{klcd} \langle kl||cd\rangle t_{ij}^{act} t_{kl}^{bd} - P(ij) \frac{1}{2} \sum_{klcd} \langle kl||cd\rangle t_{ik}^{ab} t_{jl}^{cd} + P(ab) \frac{1}{2} \sum_{kl} \langle kl||ij\rangle t_k^a t_l^b \\
& + P(ij) \frac{1}{2} \sum_{cd} \langle ab||cd\rangle t_i^c t_j^d - P(ij)P(ab) \sum_{kc} \langle kb||ic\rangle t_k^a t_j^c + P(ab) \sum_{kc} f_{kc} t_k^c t_{ij}^{bc} \\
& + P(ij) \sum_{kc} f_{kc} t_i^c t_{jk}^{ab} - P(ij) \sum_{klc} \langle kl||ci\rangle t_k^c t_{ij}^{ab} + P(ab) \sum_{kcd} \langle ka||cd\rangle t_k^c t_{ij}^{db} \\
& + P(ij)P(ab) \sum_{kcd} \langle ak||dc\rangle t_i^d t_{jk}^{bc} + P(ij)P(ab) \sum_{klc} \langle kl||ic\rangle t_l^a t_{jk}^{bc} \\
& + P(ij) \frac{1}{2} \sum_{klc} \langle kl||cj\rangle t_i^c t_{kl}^{ab} - P(ab) \frac{1}{2} \sum_{kcd} \langle kb||cd\rangle t_k^a t_{ij}^{cd} \\
& - P(ij)P(ab) \frac{1}{2} \sum_{kcd} \langle kb||cd\rangle t_i^c t_k^a t_j^d + P(ij)P(ab) \frac{1}{2} \sum_{klc} \langle kl||cj\rangle t_i^c t_k^a t_l^b \\
& - P(ij) \sum_{klcd} \langle kl||cd\rangle t_k^c t_i^d t_{lj}^{ab} - P(ab) \sum_{klcd} \langle kl||cd\rangle t_k^c t_l^a t_{ij}^{db} + P(ij) \frac{1}{4} \sum_{klcd} \langle kl||cd\rangle t_i^c t_j^d t_{kl}^{ab} \\
& + P(ab) \frac{1}{4} \sum_{klcd} \langle kl||cd\rangle t_k^a t_l^b t_{ij}^{cd} + P(ij)P(ab) \sum_{klcd} \langle kl||cd\rangle t_i^c t_l^b t_{kj}^{ad} \\
& + P(ij)P(ab) \frac{1}{4} \sum_{klcd} \langle kl||cd\rangle t_i^c t_k^a t_j^d t_l^b
\end{aligned} \tag{153}$$

The notation  $P(pq)$  indicates a permutation operator whose action on a given function is defined by

$$P(pq)f(p, q) = f(p, q) - f(q, p) \tag{154}$$

For example, from the  $\hat{T}_2$  equation above, one of the terms becomes

$$P(ij) \sum_{kc} f_{kc} t_i^c t_{jk}^{ab} = \sum_{kc} (f_{kc} t_i^c t_{jk}^{ab} - f_{kc} t_j^c t_{ik}^{ab}) \tag{155}$$

Relative to direct application of the anticommutation relations for annihilation and creation operators, Wick's theorem helps to dramatically reduce the tedium involved in deriving the rather complicated amplitude equations above. However, as illustrated by Eq. [151], Wick's theorem still does not go far enough. Even if the cluster operator is truncated to include only double excitations, the resulting algebra provides many opportunities for error. When even

higher excitations are desired, the number of algebraic manipulations required by Wick's theorem becomes rapidly insurmountable. A number of computer algorithms for the derivation of coupled-cluster-related equations have been described in the literature,<sup>33,36,118</sup> but these have thus far been difficult to apply in a general fashion. Diagrammatic techniques offer a more practical approach to the construction of complicated coupled cluster equations. They provide a simple bookkeeping system for the numerous terms generated by Wick's theorem (most of which are redundant) and allow us to identify in advance which terms will not contribute to the wavefunction and/or the energy. In the next section we will outline one diagrammatic approach that is particularly convenient for deriving a variety of coupled-cluster-like equations, including ground state energies, energy derivatives, and EOM-CC equations.

## An Introduction to Coupled Cluster Diagrams

In this section, we present a simple diagrammatic formalism popularized by Kucharski and Bartlett<sup>20</sup> by which one may construct the coupled cluster energy and amplitude equations far more quickly than by direct application of Wick's theorem.<sup>o</sup> We begin by describing some of the general features of the diagrams, including their relationship to the particle–hole formalism and how they may be used to represent normal-ordered dynamical operators. Next we describe how the operator diagrams may be connected together to form operator products in a manner analogous to Wick's theorem. We then construct the diagrammatic form of the CCSD energy and amplitude equations, and, as each new diagram is presented, we provide rules for its algebraic interpretation. The diagrams described here may be used to represent either wavefunctions, operators, or matrix elements, depending on the context of the mathematical analysis. However, the set of rules we present for interpreting the diagrams algebraically apply only to the matrix element representation, because that is the most appropriate context for the coupled cluster energy and amplitude equations.<sup>o</sup>

We make use of the particle–hole formalism in diagrammatic analyses by drawing upward- and downward-directed lines that identify those orbitals which differ from those in the reference determinant,  $\Phi_0$ , as shown in Figure 1.

---

<sup>o</sup>Many varieties of diagrams have used throughout the chemical physics literature for many years (e.g., see Refs. 1, 2, 80, 117, and 119). The diagrammatic formalism we have chosen here has been frequently used in work by the Bartlett group among others<sup>120</sup> and is particularly straightforward for “conventional” coupled cluster and many-body perturbation theories.

<sup>o</sup>The algebraic rules for interpreting the diagrams as operators or wavefunctions differ only slightly from the matrix element approach discussed here. We recommend Refs. 80 and 88 for additional information.

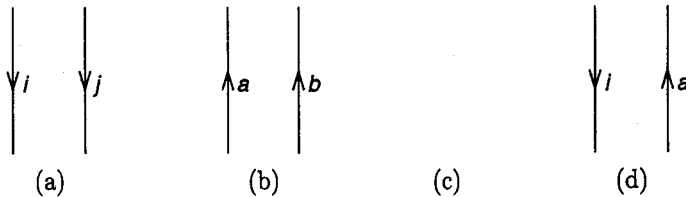


**Figure 1** Some basic components of coupled cluster diagrams: (a) hole lines; (b) particle lines; (c) the reference wavefunction,  $\Phi_0$ , represented by empty space; and (d) a single-determinant wavefunction,  $\Phi^1$  which differs from the reference by a single excitation.

Downward-directed lines represent hole states (orbitals occupied in the reference) and upward directed lines represent particle states (orbitals unoccupied in the reference). Hence, one may interpret Figure 1(d) as a single-determinant wavefunction that differs from the reference by a single excitation from orbital  $\phi_i$  to orbital  $\phi_a$ . Furthermore, this convention implies that the reference wavefunction itself is represented by empty space, as indicated in Figure 1(c).

Diagrams representing dynamical operators (such as the one- and two-electron components of the normal-ordered Hamiltonian,  $\hat{H}_N$ ) are depicted by horizontal “interaction lines,” with vertical-directed lines like those in Figure 1 representing the annihilation and creation operator strings. We will choose different interaction lines to represent different types of operator, e.g., a dashed line to indicate components of the electronic Hamiltonian, a solid line for cluster operators,  $\hat{T}_1$ ,  $\hat{T}_2$ , etc. The directed lines emanate from “vertices” on the interaction line; each vertex represents the action of the operator on individual electrons. Thus, one-electron diagrams have one vertex, two-electron diagrams have two vertices, and so on. Attached to each vertex are two directed lines, one incoming and one outgoing, which are associated with the annihilation and creation operators of the operator’s normal-ordered string. Since one-electron operators contain two second-quantized components (see, e.g., Eq. [53]), their diagrammatic representations contain two directed lines. Similarly, diagrams representing two-electron operators contain four directed lines, three-electron operators contain six directed lines, and so on. The upward and downward directions of these lines are dependent on the orbital subspaces in which the second-quantized operators act:  $q$ -creation operators lie above the interaction line, whereas  $q$ -annihilation lines lie below the interaction line.<sup>p</sup>

For example, we denote the one-electron component of the Hamiltonian,  $\hat{F}_N$ , by a dashed interaction line capped by an “X.” This operator may be

---

<sup>p</sup>For an explanation of  $q$ -creation and  $q$ -annihilation operators, see the earlier discussion of the particle-hole formalism in the section on The Fermi Vacuum and Particle-Hole Formalism.

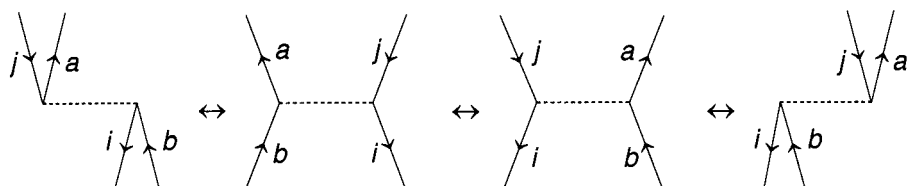
$$\hat{F}_N = \sum_{ab} f_{ab} \{a_a^\dagger a_b\} + \sum_{ij} f_{ij} \{a_i^\dagger a_j\} + \sum_{ia} f_{ia} \{a_i^\dagger a_a\} + \sum_{ia} f_{ai} \{a_a^\dagger a_i\}$$

$$= \begin{array}{c} \text{Diagram 1: } \text{Two vertical lines meeting at a dashed horizontal line labeled 'X'.} \\ 0 \end{array} + \begin{array}{c} \text{Diagram 2: } \text{Two vertical lines meeting at a dashed horizontal line labeled 'X'.} \\ 0 \end{array} + \begin{array}{c} \text{Diagram 3: } \text{Two vertical lines meeting at a dashed horizontal line labeled 'X'.} \\ -1 \end{array} + \begin{array}{c} \text{Diagram 4: } \text{Two vertical lines meeting at a dashed horizontal line labeled 'X'.} \\ +1 \end{array}$$

Figure 2 Diagrammatic representation of each fragment of the one-particle component of the Hamiltonian operator  $\hat{F}_N$ . The excitation level of each diagram is indicated beneath it. The interaction line is indicated by the dashed horizontal line capped by the "X".

written in four fragments as shown in Figure 2. The first fragment, which involves only operators in the particle (unoccupied) space, has one  $q$ -creation line above the interaction line corresponding to the  $a_a^\dagger$  component of its operator string, and one  $q$ -annihilation line below the interaction line corresponding to the  $a_b$  component. Similarly, the second fragment in the figure, which involves only operators in the hole (occupied) space, has one  $q$ -creation line above the interaction line corresponding to the  $a_i^\dagger$  component of the operator string, and one  $q$ -annihilation line below the interaction line corresponding to the  $a_j$  component. The third  $\hat{F}_N$  fragment contains only  $q$ -annihilation lines below the interaction line since the operator string consists of  $a_i^\dagger$  and  $a_a$  components only. Finally, the fourth fragment contains only  $q$ -creation lines above the interaction line representing the  $a_a^\dagger$  and  $a_i^\dagger$  components of the operator string.

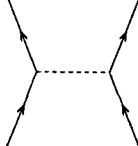
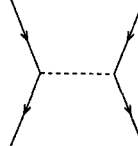
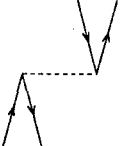
The two-electron fragment of the Hamiltonian may be partitioned in a similar manner as shown in Figure 3, with a dashed horizontal interaction line and with implicit antisymmetry with respect to permutation of the lines leaving or entering the left and right vertices. For example, in the third diagram, corresponding to a sum over the operator components,  $\langle i a || b j \rangle \{a_i^\dagger a_a^\dagger a_j a_b\}$ , the diagram as shown may be written in four equivalent ways (differing only by a sign), each formed by permuting either the two outgoing lines or the two incoming lines from the left and right vertices:



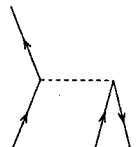
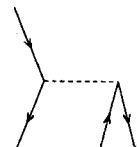
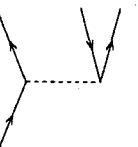
$$\hat{V}_N = \frac{1}{4} \sum_{abcd} \langle ab||cd \rangle \{a_a^\dagger a_b^\dagger a_d a_c\} + \frac{1}{4} \sum_{ijkl} \langle ij||kl \rangle \{a_i^\dagger a_j^\dagger a_l a_k\} + \sum_{iabj} \langle ia||bj \rangle \{a_i^\dagger a_a^\dagger a_j a_b\}$$

$$+ \frac{1}{2} \sum_{aibc} \langle ai||bc \rangle \{a_a^\dagger a_i^\dagger a_c a_b\} + \frac{1}{2} \sum_{ijka} \langle ij||ka \rangle \{a_i^\dagger a_j^\dagger a_a a_k\} + \frac{1}{2} \sum_{abci} \langle ab||ci \rangle \{a_a^\dagger a_b^\dagger a_i a_c\}$$

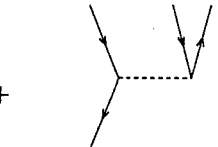
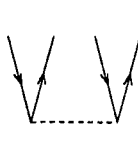
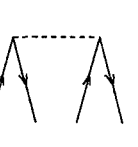
$$+ \frac{1}{2} \sum_{iajk} \langle ia||jk \rangle \{a_i^\dagger a_a^\dagger a_k a_j\} + \frac{1}{4} \sum_{abij} \langle ab||ij \rangle \{a_a^\dagger a_b^\dagger a_j a_i\} + \frac{1}{4} \sum_{ijab} \langle ij||ab \rangle \{a_i^\dagger a_j^\dagger a_b a_a\}$$

=  +  + 

0                    0                    0

+  +  + 

-1                    -1                    +1

+  +  + 

+1                    +2                    -2

**Figure 3** Diagrammatic representation of each fragment of the two-particle component of the Hamiltonian operator  $\hat{V}_N$ . The excitation level of each diagram is indicated beneath it. The interaction line is indicated by the dashed horizontal line.

Diagrammatic representations of the cluster operators,  $\hat{T}$ , are shown in Figure 4, with solid horizontal interaction lines. Since the cluster operators contain only  $q$ -creation strings (and thereby generate excited determinants from the reference wavefunction), they contain no lines below the horizontal bar. Furthermore, these representations are also fully antisymmetric in that exchange of any pair of outgoing or incoming lines introduces a change in the

$$\hat{T}_1 = \sum_{ia} t_i^a \{a_a^\dagger a_i\} = \begin{array}{c} \diagdown \quad \diagup \\ \text{V} \end{array} +1$$
  

$$\hat{T}_2 = \frac{1}{4} \sum_{ijab} t_{ij}^{ab} \{a_a^\dagger a_b^\dagger a_j a_i\} = \begin{array}{c} \diagdown \quad \diagup \quad \diagdown \quad \diagup \\ \text{V} \quad \text{V} \end{array} +2$$
  

$$\hat{T}_3 = \frac{1}{36} \sum_{ijkabc} t_{ijk}^{abc} \{a_a^\dagger a_b^\dagger a_c^\dagger a_k a_j a_i\} = \begin{array}{c} \diagdown \quad \diagup \quad \diagdown \quad \diagup \quad \diagdown \quad \diagup \\ \text{V} \quad \text{V} \quad \text{V} \quad \text{V} \end{array} +3$$

**Figure 4** Diagrammatic representation of the  $\hat{T}_1$ ,  $\hat{T}_2$ , and  $\hat{T}_3$  excitation operators. The excitation level of each diagram is indicated to its right. The interaction line is indicated by a solid horizontal bar.

sign of the diagram. We will discuss this point in greater detail later when we introduce rules for interpreting the diagrams algebraically.

Other than the operator representation above, we will interpret the diagrams in this chapter from bottom to top as matrix elements of operators (or operator products) between determinants. For the coupled cluster energy and amplitude equations shown in Eqs. [50] and [51], the pertinent matrix elements always contain the reference determinant,  $\Phi_0$ , on the right and either  $\Phi_0$  or excited determinants such as  $\Phi_i^{ab}$  on the left. Diagrams are particularly convenient for constructing such matrix elements because they provide a straightforward method for evaluating the types of determinants to which individual operator fragments in Figures 2–4 may be applied or what determinants they produce. As an example, consider the fourth  $\hat{F}_N$  fragment in Figure 2, which contains no lines below and two lines above the horizontal operator line. Since the reference wavefunction,  $\Phi_0$ , is represented by empty space, and a singly excited determinant,  $\Phi_i^a$ , by a pair of directed lines such as those in Figure 1(d), we may interpret the diagram from bottom to top to obtain the matrix element

$$\langle \Phi_i^a | \hat{F}_N | \Phi_0 \rangle = i \begin{array}{c} \diagdown \quad \diagup \\ \text{V} \end{array} a \quad [156]$$

A similar analysis may be applied to the two-electron operator in the third diagram in Figure 3, which contains particle–hole pairs of lines both above and

below the interaction line. Each of these pairs may be interpreted as singly excited determinants to obtain the general matrix element

$$\langle \Phi_i^a | \hat{V}_N | \Phi_j^b \rangle = \begin{array}{c} i \swarrow \searrow a \\ \cdots \cdots \cdots \\ j \swarrow \searrow b \end{array} [157]$$

The cluster operator diagrams are particularly simple to interpret as matrix elements; the diagrams always involve the reference determinant on the right (because they contain no lines below the interaction line) and an excited determinant on the left, for example,

$$\langle \Phi_{ij}^{ab} | \hat{T}_2 | \Phi_0 \rangle = \begin{array}{c} i \swarrow \searrow a \quad j \swarrow \searrow b \\ \cdots \cdots \cdots \end{array} [158]$$

We also make use of a simple bookkeeping system<sup>20</sup> that indicates the “excitation level” produced by a particular operator fragment. This value is determined by subtracting the number of  $q$ -annihilation lines from the number of  $q$ -creation lines and dividing the result by 2. For example, the first and second one-electron Hamiltonian fragments shown in Figure 2 are assigned an excitation level of +1, since both the wavefunction to which they are applied (at the bottom of the diagram) and the wavefunction they produce (at the top of the diagram) differ from the reference by a single orbital; no net excitation is produced. The fourth one-electron fragment, however, has an excitation level of +1 since it effectively produces a single excitation from the reference wavefunction. Two-electron Hamiltonian fragments have excitation levels ranging from +2 to -2, as indicated in Figure 3, and the  $\hat{T}$  operators have the obvious excitation levels indicated in Figure 4.

### Diagrammatic Representation of the CCSD Energy Equation

As discussed in detail earlier, products of normal-ordered operators can be simplified algebraically using Wick’s theorem by evaluating pairs of contractions between the component annihilation and creation operators. Many of these contractions produce mathematically redundant terms that can be combined after complicated manipulation to eventually produce a much simpler expression. Diagrams provide a straightforward scheme by which these redundancies may be eliminated.

As an example, consider the CCSD energy equation derived earlier in Eq. [134] using Wick’s theorem. Each term of the general expression

$$E_{\text{CCSD}} - E_0 = \langle \Phi_0 | \hat{H}_N + \left( \hat{H}_N \hat{T}_1 + \hat{H}_N \hat{T}_2 + \frac{1}{2} \hat{H}_N \hat{T}_1^2 + \dots \right)_c | \Phi_0 \rangle \quad [159]$$

is a matrix element of a component of  $e^{-\hat{T}} \hat{H}_N e^{\hat{T}}$  involving the reference determinant,  $\Phi_0$ , on both the right and left. Since  $\Phi_0$  is depicted diagrammatically by empty space, the diagrams associated with the energy equation must contain no directed lines that extend above or below the first (lowest) or last (highest) operator interaction lines; that is, the energy diagrams can contain no “external” lines. Clearly none of the diagrams representing fragments of  $\hat{H}_N$  shown in Figures 2 and 3 satisfy this criterion, and they therefore do not contribute to the CCSD energy. This is the expected result because all these diagrams represent normal-ordered operators whose reference expectation value is zero, by construction.

Next we consider the term from Eq. [159] that is linear in  $\hat{T}_1$

$$E_{\text{CCSD}} \leftarrow \langle \Phi_0 | (\hat{H}_N \hat{T}_1)_c | \Phi_0 \rangle \quad [160]$$

which we examined earlier to obtain Eq. [126]. (The left arrow indicates that this is only one of several terms that contribute to the energy on the left-hand side.) The rightmost operator in this matrix element is  $\hat{T}_1$ , so its interaction line must lie at the bottom of the final diagram. Making use of the excitation levels associated with the operator diagrams described above, we note that the  $\hat{T}_1$  diagram produces an excitation level of +1 from the reference determinant. Since the matrix element of interest must contain  $\Phi_0$  on the left, the total excitation level of the final diagram must be 0. Therefore, we require the Hamiltonian diagrams that have an excitation level of -1 and contain the reference determinant at the top of the diagram. Of the  $\hat{F}_N$  and  $\hat{V}_N$  diagrams given above, only the third diagram of Figure 2 meets these criteria. We may then connect the  $\hat{T}_1$  diagram with this  $\hat{F}_N$  fragment to obtain

$$\langle \Phi_0 | (\hat{F}_N \hat{T}_1)_c | \Phi_0 \rangle = \text{Diagram} \quad [161]$$

Note that to avoid external lines, both lines from the  $\hat{T}_1$  diagram must connect to each line from the  $\hat{F}_N$  fragment. The diagram may be interpreted algebraically using the following rules:

- Label all directed lines with appropriate indices. By the convention we have used so far, hole lines would be labeled with  $i, j, k, l, \dots$  and particle lines with  $a, b, c, d, \dots$ . Therefore, for the diagram above we label the

hole line with  $i$  and the particle line with  $a$  to obtain



- Each operator interaction line contributes an integral or amplitude to the matrix element expression. Fock matrix elements are constructed from the diagram by the rule  $\langle \text{out} | \hat{T} | \text{in} \rangle$ , where **out** indicates the index of the outgoing directed line and **in** indicates the index of the incoming directed line at the interaction line's vertex.  $\hat{T}$  operators contribute amplitudes to the expression, constructed using the hole and particle indices in their left-to-right order in the diagram. In this case, the Fock matrix element is  $f_{ia}$  and the amplitude is  $t_i^a$ .
- Summations are included over all “internal” indices—that is, all indices associated with lines that begin and end at operator interaction lines and do not extend to infinity above or below the diagram like the external lines described above. Thus, the present diagram requires a summation over indices  $i$  and  $a$ .
- The sign of the diagram is determined based on the formula  $(-1)^{h+l}$ , where  $h$  is the number of hole lines in the diagram and  $l$  is the number of “loops.” A loop is a route along a series of directed lines that either returns to its beginning or begins at one external line and ends at another. In this case, we have only one hole line ( $i$ ) and one loop, so the sign on the diagram is positive.

According to these rules, the final algebraic interpretation of the diagram above is therefore



$$= \sum_{ia} f_{ia} t_i^a \quad [162]$$

which is identical to Eq. [126] obtained earlier using Wick’s theorem.

Now consider the next term of Eq. [159] which is linear in  $\hat{T}_2$ ,

$$E_{\text{CCSD}} \leftarrow \langle \Phi_0 | (\hat{H}_N \hat{T}_2)_c | \Phi_0 \rangle \quad [163]$$

which we examined earlier in Eq. [132]. Again the cluster operator must lie at the bottom of the final diagram because it is the rightmost operator in the matrix element. Since  $\hat{T}_2$  produces an excitation level of +2 (see Figure 4), we require Hamiltonian diagrams that have an excitation level of -2 (to obtain a total excitation level of 0) and contain the reference wavefunction above the Hamiltonian interaction line. The only  $\hat{H}_N$  diagram that meets these criteria is

the last diagram of Figure 3,  , which contains four  $q$ -annihilation lines.

Connecting this diagram with that of  $\hat{T}_2$  such that there are no external lines gives

$$\langle \Phi_0 | (\hat{V}_N \hat{T}_2)_c | \Phi_0 \rangle = \text{Diagram} [164]$$

To construct the algebraic interpretation of this diagram, we first assign labels

to the hole and particle lines as before, to obtain By the rules

described above, there are four internal lines and thus four summation indices. In addition, there are two loops in this diagram (one involving the  $i$  and  $a$  lines and the other involving the  $j$  and  $b$  lines) and two hole lines, giving an overall + sign. For the remainder of the algebraic expression, we require two rules in addition to those described above:

- The  $\hat{V}_N$  fragment contributes the two-electron integral,  $\langle ij || ab \rangle$ , which is constructed by the rule `left-out, right-out||left-in, right-in`, where **left-out** and **right-out** indicate the left and right outgoing lines from the  $\hat{V}_N$  diagram vertex, respectively, and **left-in** and **right-in** indicate the left and right incoming lines, respectively. The contribution of the  $\hat{T}_2$  operator to the expression is obtained by taking the hole and particle indices from the  $\hat{T}_2$  vertex in their left-to-right ordering in the diagram. For this diagram,  $\hat{V}_N$  contributes the integral  $\langle ij || ab \rangle$  and  $\hat{T}_2$  contributes the amplitude  $t_{ij}^{ab}$ .
- This diagram contains two pairs of “equivalent” lines—that is, lines beginning at the same operator interaction line and ending at the same interaction line. For each such pair, a prefactor of  $\frac{1}{2}$  is multiplied onto the algebraic expression.<sup>9</sup>

The final algebraic interpretation of this diagram is therefore

$$\text{Diagram} = \frac{1}{4} \sum_{ijab} \langle ij || ab \rangle t_{ij}^{ab} [165]$$

We could have used a connectivity for the  $\hat{V}_N$  and  $\hat{T}_2$  diagram fragments somewhat different from the one shown above. For example, we could also have chosen instead to build this diagram as

$$\langle \Phi_0 | (\hat{V}_N \hat{T}_2)_c | \Phi_0 \rangle = \text{Diagram} [166]$$

---

<sup>9</sup>It is possible for groups of three or more lines to be identified as equivalent, though this can happen only in many-body perturbation theory, expectation value coupled cluster theory, or unitary coupled cluster theory. For such diagrams, a prefactor of  $\frac{1}{n!}$ , where  $n$  is the number of electron lines, must be included.

However, recall that the  $\hat{V}_N$  and  $\hat{T}_2$  operator diagrams from Figures 3 and 4 are antisymmetric with respect to permutation of either the pair of outgoing lines or the pair of incoming lines at the two vertices. Hence, we have the relations,

$$\begin{array}{cccccc} \text{Diagram 1} & \text{Diagram 2} & \text{Diagram 3} & \text{Diagram 4} & \text{Diagram 5} & \text{Diagram 6} \\ \text{Diagram 1} = -\text{Diagram 2} & & & & & \\ \text{Diagram 3} = -\text{Diagram 4} & & & & & \\ \text{Diagram 5} = -\text{Diagram 6} & & & & & \end{array} \quad [167]$$

Therefore, the two energy diagrams are equivalent, because the two hole lines and the two particle lines from the  $\hat{T}_2$  diagram both connect to the same  $\hat{V}_N$  diagram fragment:

$$\text{Two separate loops} = \text{Single loop with a cross inside} \quad [168]$$

The equivalence of the two diagrams can also be seen through their algebraic interpretations, which we obtain by applying the same rules given above to the new diagram from Eq. [166]. Again, we label the hole and particle lines using

the indices  $i, j, a$ , and  $b$ , to obtain . In this case, the algebraic

analysis is identical to that given for the diagram of Eq. [164], with two exceptions: (1) the two-electron integral contributed by the  $\hat{V}_N$  fragment is  $\langle ij||ba\rangle$  rather than  $\langle ij||ab\rangle$  because its two incoming particle lines have been reversed; and (2) although there are still two hole lines, there is now only one loop, which involves all four directed lines, giving rise to a negative sign for the diagram. Hence, the algebraic interpretation of the diagram is

$$\text{Loop with a cross inside} = -\frac{1}{4} \sum_{ijab} \langle ij||ba\rangle t_{ij}^{ab} = +\frac{1}{4} \sum_{ijab} \langle ij||ab\rangle t_{ij}^{ab} = \text{Two separate loops} \quad [169]$$

where we have used the antisymmetry of the Dirac notation two-electron integrals to make the equivalence of the two diagrams clearer.

Next consider the component of Eq. [159] which is quadratic in  $\hat{T}_1$ ,

$$E_{CCSD} \leftarrow \frac{1}{2} \langle \Phi_0 | (\hat{H}_N \hat{T}_1^2)_c | \Phi_0 \rangle \quad [170]$$

Since the two cluster operators act on the reference determinant to produce a total excitation level of +2, we require the same Hamiltonian –2 diagram fragment used in Eq. [164]. Also, because the cluster operators act before the Hamiltonian operator in the matrix element, they are placed at the bottom of the diagram. Furthermore, because the  $\hat{T}_1$  operators commute, their vertical

ordering in the diagram is not important. The complete diagram is formed by connecting the  $\hat{V}_N$  vertex to both of the  $\hat{T}_1$  diagrams to give

$$\frac{1}{2} \langle \Phi_0 | (\hat{V}_N \hat{T}_1^2)_c | \Phi_0 \rangle = \text{Diagram} [171]$$

For this diagram, the algebraic analysis is quite similar to that used to obtain Eq. [165]. There are two hole lines, and two particle lines, all of which are summation indices. Since there are two loops, the total sign on the diagram is positive. The two-electron integral provided by the  $\hat{V}_N$  fragment is again  $\langle ij || ab \rangle$ , but there are now two  $\hat{T}_1$  amplitude fragments, one contributing  $t_i^a$  and the other  $t_j^b$ . Note also that the two pairs of hole lines and particle lines are no longer equivalent as they were in Eq. [165]. We require only one additional rule to evaluate this diagram:

Unlike the diagram in Eq. [165], this diagram contains a pair of “equivalent” vertices; since both  $\hat{T}_1$  fragments are connected to the same  $\hat{V}_N$  interaction line in exactly the same manner (each by a hole line and a particle line), a prefactor of  $\frac{1}{2}$  is multiplied into the final expression. Generally speaking, if there are  $n$  equivalent vertices in the diagram, they contribute a prefactor of  $1/n!$  to the final expression.

Thus, the final algebraic expression for this diagram is

$$\text{Diagram} = \frac{1}{2} \sum_{ijab} \langle ij || ab \rangle t_i^a t_j^b [172]$$

The diagrammatic analysis also makes it clearer that no higher order contributions to the Hausdorff expansion in Eq. [159] can contribute to the coupled cluster energy. All remaining terms contain cluster operator products that produce excitation levels higher than +2. However, there are no Hamiltonian operator diagrams that can decrease this excitation level by more than -2. Therefore, there can be no higher-order contributions to the coupled cluster energy equation, which must have a total excitation level of 0.

Summing diagrammatic Eqs. [162], [165], and [172], we obtain the final energy equation

$$E_{CCSD} - E_0 = \text{Diagram} + \text{Diagram} + \text{Diagram} [173]$$

$$= \sum_{ia} f_{ia} t_i^a + \frac{1}{4} \sum_{ijab} \langle ij || ab \rangle t_{ij}^{ab} + \frac{1}{2} \sum_{ijab} \langle ij || ab \rangle t_i^a t_j^b$$

which is identical to that derived earlier using Wick’s theorem.

## Diagrammatic Representation of the CCSD Amplitude Equations

The same diagrammatic concepts used to derive the CCSD energy equation (Eq. [173]) may also be applied to the CCSD  $\hat{T}_1$  and  $\hat{T}_2$  amplitude equations, with a few additional rules. Here we consider the contribution of each term of  $\bar{H}$  given in Eq. [122] to the amplitude equations in the same order as we did using Wick's theorem before. The resulting matrix elements always contain the reference determinant,  $\Phi_0$ , on the right and an excited determinant on the left (e.g.,  $\Phi_i^a$  for the  $\hat{T}_1$  equation and  $\Phi_{ij}^{ab}$  for the  $\hat{T}_2$  equation). The corresponding diagrams always have the same general structure: no  $q$ -annihilation lines below the diagram and a certain number of  $q$ -creation lines extending above. For example, diagrams contributing to the  $\hat{T}_1$  amplitude equation contain exactly two  $q$ -creation lines above (and therefore a total excitation level of +1), and diagrams contributing to the  $\hat{T}_2$  amplitude equation contain four  $q$ -creation lines above (and a total excitation level of +2).

The leading term of  $\bar{H}$  is just the electronic Hamiltonian itself. For its contribution to the  $\hat{T}_1$  amplitude equation, we must evaluate the matrix elements,  $\langle \Phi_i^a | (\hat{F}_N + \hat{V}_N) | \Phi_0 \rangle$ , as before. Since these elements contain the reference determinant on the right and a singly excited determinant on the left, we require those +1 Hamiltonian diagrams that contain no lines below the interaction line and a single pair of lines above it. The only diagram from Figures 2 and 3 that meets this criterion is the fourth fragment of the one-electron operator,  $\hat{F}_N$ . Hence, there is no contribution from  $\hat{V}_N$  in this case, and the matrix element is represented diagrammatically as

$$\langle \Phi_i^a | \hat{F}_N | \Phi_0 \rangle = \begin{array}{c} \diagup \quad \diagdown \\ i \quad a \\ \diagup \quad \diagdown \\ \dots \end{array} X \quad [174]$$

The algebraic interpretation of this diagram is straightforward: (1) we label the two lines using indices  $i$  and  $a$  to maintain consistency with the singly excited determinant,  $\Phi_i^a$ , used in the matrix element itself; (2) there are no internal lines and therefore no summation indices; (3) the  $\hat{F}_N$  fragment contributes the Fock matrix element,  $f_{ai}$ ; and (4) there is only one loop (which starts at one external line and ends at another) and one hole line, giving a positive sign. Thus, the final expression is simply

$$\begin{array}{c} \diagup \quad \diagdown \\ i \quad a \\ \diagup \quad \diagdown \\ \dots \end{array} = f_{ai} \quad [175]$$

which we derived earlier in Eq. [139] using Wick's theorem.

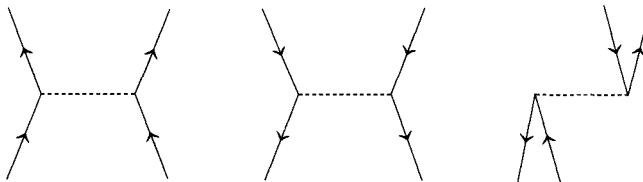
For the contribution of  $\hat{H}_N$  to the  $\hat{T}_2$  amplitude equation, we must evaluate the matrix element,  $\langle \Phi_{ij}^{ab} | (\hat{F}_N + \hat{T}_N) | \Phi_0 \rangle$ , which contains the reference deter-

minant on the right and a doubly excited determinant on the left. Therefore, we require the  $\hat{H}_N$  diagrams that produce a +2 excitation and have no  $q$ -annihilation lines. Only the eighth diagram of Figure 3,  , meets this criterion. Its algebraic interpretation is carried out as follows: (1) we label the lines (in order) as  $i$ ,  $a$ ,  $j$ , and  $b$ , for consistency with the doubly excited determinant in the matrix element; (2) there are no internal lines and therefore no summation indices; (3) the two-electron integral contributed by the  $\hat{V}_N$  interaction line is  $\langle ab||ij\rangle$ ; and (4) there are two hole lines and two loops, giving a positive sign. Therefore, this matrix element may be written as

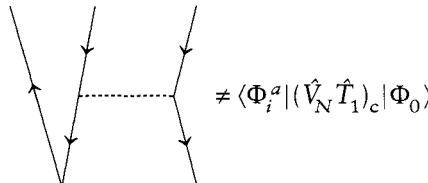
$$\langle \Phi_{ij}^{ab} | \hat{V}_N | \Phi_0 \rangle = i \begin{array}{c} \diagdown \\ \diagup \end{array} a \quad j \begin{array}{c} \diagup \\ \diagdown \end{array} b = \langle ab || ij \rangle \quad [176]$$

which is the same as that derived earlier in Eq. [141].

The contribution of the second term of Eq. [122] to the  $\hat{T}_1$  amplitude equation is only slightly more complicated. This term involves the matrix element,  $\langle \Phi_i^a | (\hat{F}_N + \hat{V}_N) \hat{T}_1 | \Phi_0 \rangle$ , and, as before, we will consider only the contribution of  $\hat{V}_N$ . The  $\hat{T}_1$  operator, which acts first and is therefore placed at the bottom of the diagram, produces a +1 excitation from the reference on the right. Since the singly excited determinant on the left-hand side of the matrix element indicates an overall +1 excitation level, we require the three diagram fragments of  $\hat{V}_N$  that have an overall excitation level of 0:



However, the first two of these fragments can connect to the  $\hat{T}_1$  diagram in only one index—via either a single hole line or particle line—thus leaving an additional line extending below the  $\hat{T}_1$  interaction line in the final diagram, for example,



$$\neq \langle \Phi_i^a | (\hat{V}_N \hat{T}_1)_c | \Phi_0 \rangle \quad [177]$$

Because such diagrams cannot represent matrix elements that have the reference wavefunction on the right, only the third diagram above can contribute to

the  $\hat{T}_1$  amplitude equation. Connecting this  $\hat{V}_N$  fragment to the  $\hat{T}_1$  diagram gives

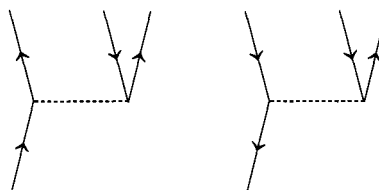
$$\langle \Phi_i^a | (\hat{V}_N \hat{T}_1)_c | \Phi_0 \rangle = \text{Diagram} [178]$$

The algebraic interpretation of this diagram proceeds exactly as before: (1) we label the external lines using  $i$  and  $a$  for consistency with the singly excited determinant in the matrix element, and the internal lines are labeled with the summation indices  $j$  and  $b$ ; (2) the appropriate two-electron integral contributed by the  $\hat{V}_N$  component is  $\langle ja||bi \rangle$ , and the  $\hat{T}_1$  amplitude is  $t_j^b$ ; and (3) there are two loops and two hole lines, giving the diagram a positive sign. The final expression for this diagram is therefore

$$\text{Diagram} = \sum_{jb} \langle ja||bi \rangle t_j^b [179]$$

which is identical to the result in Eq. [143].

The contribution of  $(\hat{V}_N \hat{T}_1)_c$  to the  $\hat{T}_2$  amplitude equation involves the matrix element  $\langle \Phi_{ij}^{ab} | (\hat{V}_N \hat{T}_1)_c | \Phi_0 \rangle$ . In this case, we require an overall excitation level of +2 as dictated by the doubly excited determinant on the left. Since the  $\hat{T}_1$  operator produces a +1 excitation from  $\Phi_0$ , we require the sixth and seventh diagrams of  $\hat{V}_N$  in Figure 3, which produce a +1 excitation:



These may be connected to the  $\hat{T}_1$  amplitude diagram from below to give two terms

$$\langle \Phi_{ij}^{ab} | (\hat{V}_N \hat{T}_1)_c | \Phi_0 \rangle = \text{Diagram} + \text{Diagram} [180]$$

These two diagrams may be interpreted using the rules described above: (1) we assign indices  $i$ ,  $j$ ,  $a$ , and  $b$  (from left to right) to the external lines for consistency with the doubly excited determinant in the matrix element; (2) there is only one internal (summation) line in each diagram to which we assign the indices  $c$  in the left diagram and  $k$  in the right diagram; (3) in the left diagram, there are two loops and two hole lines giving a positive sign, and in the right diagram there are two loops and three hole lines giving a negative sign; (4) the two-electron integral in the left diagram is  $\langle ab||cj\rangle$  and in the right diagram is  $\langle kb||ij\rangle$ ; (5) the  $\hat{T}_1$  amplitude in the left diagram is  $t_i^c$  and in the right diagram is  $t_k^i$ ; and (6) there are neither equivalent lines nor equivalent vertices, so no additional factors of  $1/2$  appear in the final expression.

Before the algebraic interpretation is complete, however, we require one additional rule:

Each pair of unique, external hole or particle lines introduces a permutation function,  $P(pq)$  (as defined earlier in Eq. [154]), to ensure antisymmetry of the final expression.

Note again that the four external  $q$ -creation lines of the  $\hat{T}_2$  amplitude diagrams correspond to the wavefunction lines of a doubly excited determinant; in the diagrams above, the  $i$ ,  $j$ ,  $a$ , and  $b$  external lines correspond to the excitation orbitals of the determinant,  $\Phi_{ij}^{ab}$ . Since this determinant is antisymmetric with respect to permutation of either the  $i$  and  $j$  indices or the  $a$  and  $b$  indices, this antisymmetry must be maintained in the final algebraic expression. Pairs of external lines that originate from the same operator interaction line (such as the two particle lines in the leftmost diagram of Eq. [180]) are not unique, and the expression is already antisymmetric with respect to permutation of such pairs. Pairs of external lines that do not originate on the same operator interaction line (such as the hole lines of the leftmost diagram) are unique, and a permutation operator must be included in the algebraic interpretation to ensure proper antisymmetry. For example, in the left-hand diagram above, there are two external particle lines and two external hole lines. The diagram is already antisymmetric to permutation of the two particle lines because they both connect to the  $\hat{V}_N$  diagram fragment. The hole lines, on the other hand, connect to different vertices—one to  $\hat{T}_1$  and the other to  $\hat{V}_N$ . Therefore, the diagram is not antisymmetric to permutation of these lines, and we must include the operator  $P(ij)$  in the algebraic expression corresponding to this diagram:

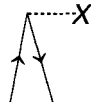
$$= P(ij) \sum_c \langle ab || cj \rangle t_i^c \quad [181]$$

Similarly, the external particle lines in the rightmost diagram must be permuted in its algebraic expression:

$$= -P(ab) \sum_k \langle kb || ij \rangle t_k^a \quad [182]$$

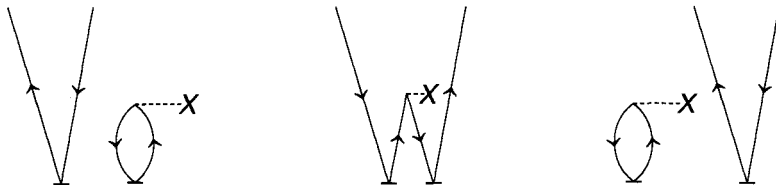
When the permutation operators are expanded, these expressions are identical to those given in Eq. [145] derived earlier using Wick's theorem and some complicated algebra.

The next example is the contribution of  $(\hat{F}_N \hat{T}_1^2)_c$  to the  $\hat{T}_1$  amplitude equation, which requires the matrix element  $\langle \Phi_i^a | (\hat{F}_N \hat{T}_1^2)_c | \Phi_0 \rangle$ . To obtain an overall excitation level of +1, as dictated by the singly excited determinant on the left and the reference on the right, we must use the -1 diagram fragment of



, since the two  $\hat{T}_1$  operators produce an excitation level of +2. There

are three ways to connect this  $\hat{F}_N$  diagram fragment to the cluster operator diagrams to produce a matrix element with the appropriate determinants above and below the diagrams:



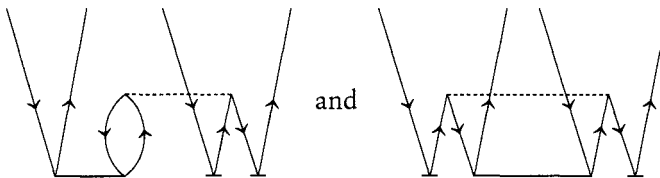
The first and third diagrams above are equivalent and correspond to the contractions indicated in Eq. [149]. These violate the “connected cluster” form of  $e^{-\hat{T}} \hat{H}_N e^{\hat{T}} \equiv (\hat{H}_N e^{\hat{T}})_c$  discussed earlier, which requires that the Hamiltonian fragment share at least one index with every cluster operator on its right. The second diagram is therefore the only acceptable contribution from this matrix element to the  $\hat{T}_1$  amplitude equation. Its algebraic interpretation proceeds as usual: (1) the external lines are labeled  $i$  and  $a$  to match the singly excited determinant,  $\Phi_i^a$  in the matrix element; (2) the internal (summation) lines are labeled by the dummy indices  $k$  and  $c$ ; (3) the Fock operator contributes the element  $f_{kc}$ , and the  $\hat{T}_1$  operators contribute the amplitudes  $t_k^c$  and  $t_k^a$ ; (4) there are two hole lines and only one loop, giving an overall negative sign to the diagram; and (5) there are no equivalent, internal lines, nor are the two  $\hat{T}_1$  fragments equivalent since they do not connect to the  $\hat{F}_N$  diagram fragment in

the same way (one connects via a hole line and the other via a particle line). The final expression is therefore

$$\frac{1}{2} \langle \Phi_i^a | (\hat{F}_N \hat{T}_1^2)_c | \Phi_0 \rangle = \begin{array}{c} \text{Diagram showing two V-shaped lines meeting at a central point labeled } X. \end{array} = -\sum_{kc} f_{kc} t_i^c t_k^a \quad [183]$$

which is the same as the result given in Eq. [148].

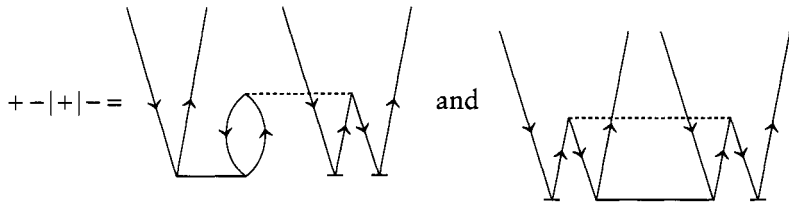
As a final example, consider the contribution of the  $\frac{1}{2}(\hat{V}_N \hat{T}_1^2 \hat{T}_2)_c$  operator to the  $\hat{T}_2$  equation. As discussed earlier, the corresponding matrix element, which involves a doubly excited determinant on the left and the reference determinant on the right, requires considerable effort if analyzed using Wick's theorem. Diagrammatically, however, this analysis is much simpler. The only difficulty arises in the construction of only uniquely connected diagrams. For example, one might construct the two seemingly different diagrams:



Careful inspection, however, reveals that the diagrams are equivalent because one can be produced from the other by permutation of the hole or particle lines on the  $\hat{T}_2$  fragment. (This equivalence can also be proven algebraically, and the reader is encouraged to carry this analysis out independently.)

One can ensure that only unique diagrams are produced by using a straightforward procedure developed by Kucharski and Bartlett.<sup>20</sup> In this approach, one first assigns + symbols to particle lines and - symbols to hole lines lying below the interaction line of the Hamiltonian fragment or above the interaction line for the cluster operators. Unique connectivities of the operator diagrams are produced by combining these signs in all unique ways. In the present example, the two  $\hat{T}_1$  operators each contribute one + sign and one - sign, the  $\hat{T}_2$  operator contributes two + signs and two - signs, and the -2 excitation level fragment of  $\hat{V}_N$  contributes two + signs and two - signs. Since in this case every directed line from the Hamiltonian fragment must connect to lines from the cluster operators, we must match the + and - signs from  $\hat{V}_N$  to the same signs on the cluster operators. For example, we might choose one + and one - from the  $\hat{T}_2$  operator, leaving one + for one of the  $\hat{T}_1$  fragments and one - for the remaining  $\hat{T}_1$ . We will denote this "sign sequence" as + - | + | -, where the first pair of signs belong to the  $\hat{T}_2$  operator, and the remaining signs (sepa-

rated by the vertical bars) belong to the  $\hat{T}_1$  operator fragments. The corresponding diagram would be



where the connectivity dictated by the sign sequence is maintained in the diagram. The sign sequence helps to reveal the equivalence of the two diagrams; the  $\hat{T}_2$  operator in each diagram connects to the  $\hat{V}_N$  fragment by a particle-hole pair of lines, while the  $\hat{T}_1$  operators connect by either a particle or a hole line. Note that this sequence is equivalent to the sequence  $+ - | - | +$  because the  $\hat{T}_1$  operators commute. For this matrix element, there are only five unique sign sequences, including the one given above: (1)  $+ - | + | -$ , (2)  $+ + | - | -$ , (3)  $- - | + | +$ , (4)  $- | + | + -$ , and (5)  $+ | - | + -$ . These five Kucharski-Bartlett sign sequences give rise to the diagrams (in order)

$$\frac{1}{2} \langle \Phi_{ij}^{ab} | (\hat{V}_N \hat{T}_1^2 \hat{T}_2)_c | \Phi_0 \rangle =$$

[184]

The algebraic interpretation of each of these diagrams, using the rules described earlier, is easily shown to be (in the same order as the diagrams above)

$$\begin{aligned} \frac{1}{2}\langle\Phi_{ij}^{ab}|\hat{V}_N\hat{T}_1^2\hat{T}_2\rangle_c|\Phi_0\rangle &= -P(ij)P(ab)\sum_{klcd}\langle kl||cd\rangle t_{ik}^{ac}t_j^dt_l^b \\ &\quad + \frac{1}{4}P(ab)\sum_{klcd}\langle kl||cd\rangle t_{ij}^{cd}t_k^at_l^b + \frac{1}{4}P(ij)\sum_{klcd}\langle kl||cd\rangle t_{kl}^{ab}t_i^ct_l^d \\ &\quad - P(ij)\sum_{klcd}\langle kl||cd\rangle t_{ik}^{ab}t_j^ct_l^d - P(ab)\sum_{klcd}\langle kl||cd\rangle t_{ij}^{ac}t_k^bt_l^d \end{aligned} \quad [185]$$

The permutation operators appear in order to maintain the antisymmetry of the algebraic expressions, as explained earlier. Note that the factors of  $\frac{1}{4}$  appearing in the second and third terms result from both a pair of equivalent lines and a pair of equivalent vertices in each of the corresponding diagrams.

### Size Extensivity of the Coupled Cluster Energy

Earlier in the chapter we discussed the property of the coupled cluster energy known as size consistency, which implies that the energy of two noninteracting fragments computed separately is the same as that computed for both fragments simultaneously. A related property is known as size extensivity, which is applied to methods whose energy scales linearly with  $N$  (the number of electrons), just as the exact energy scales. Whereas size consistency applies only to noninteracting molecular fragments, size extensivity is a more general mathematical concept that applies to any point on the potential energy surface. The term was popularized in electronic structure theory by Bartlett<sup>87</sup> and is based on analogous extensive thermodynamic properties. In this section, we show that the exponential ansatz of coupled cluster theory guarantees size extensivity, but the truncated CI approach does not.

Consider the structure of the CI Schrödinger equation (assuming intermediate normalization as well as normal-ordered  $\hat{H}_N$  and  $\hat{C}$  operators), beginning from the linear ansatz of Eq. [32]:

$$\hat{H}_N(1 + \hat{C}_1 + \hat{C}_2 + \dots)|\Phi_0\rangle = (E_{\text{CI}} - E_0)(1 + \hat{C}_1 + \hat{C}_2 + \dots)|\Phi_0\rangle \quad [186]$$

Left-projection of this equation by the reference determinant,  $\Phi_0$ , leads to the energy equation,

$$E_{\text{CI}} - E_0 = \langle\Phi_0|(\hat{H}_N(\hat{C}_1 + \hat{C}_2))|\Phi_0\rangle \quad [187]$$

where truncation of the CI expansion is a natural consequence of Slater's rules. By application of Wick's theorem (or the corresponding diagrams, of course), this equation may be written in algebraic form as

$$E_{\text{CI}} - E_0 = \sum_{ia}f_{ia}c_i^a + \frac{1}{4}\sum_{ijab}\langle ij||ab\rangle c_{ij}^{ab} \quad [188]$$

If canonical Hartree–Fock orbitals are chosen, the first term is zero by Bril-louin’s theorem.

How do the individual terms on the right-hand side of Eq. [188] scale as more electrons are added to the system? If we assume a localized orbital basis (which does not limit the validity of this analysis), then, for a given occupied orbital,  $\phi_i$ , the two-electron integral,  $\langle ij||ab\rangle$ , for example, will be zero unless the orbitals,  $\phi_j$ ,  $\phi_a$ , and  $\phi_b$ , are in reasonably close proximity to  $\phi_i$ , owing to the relatively short range of the interelectronic potential. Assuming that the number of orbitals that fulfill this proximity requirement for (i.e., are “local” to)  $\phi_i$  is finite, then all the individual two-electron integrals,  $\langle ij||ab\rangle$ , associated with  $\phi_i$  are *independent* of the number of electrons in the system. That is, as more electrons (and therefore more occupied and virtual orbitals) enter the calculation, the set of individual two-electron integrals associated with orbital  $\phi_i$  remains unaffected. Assuming that the CI coefficients,  $c_{ij}^{ab}$ , in the second term of Eq. [188] have the same independence—an assumption we will examine momentarily—then the  $i$ -independent summation,

$$Z_i \equiv \sum_{jab} \langle ij||ab\rangle c_{ij}^{ab} \quad [189]$$

will be unaffected as the size of the system increases. Since there are  $N$  electrons, the final summation over occupied orbital index  $i$  produces  $N$  independent  $Z_i$  contributions,

$$E_{\text{CI}} \leftarrow \sum_i Z_i \quad [190]$$

(The left arrow indicates that the term on the right-hand side is one of several terms that contribute to  $E_{\text{CI}}$ .) Therefore the second term of Eq. [188] scales *linearly* with the number of electrons if and only if the CI coefficients,  $c_{ij}^{ab}$ , are independent of  $N$ . A similar argument holds for the first term on the right-hand side of the equation as well.

The CI coefficient equations are obtained by left-projection of Eq. [186] by excited determinants. For example, the  $\hat{C}_1$  equation from full CI is

$$\langle \Phi_i^a | \hat{H}_N (1 + \hat{C}_1 + \hat{C}_2 + \hat{C}_3) | \Phi_0 \rangle = (E_{\text{CI}} - E_0) \langle \Phi_i^a | \hat{C}_1 | \Phi_0 \rangle = E_{\text{CI}} \xi_i^a \quad [191]$$

which is energy dependent, unlike the corresponding coupled cluster amplitude equation. Every term on the left-hand side of this equation involves either bare Hamiltonian matrix elements, which are independent of  $N$ , or contractions of such matrix elements with CI coefficients, whose  $N$ -scaling is not yet known. The term on the right-hand side, which contains the CI energy, on the other hand, does depend on the system size—as  $N$  increases,  $E_{\text{CI}}$  increases (with some undetermined order). This nonunit scaling implies that if size extensivity is to be

maintained, terms on the left-hand side of Eq. [191] must scale similarly with  $N$  in order to cancel out the “errors” introduced by the presence of  $E_{\text{CI}}$ . If all excitation operators are included in the CI ansatz, this compensation is included in the corresponding coefficient equations. For example, we see that in Eq. [191],  $\hat{C}_3$  can contribute to  $\hat{C}_1$  by Slater’s rules. The  $\hat{C}_3$  equation itself is

$$\langle \Phi_{ijk}^{abc} | \hat{H}_N (\hat{C}_1 + \hat{C}_2 + \hat{C}_3 + \hat{C}_4 + \hat{C}_5) | \Phi_0 \rangle = (E_{\text{CI}} - E_0) c_{ijk}^{abc} \quad [192]$$

which includes contributions from up to  $\hat{C}_5$ . The first term on the left-hand side involving  $\hat{C}_1$  may be written as

$$c_{ijk}^{abc} \leftarrow \frac{1}{4} \sum_{jkbc} c_{ijk}^{abc} \langle jk||bc \rangle = c_i^a \langle jk||bc \rangle \quad [193]$$

where the thick bar in the diagram distinguishes the  $\hat{C}_1$  operator from the corresponding  $\hat{T}_1$  operator. Since the orbitals on the  $\hat{C}_1$  component are completely independent of those of the two-electron integral (i.e., the diagram is “disconnected”), this term will produce nonzero  $\hat{C}_3$  components involving orbitals that are spatially distant as the size of the system is increased. That is, for a given orbital,  $\phi_i$ , the number of nonzero coefficients,  $c_{ijk}^{abc}$ , involving the orbitals  $\phi_j$ ,  $\phi_k$ , etc., increases as more electrons (orbitals) are added to the system. Therefore, the term from Eq. [191] involving  $\hat{C}_3$ , which may be written as

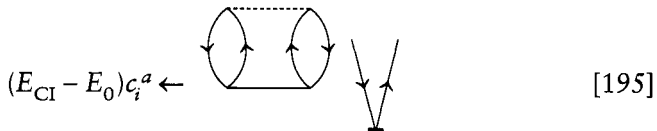
$$c_i^a \leftarrow \frac{1}{4} \sum_{jkbc} c_{ijk}^{abc} \langle jk||bc \rangle \quad [194]$$

scales approximately linearly as  $N$  increases. This term would therefore contribute to the “compensating errors” described above to ensure appropriate linear scaling of the CI energy with respect to the number of electrons. Similarly, the  $N$ -scaling of the  $\hat{C}_3$  equation itself is corrected by such disconnected terms arising from higher excitation levels such as  $\hat{C}_4$  and  $\hat{C}_5$ . Therefore, if the CI equations are truncated at a particular excitation level, the higher excitation terms needed to cancel the incorrect  $N$ -scaling of the energy-dependent term in each coefficient equation will be lost, and the errors in the truncated CI energy relative to the exact (full CI) energy will be compounded as the size of the system increases. The well-known Davidson correction for the CISD energy is designed to account for the size extensivity error of this method.<sup>121,122</sup>

The coupled cluster energy, on the other hand, does not suffer from this lack of size extensivity for two reasons: (1) the amplitude equations in Eq. [50] are independent of the coupled cluster energy; and (2) the Hausdorff expansion of the similarity-transformed Hamiltonian in Eq. [106], for example, guarantees that the only nonzero terms are those in which the Hamiltonian is con-

nected to all the cluster operators on its right, regardless of the truncation of  $\hat{T}$ . Hence, no diagrams such as that in Eq. [193] appear in the coupled cluster amplitude equations. As a result, the  $\hat{T}$  amplitudes are independent of the system size, and the coupled cluster energy computed via Eq. [123] scales linearly with the number of electrons.

A size extensive method is frequently defined esoterically as one whose energy and amplitude/coefficient equations contain no “unlinked” diagrams, such as



in which the two diagram components cannot be connected to each other even by application of other interaction lines.<sup>7</sup> Although such terms are indeed absent in the coupled cluster equations (as well as those of many-body perturbation theory), the disconnected amplitude components, such as those in Eq. [193] (which also contribute to the improper  $N$ -dependence of the amplitudes), must be excluded to ensure correct scaling of the energy.

## CONNECTION TO MANY-BODY PERTURBATION THEORY

In this section we examine the fundamental relationship between many-body perturbation theory (MBPT) and coupled cluster theory. As originally pointed out by Bartlett,<sup>87,123</sup> this connection allows one to construct finite-order perturbation theory energies and wavefunctions via “iterations” of the coupled cluster equations. The essential aspects of MBPT have been discussed in Volume 5 of *Reviews in Computational Chemistry*,<sup>77</sup> as well as in numerous other texts.<sup>80,82,124,125</sup> We therefore only summarize the main points of MBPT and focus on its intimate link to coupled cluster theory, as well as how MBPT can be used to construct energy corrections for higher order cluster operators such as the popular ( $T$ ) correction for connected triple excitations.

<sup>7</sup>The “disconnected” diagram of Eq. [193] is not unlinked because the inclusion of an additional  $\hat{V}_N$  fragment can connect its two components—Harris et al. (Ref. 80) have recommended that such terms be called “linkable.” With terms such as “disconnected,” “connected,” “linked,” and “unlinked” used to describe diagrams, it is not surprising that these techniques caused much confusion in the past.

## Perturbational Decomposition of the Cluster Operators

Two essential concepts underlie the construction of MBPT from basic Rayleigh–Schrödinger perturbation theory:<sup>77,82</sup>

The zeroth-order component of the electronic Hamiltonian is taken to be the Fock operator such that the perturbation operator (sometimes called the fluctuation potential) is then the remaining two-electron operator,  $\hat{V}_N$ :

$$\hat{H}_N = \hat{H}^{(0)} + \hat{H}^{(1)} = \hat{F}_N + \hat{V}_N \quad [196]$$

This partitioning, when applied in conjunction with the set of canonical Hartree–Fock orbitals (in which  $\hat{F}_N$  is diagonal), corresponds to the Møller–Plesset variant of many-body perturbation theory.<sup>126</sup> A Hartree–Fock determinant, which is an eigenfunction of  $\hat{F}_N$ , is therefore the natural choice for the zeroth-order wavefunction.<sup>s</sup>

Each perturbed wavefunction,  $\Psi^{(n)}$ , is expanded in a CI-like fashion as a linear combination of excited determinants,

$$\Psi^{(n)} = \sum_{ia} a_i^{a(n)} \Phi_i^a + \frac{1}{4} \sum_{ijab} a_{ij}^{ab(n)} \Phi_{ij}^{ab} + \dots \quad [197]$$

As discussed in detail in Refs. 77 and 82, for example, this expansion is not  $N$ -fold (where  $N$  is the number of electrons in the system) for the lower perturbational orders, but truncates to include only modest excitation levels. For example, the first-order wavefunction, which may be used to compute both the second- and third-order energies, contains contributions from doubly excited determinants only, whereas the second-order wavefunction, which contributes to the fourth- and fifth-order perturbed energies, contains contributions from singly, doubly, triply, and quadruply excited determinants. Furthermore, the sum of the zeroth- and first order energies is equal to the SCF energy. This determinantal expansion of the perturbed wavefunctions suggests that we may also decompose the cluster operators,  $\hat{T}_n$ , by orders of perturbation theory:

$$\hat{T}_n = \hat{T}_n^{(1)} + \hat{T}_n^{(2)} + \hat{T}_n^{(3)} + \dots \quad [198]$$

Depending on the choice of molecular orbital basis, the earliest terms for certain excitation levels are naturally zero. For example, in Møller–Plesset theory, only

---

<sup>s</sup>The choice of  $\hat{F}_N$  as the zeroth-order Hamiltonian requires the use of either a spin-restricted (closed-shell) Hartree–Fock (RHF) or spin-unrestricted Hartree–Fock (UHF) determinant as the zeroth-order (reference) wavefunction. Since spin-restricted open-shell Hartree–Fock (ROHF) reference functions are not eigenfunctions of the spin-orbital  $\hat{F}_N$ , other partitions are required (Refs. 127–134).

$\hat{T}_2$  contains a nonzero first-order component; contributions to  $\hat{T}_1$ ,  $\hat{T}_3$ , and  $\hat{T}_4$  first appear in second order because the corresponding second-order wavefunction contains single, double, triple, and quadruple excitations.

## Perturbation Theory Energies from the Coupled Cluster Hamiltonian

The partitioning of the electronic Hamiltonian and the corresponding breakdown of the cluster operators leads to an expansion of the coupled cluster effective Hamiltonian,  $\bar{H}$ , in orders of perturbation theory through the Hausdorff expansion given in Eq. [122]:

$$\bar{H} = \bar{H}^{(0)} + \bar{H}^{(1)} + \bar{H}^{(2)} + \dots \quad [199]$$

Since the zeroth-order component of  $\bar{H}$  consists of just the Fock operator in Møller–Plesset theory, the first-order components of  $\bar{H}$  may be written as

$$\bar{H}^{(1)} = \hat{V}_N + (\hat{F}_N \hat{T}_2^{(1)})_c \quad [200]$$

and the second-order term as

$$\bar{H}^{(2)} = (\hat{F}_N \hat{T}_1^{(2)} + \hat{V}_N \hat{T}_2^{(1)} + \frac{1}{2} \hat{F}_N (\hat{T}_2^{(1)})^2)_c \quad [201]$$

Each of these expressions is constructed by simply assigning the appropriate perturbational orders to each operator in Eq. [122] and retaining only the terms that correspond to the desired order,  $n$ . Using  $\bar{H}^{(n)}$  as an approximate Hamiltonian, one may construct  $n$ th-order Schrödinger equations of the form

$$\bar{H}^{(n)} |\Phi_0\rangle = E^{(n)} |\Phi_0\rangle \quad [202]$$

One computes the energy in the  $n$ th order of MBPT via a zeroth-order expectation value, namely,

$$E^{(n)} = \langle \Phi_0 | \bar{H}^{(n)} | \Phi_0 \rangle \quad [203]$$

obtained by left-projection of Eq. [202] by  $\Phi_0$ . For example, the second-order energy (often referred to as the MP2 energy) may be computed from

$$E^{(2)} = \langle \Phi_0 | (\hat{F}_N \hat{T}_1^{(2)})_c | \Phi_0 \rangle + \langle \Phi_0 | (\hat{V}_N \hat{T}_2^{(1)})_c | \Phi_0 \rangle + \frac{1}{2} \langle \Phi_0 | (\hat{F}_N (\hat{T}_2^{(1)})^2)_c | \Phi_0 \rangle \quad [204]$$

which may be evaluated as usual using Wick's theorem or the diagrammatic techniques described earlier in the chapter. We denote the cluster operators of a

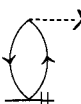
particular order diagrammatically by adding hash marks to the corresponding interaction line. For example, the first-order  $\hat{T}_2$  operator may be written as

$$\hat{T}_2^{(1)} = \begin{array}{c} \diagdown \quad \diagup \\ \diagdown \quad \diagup \\ + \end{array} \quad [205]$$

and the second-order  $\hat{T}_1$  operator as

$$\hat{T}_1^{(2)} = \begin{array}{c} \diagdown \quad \diagup \\ \diagdown \quad \diagup \\ + \end{array} \quad [206]$$

The first term on the right-hand side of Eq. [204] involving  $\hat{T}_1^{(2)}$  must be zero in

MBPT because the corresponding diagram, , involves the  $f_{ia}$  elements

of the spin-orbital Fock matrix, which are necessarily zero in the basis of canonical Hartree–Fock orbitals. Furthermore, the third term on the right-hand side of the equation cannot contribute to the energy because  $\hat{F}_N$  cannot cancel the +4 excitation level produced by the cluster operators. Therefore, Eq. [204] may be written as

$$E^{(2)} = \begin{array}{c} \text{---} \\ \diagdown \quad \diagup \\ \diagdown \quad \diagup \\ + \end{array} = \frac{1}{4} \sum_{ijab} \langle ij || ab \rangle t_{ij}^{ab(1)} \quad [207]$$

The first-order  $\hat{T}_2$  amplitudes, which are required for Eq. [207], may be determined by left-projecting the first-order variant of Eq. [202] involving  $\bar{H}^{(1)}$  by a doubly excited determinant,  $\Phi_{ij}^{ab}$ , as we did earlier in the construction of the coupled cluster amplitude equations,

$$0 = \langle \Phi_{ij}^{ab} | \bar{H}^{(1)} | \Phi_0 \rangle = \langle \Phi_{ij}^{ab} | \hat{V}_N | \Phi_0 \rangle + \langle \Phi_{ij}^{ab} | (\hat{F}_N \hat{T}_2^{(1)})_c | \Phi_0 \rangle \quad [208]$$

Evaluating this expression diagrammatically, we obtain

$$0 = \begin{array}{c} \diagdown \quad \diagup \\ \diagdown \quad \diagup \\ + \end{array} + \begin{array}{c} \diagdown \quad \diagup \\ \diagdown \quad \diagup \\ + \end{array} \text{---} X + \begin{array}{c} \diagdown \quad \diagup \\ \diagdown \quad \diagup \\ + \end{array} \text{---} X \quad [209]$$

$$= \langle ab || ij \rangle + \sum_c (f_{bc} t_{ij}^{ac(1)} - f_{ac} t_{ij}^{bc(1)}) - \sum_k (f_{kj} t_{ik}^{ab(1)} - f_{ki} t_{jk}^{ab(1)})$$

Again assuming canonical Hartree–Fock orbitals, the terms containing Fock matrix elements are reduced to include the diagonal elements only:

$$(f_{ii} + f_{jj} - f_{aa} - f_{bb})t_{ij}^{ab(1)} = \langle ab || ij \rangle \quad [210]$$

Thus, the diagrammatic equation could be rewritten more simply as

$$D_2 \begin{array}{c} \diagdown \\ \diagup \end{array} \begin{array}{c} \diagup \\ \diagdown \end{array} = \begin{array}{c} \diagdown \\ \diagup \end{array} \begin{array}{c} \diagup \\ \diagdown \end{array} \quad [211]$$

where  $D_2 \equiv D_{ij}^{ab} \equiv f_{ii} + f_{jj} - f_{aa} - f_{bb}$  denotes the separation of the orbital energies (the diagonal Fock matrix elements) from the terms involving the Fock operator. This equation may be rearranged further by another slight modification of our current diagrammatic notation:

$$t_{ij}^{ab(1)} = \begin{array}{c} \diagdown \\ \diagup \end{array} \begin{array}{c} \diagup \\ \diagdown \end{array} = \begin{array}{c} \diagdown \\ \diagup \end{array} \begin{array}{c} \diagup \\ \diagdown \end{array} = \frac{\langle ab || ij \rangle}{D_{ij}^{ab}} \quad [212]$$

The extra horizontal bar across the lines emanating from the  $\hat{V}_N$  fragment denotes division by the  $D_{ij}^{ab}$  “energy denominator” from the foregoing algebraic expression. This new diagrammatic feature may be used to indicate other such denominators, including those from the  $\hat{T}_1^{(n)}$  and  $\hat{T}_3^{(n)}$  equations, as we will see later in the chapter. Inserting Eq. [212] into Eq. [207], we may write the final MBPT(2) energy expression as

$$E^{(2)} = \begin{array}{c} \diagdown \\ \diagup \end{array} \begin{array}{c} \diagup \\ \diagdown \end{array} = \frac{1}{4} \sum_{ijab} \frac{\langle ij || ab \rangle \langle ab || ij \rangle}{D_{ij}^{ab}} \quad [213]$$

This expression is identical to that derived directly from perturbation theory in Refs. 77 and 82.

As the preceding analysis clearly shows, the MBPT(2) energy may be determined by approximating the CCSD energy using only those components which contribute to  $\bar{H}^{(2)}$ . The CCSD energy is therefore “complete” through at least the second order of MBPT. One can carry this discussion further to construct the MBPT(3) energy as well. However, beginning with fourth order, the CCSD fails to include all the necessary terms. This result makes sense, of course, because of the excitation level included in each perturbed wavefunction. The MBPT(2) and MBPT(3) energies require only doubly excited determinants, which are included explicitly in the CCSD approximation; but the MBPT(4) energy includes contributions from singly, doubly, triply, and quadruply excited determinants. It may be shown<sup>6,87,135,136</sup> that the MBPT(4) quadruple-exci-

tation contributions may be factored exactly into products of double excitations, but no such factorization is possible for the corresponding triples. As a result, the CCSD energy lacks only triple excitation contributions to be complete through fourth order.

Recognition of this relationship between coupled cluster theory and MBPT has inspired research efforts to construct perturbation-based corrections to the CCSD energy to account for higher excitation contributions. Undoubtedly, the most successful and popular of these is the (T) correction first described for closed-shell molecular systems by Raghavachari et al.<sup>24</sup> In the next section, we will describe the structure of this correction using diagrammatic techniques.

### The (T) Correction

Numerous studies over the last 15 years have confirmed the importance of triple and higher excitations for the accurate prediction of many molecular properties.<sup>15–17,24,25,27,51,137,138</sup> Unfortunately, the full CCSDT approach,<sup>22,23,26</sup> in which triple excitations are included explicitly via the  $\hat{T} \equiv \hat{T}_1 + \hat{T}_2 + \hat{T}_3$  cluster operator, is far too computationally expensive for general application to most systems of chemical interest.

As pointed out in the preceding section, the CCSD energy contains contributions identical to those of the MBPT(2) and MBPT(3) energy, but lacks triple-excitation contributions necessary for MBPT(4). Thus, a natural approach to the “triples problem” is to correct the CCSD energy for the missing MBPT(4) terms,<sup>18</sup> using the CCSDT similarity-transformed Hamiltonian,

$$\bar{H}_{\text{CCSDT}} = e^{-\hat{T}_1 - \hat{T}_2 - \hat{T}_3} \hat{H}_N e^{\hat{T}_1 + \hat{T}_2 + \hat{T}_3} \quad [214]$$

for the perturbational decomposition. The fourth-order energy depends on this effective Hamiltonian as

$$E^{(4)} = \langle \Phi_0 | \bar{H}^{(4)} | \Phi_0 \rangle = \langle \Phi_0 | (\hat{V}_N \hat{T}_2^{(3)})_c | \Phi_0 \rangle = \begin{array}{c} \text{Diagram of two circles connected by a horizontal line with three vertical bars below it} \end{array} = \frac{1}{4} \sum_{ijab} \langle ij || ab \rangle t_{ij}^{ab(3)} \quad [215]$$

(Note that we have omitted numerous  $\bar{H}^{(4)}$  components, which cannot contribute to the energy expression.) The third-order  $\hat{T}_2$  component of this equation is determined via

$$\begin{aligned} 0 &= \langle \Phi_{ij}^{ab} | \bar{H}^{(3)} | \Phi_0 \rangle \\ &= \langle \Phi_{ij}^{ab} | (\hat{F}_N \hat{T}_2^{(3)} + \hat{V}_N \hat{T}_1^{(2)} + \hat{V}_N \hat{T}_2^{(2)} + \hat{V}_N \hat{T}_3^{(2)} + \frac{1}{2} \hat{V}_N (\hat{T}_2^{(1)})^2)_c | \Phi_0 \rangle \end{aligned} \quad [216]$$

Note the appearance of the  $\hat{T}_3$  operator through the use of  $\bar{H}_{\text{CCSDT}}$ . Since we wish to construct a correction to the CCSD energy, which already contains the contributions from the  $\hat{T}_1$  and  $\hat{T}_2$  terms, we need to construct only the  $(\hat{V}_N \hat{T}_3^{(2)})_c$  component of Eq. [216], which may be represented diagrammatically as

$$\hat{T}_2^{(3)} = \begin{array}{c} \text{Diagram 1: } \text{Two vertical lines with arrows pointing down, meeting at a V-shape with a horizontal bar below it.} \\ \leftarrow \end{array} + \begin{array}{c} \text{Diagram 2: } \text{Two vertical lines with arrows pointing down, meeting at a V-shape with a horizontal bar below it. A dashed horizontal line connects the top of the V to a circle with a clockwise arrow.} \\ \text{Diagram 3: } \text{Two vertical lines with arrows pointing down, meeting at a V-shape with a horizontal bar below it. A dashed horizontal line connects the top of the V to a circle with a clockwise arrow.} \end{array} [217]$$

where we have indicated the two-electron denominator  $D_2$  using the horizontal bar notation described earlier. The  $\hat{T}_3^{(2)}$  amplitudes needed for this equation may be determined from the corresponding second-order amplitude equation:

$$0 = \langle \Phi_{ijk}^{abc} | (\hat{V}_N \hat{T}_2^{(1)} + \hat{F}_N \hat{T}_3^{(2)})_c | \Phi_0 \rangle [218]$$

which we may write using the denominator notation from the preceding section as

$$D_3 \begin{array}{c} \text{Diagram 1: } \text{Three vertical lines with arrows pointing down, meeting at a V-shape with a horizontal bar below it.} \end{array} = \begin{array}{c} \text{Diagram 1: } \text{Three vertical lines with arrows pointing down, meeting at a V-shape with a horizontal bar below it. A dashed horizontal line connects the top of the V to a circle with a clockwise arrow.} \\ + \end{array} \begin{array}{c} \text{Diagram 2: } \text{Three vertical lines with arrows pointing down, meeting at a V-shape with a horizontal bar below it. A dashed horizontal line connects the top of the V to a circle with a clockwise arrow.} \end{array} [219]$$

This equation may be interpreted algebraically as

$$\begin{aligned} D_{ijk}^{abc} t_{ijk}^{abc(2)} &= P(k|ij)P(a|bc) \sum_d \langle bc || dk \rangle t_{ij}^{ad(1)} \\ &\quad - P(i|jk)P(c|ab) \sum_l \langle lc || jk \rangle t_{il}^{ab(1)} \end{aligned} [220]$$

where the  $P(p|qr)$  permutation operators perform antisymmetric permutations of index  $p$  with indices  $q$  and  $r$ , in analogy to the two-index  $P(pq)$  operator defined earlier in the chapter. The first-order  $\hat{T}_2$  amplitudes here are computed using Eq. [212]. These  $\hat{T}_3^{(2)}$  amplitudes may then be inserted into Eq. [217] to compute the  $\hat{T}_2^{(3)}$  amplitudes, which may then be used in Eq. [215] to compute

the triple-excitation contribution to the fourth-order energy,  $E_{\text{T}}^{(4)}$ .<sup>t</sup> The corrected CCSD energy,

$$E_{\text{CCSD+T(4)}} = E_{\text{CCSD}} + E_{\text{T}}^{(4)} \quad [221]$$

was referred to as CCSD+T(4) by Urban et al.<sup>18</sup> because  $E_{\text{T}}^{(4)}$  is the true fourth-order triples energy when Eq. [220] is used to compute  $\hat{T}_3^{(2)}$ . If, on the other hand, we choose to use the *converged* CCSD  $\hat{T}_2$  amplitudes rather than first-order  $\hat{T}_2$  in Eq. [220]—that is, amplitudes that solve Eq. [153]—we obtain a different correction, which Urban et al. denoted CCSD+T(CCSD) (although more recently this method has been called CCSD[T]):

$$E_{\text{CCSD+T(CCSD)}} = E_{\text{CCSD}} + E_{\text{T}}^{[4]} \quad [222]$$

where the superscript [4] indicates that the usual fourth-order triples energy formula is evaluated using CCSD  $\hat{T}_2$  amplitudes. It has been shown<sup>24,140</sup> that the CCSD+T(CCSD)/CCSD[T] approach has a tendency to overestimate triple-excitation effects, which for some systems leads to qualitatively incorrect predictions of molecular properties.<sup>24</sup>

A few years after the work by Urban et al., Pople and coworkers<sup>17</sup> developed a triples correction for the QCISD (quadratic configuration interaction—a method commonly viewed as an approximation to CCSD) energy. In their work,<sup>17</sup> they noted that to properly balance the contribution of single and double excitations to the triples correction, an additional term beyond  $E_{\text{T}}^{[4]}$  must be included. In 1989 a similar analysis was developed by Raghavachari et al., who determined that a fifth-order energy contribution involving single excitations, denoted  $E_{\text{ST}}^{[5]}$ , should be included in the CCSD correction, as well.<sup>24</sup> This component may be derived based on the second-order  $\hat{T}_3$  contribution to the third-order  $\hat{T}_1$  operator, which subsequently contributes to fourth-order  $\hat{T}_2$ . Although the diagrammatic techniques described above are particularly convenient for deriving  $E_{\text{ST}}^{[5]}$ , we will avoid this task here, and simply present the final equation

$$E_{\text{ST}}^{[5]} = \frac{1}{4} \sum_{ijkabc} \langle jk \| bc \rangle t_i^a t_{ijk}^{abc} \quad [223]$$

---

<sup>t</sup>It should be noted that the “procedure” outlined here for computing  $E_{\text{T}}^{(4)}$  is certainly not the most efficient approach. As discussed more than two decades ago (Refs. 136, 139), the expression for  $E_{\text{T}}^{(4)}$  may be cast into the form

$$E_{\text{T}}^{(4)} = \frac{1}{36} \sum_{ijkabc} t_{ijk}^{abc(2)} D_{ijk}^{abc} t_{ijk}^{abc(2)}$$

where  $D_{ijk}^{abc}$  is the three-electron counterpart of  $D_{ij}^{ab}$ . Instead of storing individual triple-excitation amplitudes, however, each contribution to the summation above is computed separately using equations involving only two-electron integrals and energy denominators.

where the triple-excitation amplitudes are determined using a modified form of Eq. [220] that includes converged  $\hat{T}_2$  amplitudes

$$D_{ijk}^{abc} t_{ijk}^{abc} = P(i/jk)P(a/bc) \left[ \sum_d \langle bc \parallel di \rangle t_{jk}^{ad} - \sum_l \langle la \parallel jk \rangle t_{il}^{bc} \right] \quad [224]$$

Hence, the total CCSD(T) energy may be succinctly written as

$$E_{\text{CCSD(T)}} = E_{\text{CCSD}} + E_{\text{T}}^{[4]} + E_{\text{ST}}^{[5]} \quad [225]$$

We again note that large-scale computer implementations of the (T) method do not actually use Eq. [224] to compute and subsequently store the  $\hat{T}_3$  amplitudes. Instead, a much more efficient algorithm is employed in which the contributions to  $E_{\text{T}}^{[4]}$  and  $E_{\text{ST}}^{[5]}$  are computed for each unique combination of  $i$ ,  $j$ , and  $k$  indices,<sup>141,142</sup> thus avoiding the  $\mathcal{O}(N^6)$  storage requirement associated with solving Eq. [224] explicitly. We also note that Deegan and Knowles constructed an augmented triples correction, denoted CCSD+T, which includes additional fifth-order terms missing in CCSD.<sup>30</sup>

What is the motivation for the inclusion of this particular fifth-order term over other such terms in the (T) correction? There have been influential numerical studies that serve to rationalize the success of the (T) correction from a purely empirical standpoint,<sup>24,25,143,144</sup> but here we are more interested in a physical motivation. Pople and coworkers<sup>17</sup> referred to  $E_{\text{ST}}^{[5]}$  as necessary to “balance” single and double excitation contributions. A more complete fifth-order analysis than that presented here<sup>20,24,143,144</sup> would show that CCSD alone already includes fifth-order double-triple interaction terms. Hence, we may consider this apparent mismatch to be the explanation for the inadequacy of CCSD [and especially CCSD+T(CCSD)] in certain difficult cases, such as the asymmetric stretching frequency of O<sub>3</sub>.<sup>24</sup> However, the physical interpretation behind a balancing of single and double excitation contributions is unclear. For Møller–Plesset perturbation theory, single excitations do not contribute until the second-order wavefunction, and double excitations provide the earliest correction of the zeroth-order state. This suggests, then, that double excitations should be more important in the perturbational analysis than single excitations and that no such balancing of the two is important. On the other hand, we recognize that the delayed appearance of single excitations in the perturbed wavefunctions is an artifact of Brillouin’s theorem.<sup>82</sup> That is, it is strictly because of the form of the arbitrarily chosen molecular orbitals that single excitations do not appear in first order. If we make our perturbational analysis more general, such that single excitations appear alongside double excitations in the wavefunction expansion, then the  $E_{\text{ST}}^{[5]}$  energy term shifts to fourth order rather than fifth order. From this perspective, then, single and double excitations should perhaps be treated alike, and the perturbational order has less to do with the selection of corrections terms than the excitation types themselves. This

shifting of perturbational orders is seen, for example, in certain types of open-shell perturbation theory.<sup>134</sup> Extension of the (T) correction to open-shell systems based on a spin-restricted reference wavefunction presents numerous difficulties,<sup>31</sup> and recent work in this area has produced a number of interesting techniques.<sup>27,29,33,51</sup>

Recently, it has been shown<sup>32</sup> that equation-of-motion coupled cluster theory (EOM-CC)<sup>5,60–63,65</sup> provides a unique perspective on the CCSD(T) method. Instead of taking the Hartree-Fock determinant as the zeroth-order wavefunction and subsequently decomposing the CCSD and CCSDT equations in terms of the many-body perturbation expansion, as we have done above, the CCSD wavefunction is taken as zeroth-order and the energy viewed as the lowest eigenvalue of an effective Hamiltonian with associated left and right eigenvectors. By substituting converged CCSD cluster amplitudes in place of the left eigenvector in the lowest order energy correction, the usual (T) energy expression is obtained. In such an analysis, both single and double contributions arrive in the same order (third) of this “perturbation theory,” and no arguments based on balancing the two are necessary. This unique perspective on the (T) correction has also led to the construction of a new “asymmetric” triples correction, denoted a-CCSD(T),<sup>34,145</sup> which utilizes the left eigenvector for the ground state CCSD eigenvalue problem.

---

## COMPUTER IMPLEMENTATION OF COUPLED CLUSTER THEORY

In this section we discuss many of the issues involved in writing an efficient computer program for solving the coupled cluster amplitude and energy equations derived earlier in the chapter. Since the original implementations of the CCD<sup>6,7</sup> and CCSD<sup>8</sup> methods, streamlining the complicated coupled cluster equations has been the subject of intense research. Here we focus on five main ideas used in practical CCSD programs: (1) factorization of the amplitude equations [Eqs. (152) and (153)] into terms that are at most linear in the cluster amplitudes,  $\hat{T}_1$  and  $\hat{T}_2$ ; (2) matrix-based storage and manipulation of the amplitudes and integrals; (3) spatial symmetry simplifications; (4) inclusion of spin factorization in calculations for both closed- and open-shell molecules; and (5) atomic-orbital-based algorithms for the reduction of disk storage requirements.

It is perhaps not immediately clear how one may go about solving the  $\hat{T}_1$  and  $\hat{T}_2$  amplitude equations given in Eqs. [152] and [153] for the individual amplitudes,  $t_i^a$  and  $t_{ij}^{ab}$ . A simple rearrangement of the equations, however, provides a more palatable form of these expressions that leads to a simple iterative approach for determining the coupled cluster wavefunction amplitudes. For example, the first few terms of Eq. [152] may be written as

$$0 = f_{ai} + f_{aa}t_i^a - f_{ii}t_i^a + \sum_c (1 - \delta_{ca})f_{ac}t_i^c - \sum_k (1 - \delta_{ik})f_{ik}t_k^a + \dots \quad [226]$$

where the diagonal components of the second and third terms on the right-hand side of Eq. [152] have been separated from the summation. Defining

$$D_i^a \equiv f_{ii} - f_{aa} \quad [227]$$

we may rewrite the amplitude equation as

$$D_i^a t_i^a = f_{ai} + \sum_c (1 - \delta_{ca})f_{ac}t_i^c - \sum_k (1 - \delta_{ik})f_{ik}t_k^a + \dots \quad [228]$$

Similarly, if we define

$$D_{ij}^{ab} \equiv f_{ii} + f_{jj} - f_{aa} - f_{bb} \quad [229]$$

the  $\hat{T}_2$  amplitude equation may be rewritten as

$$D_{ij}^{ab} t_{ij}^{ab} = \langle ab || ij \rangle + P(ab) \sum_c (1 - \delta_{bc})f_{bc}t_{ij}^{ac} - P(ij) \sum_k (1 - \delta_{kj})f_{kj}t_{ik}^{ab} + \dots \quad [230]$$

To determine the values of the amplitudes, one must solve this set of coupled nonlinear equations iteratively. A simple starting approximation for  $t_i^a$  and  $t_{ij}^{ab}$  on the left-hand sides of the equations may be obtained by setting all the amplitudes on the right-hand side to zero. Hence, for the  $\hat{T}_1$  amplitudes we have

$$t_i^a = f_{ai}/D_i^a \quad [231]$$

and for the  $\hat{T}_2$  amplitudes,

$$t_{ij}^{ab} = \langle ab || ij \rangle / D_{ij}^{ab} \quad [232]$$

This initial guess may then be inserted on the right-hand sides of the equations and subsequently used to obtain new amplitudes. The process is continued until self-consistency is reached. For the special case in which canonical Hartree-Fock molecular orbitals are used, the Fock matrix is diagonal and the  $\hat{T}_2$  amplitude approximation above is exactly the same as the first-order perturbed wavefunction parameters derived from Møller-Plesset theory (cf. Eq. [212]). In that case, the  $D_i^a$  and  $D_{ij}^{ab}$  arrays contain the usual molecular orbital energies, and the initial guess for the  $\hat{T}_1$  amplitudes vanishes.

## Factorization of the Coupled Cluster Equations

The form of Eqs. [152] and [153] is perhaps misleading in that many of the terms appear to be computationally more expensive than is necessary. For example, Eq. [153] contains the following term which is quadratic in the  $\hat{T}_2$  amplitudes:

$$D_{ij}^{ab} t_{ij}^{ab} \leftarrow \frac{1}{4} \sum_{klcd} \langle kl || cd \rangle t_{ij}^{cd} t_{kl}^{ab} \quad [233]$$

where the left arrow indicates that we are examining only one of several terms which contribute to the expression on the left-hand side. This term scales as  $\mathcal{O}(h^4 p^4)$ , where  $h$  denotes the number of occupied orbitals and  $p$  denotes the number of unoccupied orbitals. However, this expression may be factored into a product of two terms, for example,

$$\frac{1}{4} \sum_{klcd} \langle kl || cd \rangle t_{ij}^{cd} t_{kl}^{ab} = \frac{1}{2} \sum_{kl} t_{kl}^{ab} \frac{1}{2} \sum_{cd} \langle kl || cd \rangle t_{ij}^{cd} \equiv \frac{1}{2} \sum_{kl} t_{kl}^{ab} X_{ij}^{kl} \quad [234]$$

where the  $X$  intermediate is defined as

$$X_{ij}^{kl} \equiv \frac{1}{2} \sum_{cd} \langle kl || cd \rangle t_{ij}^{cd} \quad [235]$$

Now the original term may be evaluated in two steps: (1) construction and storage of  $X$ ; and (2) contraction of the  $X$  array with the  $t_{kl}^{ab}$  amplitudes. Each of these steps scales as  $\mathcal{O}(h^4 p^2)$ —a significant reduction from the original  $\mathcal{O}(h^4 p^4)$ .

Every term in the coupled cluster amplitude equations that is nonlinear in  $\hat{T}$  may be factored into linear components. As a result, each step of the iterative solution of the CCSD equations scales at worst as ca.  $\mathcal{O}(N^6)$  (where  $N$  is the number of molecular orbitals). The full CCSDT method in which all  $\hat{T}_3$ -containing terms are included requires an iterative  $\mathcal{O}(N^8)$  algorithm, whereas the CCSD(T) method, which is designed to approximate CCSDT, requires a non-iterative  $\mathcal{O}(N^7)$  algorithm. The inclusion of all  $\hat{T}_4$  clusters in the CCSDTQ method scales as  $\mathcal{O}(N^{10})$ .

The most efficient scheme for factorization of the amplitude equations as described above is not obvious, however, and over the past 20 years numerous researchers have developed sets of intermediates to streamline their own coupled cluster programs.<sup>6–8,11–13,21,22,146,147</sup> Many of these factorizations have been based on careful inspection of the amplitude equations.<sup>6–8,11–13</sup> Scuseria, Janssen, and Schaefer, for example, developed a set of intermediates based on their reformulation of the CCSD amplitude and energy equations<sup>13</sup> in a unitary group formalism designed to offer special efficiency when the refer-

ence wavefunction,  $\Phi_0$ , is a spin-restricted closed-shell Hartree–Fock determinant. Closely related intermediates were utilized in certain open-shell theories developed by Scuseria<sup>27</sup> for the PSI program package<sup>148</sup> and by Knowles, Hampel, and Werner<sup>37</sup> for the MOLPRO package.<sup>149</sup>

Diagrammatic techniques also provide a route to the construction of efficient coupled cluster intermediates.<sup>21,146,147</sup> Kucharski and Bartlett,<sup>147</sup> for example, described a particularly clever approach by which one uses matrix elements of the similarity transformed Hamiltonian as the desired intermediates. Consider the matrix element of  $\bar{H}$  between the reference (on the left) and a singly excited determinant (on the right). Diagrammatically, this matrix element is resolved into two terms as

$$\begin{aligned} \langle \Phi_0 | \bar{H} | \Phi_i^a \rangle &= \text{Diagram A} + \text{Diagram B} \\ &= f_{ia} + \sum_{kc} \langle ik \| ac \rangle t_k^c \quad [236] \\ &\equiv \text{Diagram C} \end{aligned}$$

We have chosen the double bar with the “#” sign in the final diagram to simply denote the sum of the two diagrams corresponding to the matrix element. If we contract this diagram with a  $\hat{T}_2$  operator fragment from below, we obtain two contributions to the  $\hat{T}_1$  amplitude equations, namely,

$$\text{Diagram C} = \text{Diagram D} + \text{Diagram E} \quad [237]$$

The last two diagrams are equivalent to the fifth and twelfth terms from the  $\hat{T}_1$  amplitude equation in Eq. [152]. These intermediates have the particular advantage that, if the final goal of the calculation is actually an analytic energy gradient or an EOM-CCSD-based approach, for example, one need not recompute the required matrix elements of  $\bar{H}$ . Intermediates derived in this manner have been utilized in the coupled cluster programs found in the ACES II<sup>150</sup> and PSI<sup>148</sup> ab initio program packages.

## Matrix-Based Storage of Integrals and Amplitudes

Additional computational efficiency in the solution of the coupled cluster equations may be employed by formulating each of the terms as matrix–matrix or matrix–vector products,<sup>14</sup> for which modern workstations and supercom-

puters are particularly adept.<sup>151</sup> For example, the set of  $\hat{T}_2$  amplitudes,  $t_{ij}^{cd}$ , could be stored as a matrix by defining compound row and column indices  $ij$  and  $cd$ , respectively, in terms of the individual orbital indices  $i$ ,  $j$ ,  $c$ , and  $d$ . Ignoring permutational symmetry, this storage scheme produces a “supermatrix” with  $b^2$  rows and  $p^2$  columns and whose elements may be labeled  $T_2(ij, cd)$ . Similarly, the set of two-electron integrals used in the construction of the  $X$  intermediate above could be stored as a matrix by defining a compound row index  $kl$  and a compound column index  $cd$  to give a supermatrix with elements  $I(kl, cd)$ . The contraction between these matrices given explicitly in Eq. [235] could then be written as a multiplication between the amplitude matrix  $\mathbf{T}_2$  and the transpose of the integral matrix  $\mathbf{I}$  to produce the new matrix  $\mathbf{X}$ :

$$\mathbf{X} = \mathbf{T}_2 \mathbf{I}^+ \quad [238]$$

where the individual elements of  $\mathbf{X}$  may be denoted as  $X(ij, kl)$ . This type of notation is often used in the coupled cluster literature because it provides a much more compact presentation of the energy and amplitude equations than that given above, and it relates directly to a streamlined computer implementation.

## Spatial Symmetry Simplifications

Spatial symmetry also provides a means for improving the efficiency of coupled cluster programs. As shown by the work of Čársky and coworkers,<sup>152</sup> the solution of the coupled cluster equations may be greatly simplified by exploiting constraints on the cluster amplitudes imposed by the point group symmetry of the molecule of interest. In particular, given that the molecular orbital basis is based on symmetry-adapted functions (as is commonly done in ab initio programs such as PSI,<sup>148</sup> ACES II,<sup>150</sup> and MOLPRO<sup>149</sup>), the cluster amplitudes (as well as one- and two-electron integrals) vanish unless the direct product of the irreducible representations (“irreps”) associated with each orbital component contains the totally symmetric irrep. For example, a given  $\hat{T}_2$  amplitude,  $t_{ij}^{ab}$ , is zero unless

$$\Gamma_i \otimes \Gamma_j \otimes \Gamma_a \otimes \Gamma_b = A_1 \quad [239]$$

where  $A_1$  is the totally symmetric irrep of the molecular point group. Since the direct product ( $\otimes$ ) of any irrep with itself always contains  $A_1$ , Eq. [239] implies that, for example,<sup>“</sup>

$$\Gamma_{ij} \equiv \Gamma_i \otimes \Gamma_j = \Gamma_a \otimes \Gamma_b \equiv \Gamma_{ab} \quad [240]$$

---

<sup>“</sup>Of course, other partitionings of the four indices  $i$ ,  $j$ ,  $a$ , and  $b$  are equally valid. For example, the following equality also holds based on Eq. [239]:

$$\Gamma_i = \Gamma_{jab} \equiv \Gamma_j \otimes \Gamma_a \otimes \Gamma_b.$$

If the molecular orbitals are organized such that all orbitals of a given irrep are grouped together, the matrix-based storage scheme described above takes on a particularly convenient form.<sup>14</sup> Using the  $C_{2v}$  point group as an example, the  $T_2$  matrix of Eq. [238] may be schematically written as

		<i>cd</i>			
		$A_1$	$A_2$	$B_1$	$B_2$
$T_2 = ij$	$A_1$	X	0	0	0
	$A_2$	0	X	0	0
	$B_1$	0	0	X	0
	$B_2$	0	0	0	X

where X implies a submatrix of nonzero values, and we have labeled the rows and columns of the supermatrix by the appropriate compound indices  $ij$  and  $cd$ . In addition, we have indicated the  $C_{2v}$  irrep labels for the given compound index. The  $B_2$  label for the  $ij$  row index, for example, denotes the set of  $i$  and  $j$  index combinations with  $\Gamma_{ij} \equiv \Gamma_i \otimes \Gamma_j = B_2$ . If a given amplitude falls within the  $A_2$  diagonal subblock, then the compound indices meet the criterion,  $\Gamma_{ij} = \Gamma_{cd} = A_2$ .

Clearly, one needs to store only the nonzero diagonal subblocks of the matrix above. Assuming that the same number of molecular orbitals belong within each irrep of the point group, this corresponds to memory/disk savings of the order of the group (4 in the case of the  $C_{2v}$  group). Furthermore, if this symmetry scheme were also used to store the X and I matrices of Eq. [238], then the matrix multiplication would be reduced to four independent products involving only the symmetry-restricted diagonal blocks—a computational savings of the square of the order of the point group (16 for  $C_{2v}$ ). This matrix-based approach to symmetry simplification of the coupled cluster equations has been referred to as the “direct product decomposition” (DPD) technique<sup>14</sup> and has been discussed in the literature for both energies<sup>14</sup> and analytic gradients<sup>50</sup> for nondegenerate (Abelian) point groups. In their recent work on coupled cluster analytic second derivatives, Stanton and Gauss have extended their DPD approach for derivatives of cluster amplitudes, which are generally not totally symmetric quantities.<sup>57,58</sup> Furthermore, work on the extension of symmetry methods to include non-Abelian point groups has also been reported.<sup>153–155</sup>

## Spin Factorization of the Coupled Cluster Equations

The coupled cluster and configuration interaction equations presented thus far in this chapter have implicitly used spin-dependent molecular orbitals for their definitions of determinants, integrals, and wavefunction amplitudes.

This spin-orbital formulation has the advantage that it may be used with any set of orbitals, including spin-restricted Hartree–Fock (RHF), spin-unrestricted Hartree–Fock (UHF), spin-restricted open-shell Hartree–Fock (ROHF), quasi-restricted Hartree–Fock (QRHF), and Brueckner orbitals. That is, by inclusion of all components of the spin-orbital Fock matrix,  $\hat{F}_N$ , the CCSD equations in Eqs. [134], [152], and [153], for example, are valid for any choice of orbitals.<sup>v</sup> By assigning the conventional spin functions,  $\alpha$  and  $\beta$ , to each occupied and virtual orbital, we may factor the coupled cluster energy and amplitude equations into their spin-dependent components. Owing to the spin-symmetry associated with the one- and two-electron integrals, most of these components will be zero following spin integration, and may be ignored in the computational implementation of the equations. For example, consider the linear  $\hat{T}_1$  contribution to the CCSD energy given in Eq. [134],

$$E_{\text{CCSD}} \leftarrow \sum_{ia} f_{ia} t_i^a \quad [241]$$

The summation may be factored into a number of spin cases as

$$\begin{aligned} \sum_{ia} f_{ia} t_i^a &= \sum_{i_\alpha a_\alpha} f_{i_\alpha a_\alpha} t_{i_\alpha}^{a_\alpha} + \sum_{i_\beta a_\beta} f_{i_\beta a_\beta} t_{i_\beta}^{a_\beta} + \sum_{i_\alpha a_\beta} f_{i_\alpha a_\beta} t_{i_\alpha}^{a_\beta} + \sum_{i_\beta a_\alpha} f_{i_\beta a_\alpha} t_{i_\beta}^{a_\alpha} \\ &= \sum_{i_\alpha a_\alpha} f_{i_\alpha a_\alpha} t_{i_\alpha}^{a_\alpha} + \sum_{i_\beta a_\beta} f_{i_\beta a_\beta} t_{i_\beta}^{a_\beta} \end{aligned} \quad [242]$$

where the mixed spin terms vanish after spin integration of the Fock matrix integrals over the orthogonal spin functions  $\alpha$  and  $\beta$ . Similarly, the  $\hat{T}_2$  contribution to  $E_{\text{CCSD}}$  may be factored into three nonvanishing spin cases, namely,

$$\begin{aligned} \frac{1}{4} \sum_{ijab} \langle ij \| ab \rangle t_{ij}^{ab} &= \frac{1}{4} \sum_{i_\alpha j_\alpha a_\alpha b_\alpha} \langle i_\alpha j_\alpha \| a_\alpha b_\alpha \rangle t_{i_\alpha j_\alpha}^{a_\alpha b_\alpha} + \frac{1}{4} \sum_{i_\beta j_\beta a_\beta b_\beta} \langle i_\beta j_\beta \| a_\beta b_\beta \rangle t_{i_\beta j_\beta}^{a_\beta b_\beta} \\ &\quad + \sum_{i_\alpha j_\beta a_\alpha b_\beta} \langle i_\alpha j_\beta \| a_\alpha b_\beta \rangle t_{i_\alpha j_\beta}^{a_\alpha b_\beta} \end{aligned} \quad [243]$$

where we have used the permutational antisymmetry of the cluster amplitudes and the two-electron integrals to simplify the nonzero mixed spin cases into a single term. Similar factorization of the  $\hat{T}_1$  and  $\hat{T}_2$  amplitude equations is possible. To avoid wasted storage and computation of the many vanishing

<sup>v</sup>Although a spin-orbital formulation is conceptually simple, desirable properties such as spin-adaptation may be lost when the electronic state of interest is open shell, for example. A rigorously spin-adapted theory must include spin-free definitions of the cluster operators,  $\hat{T}$ , and an appropriate (perhaps multideterminant) reference wavefunction (Refs. 39, 41, 42, 156–158). Such general coupled cluster derivations are beyond the scope of this chapter, though some of the issues associated with difficult open-shell problems are discussed in the next section.

amplitudes, the most computationally efficient implementation of the CCSD equations must take these factorizations into account.

### Atomic-Orbital-Basis Algorithms

The iterative procedure for solving the amplitude equations described above requires storage of a number of quantities, including  $\hat{T}_1$  and  $\hat{T}_2$  amplitudes, as well as one- and two-electron integrals in the molecular orbital (MO) basis. Of these, the set of two-electron integrals involving four virtual orbitals (e.g.,  $\langle ab||cd\rangle$ ) requires the most disk space and quickly becomes the computational bottleneck as the size of the basis set is increased. One way of circumventing this problem is to avoid the transformation and storage of this integral class completely and to instead evaluate their contribution to the  $\hat{T}_2$  amplitude equation (cf. Eq. [153]),

$$t_{ij}^{ab} \leftarrow \sum_{cd} t_{ij}^{cd} \langle ab||cd \rangle \quad [244]$$

using the two-electron integrals in the atomic-orbital (AO) [or, symmetry-orbital (SO)] basis. The advantage is that, unlike the MO basis functions, the AO functions are often strongly localized at the atomic centers and, as a result, only a fraction of the total number of associated two-electron integrals are nonzero for large basis sets. The outline of this AO-basis algorithm may become clearer if we rewrite Eq. [244] in terms of the untransformed integrals:

$$t_{ij}^{ab} \leftarrow \sum_{cd} t_{ij}^{cd} \sum_{\mu\nu\lambda\sigma} C_\mu^a C_\nu^b C_\lambda^c C_\sigma^d \langle \mu\nu||\lambda\sigma \rangle \quad [245]$$

where the indices  $\mu$ ,  $\nu$ ,  $\lambda$ , and  $\sigma$  are used to denote AO-basis functions, and, for convenience, we assume that the MO-basis transformation coefficients such as  $C_\mu^a$  are real. Reordering the summations in this equation we obtain

$$t_{ij}^{ab} \leftarrow \sum_{\mu\nu} C_\mu^a C_\nu^b \sum_{\lambda\sigma} \langle \mu\nu||\lambda\sigma \rangle \sum_{cd} C_\lambda^c C_\sigma^d t_{ij}^{cd} \quad [246]$$

The last summation may be interpreted as the “back-transformation” of the two virtual indices on the  $\hat{T}_2$  amplitude into the AO basis, that is,

$$t_{ij}^{\lambda\sigma} = \sum_{cd} C_\lambda^c C_\sigma^d t_{ij}^{cd} \quad [247]$$

If this set of “half-AO” amplitudes is computed and stored (using two standard  $\mathcal{O}(N^5)$  steps<sup>159</sup>), the amplitudes may be subsequently contracted with the AO-basis integrals to give

$$t_{ij}^{\mu\nu} = \sum_{\lambda\sigma} \langle \mu\nu || \lambda\sigma \rangle t_{ij}^{\lambda\sigma} \quad [248]$$

which requires an  $\mathcal{O}(N^6)$  algorithm. The final summation is then evaluated to transform the final half-AO amplitudes back to the MO basis to obtain the complete contribution to  $\hat{T}_2$ ,

$$t_{ij}^{ab} \leftarrow \sum_{\mu\nu} C_{\mu}^a C_{\nu}^b t_{ij}^{\mu\nu} \quad [249]$$

A similar procedure may be constructed for terms involving three virtual index integrals,  $\langle ab || ci \rangle$ .<sup>160</sup>

AO-basis algorithms have been exploited for many years in the construction of correlated wavefunctions,<sup>161</sup> particularly in MBPT(2).<sup>154,162</sup> In coupled cluster theory, a number of approaches have recently been discussed in the literature. For example, Hampel, Peterson, and Werner<sup>160</sup> have reported an efficient implementation of the Brueckner-orbital-based CCD method that avoids the transformation and storage of the  $\langle ab || cd \rangle$  integrals and computes the appropriate contributions as described above. Koch, Helgaker, Christiansen, and coworkers<sup>163,164</sup> have carried the approach even further by avoiding storage of even the AO-basis two-electron integrals and computing limited distributions of these “on the fly” as they are needed. Their largest single-point CCSD energy calculations using this algorithm have involved more than 500 basis functions.<sup>164</sup> Rendell and Lee<sup>165</sup> have taken a somewhat different tack in CCSD(T) energy calculations by approximating the  $\langle ab || ci \rangle$  and  $\langle ab || cd \rangle$  integrals via a “resolution of the identity” technique. In their approach, a set of auxiliary functions is used to rewrite these four-center electron repulsion integrals as products of three-center integrals, which require significantly less storage space. Finally, we note that AO-basis techniques have proven to be vital to the recent work of Stanton and Gauss on analytic second derivatives for a number of correlated techniques, including SDQ-MBPT(4), CCSD, and CCSD(T).<sup>57,58</sup>

---

## CURRENT RESEARCH AND FUTURE DIRECTIONS

In this final section, we examine in detail a number of recent research efforts in coupled cluster theory. This review is far from exhaustive, and because of space considerations, we choose to focus primarily on two specific areas in which the present authors have made contributions. We will then discuss some of the most important theoretical and computational advances expected in the near future. We also recommend Refs. 78 and 79 for a discussion of other recent work.

## Coupled Cluster Theory for Open-Shell Molecules

For the closed-shell electronic states of many small molecules, the task of determining molecular properties is generally well understood, and coupled cluster methods—particularly the CCSD(T) approach—in conjunction with large basis sets, have been found to give exceptionally accurate results relative to experiment for properties such as molecular geometries, harmonic vibrational frequencies, infrared intensities, and electric dipole moments.<sup>78,79,137,138,166</sup> The potential energy surfaces of open-shell species,<sup>w</sup> on the other hand, often present serious computational problems. In the most widely used open-shell CCSD(T) approaches,<sup>27,35,51</sup> a calculation for a radical cation, for example, requires approximately *three times* the computational effort of its closed-shell counterpart, even if a spin-restricted open-shell Hartree–Fock (ROHF) determinant is chosen as the reference wavefunction. This difficulty is due to an unbalanced exchange interaction between open- and closed-shell electrons such that the Fock matrix, which appears in the spin-orbital coupled cluster expressions presented in Eqs. [152] and [153], contains *different*  $\alpha$  and  $\beta$  components. As a result, the cluster operators may be factored into two different spin cases for  $\hat{T}_2$  ( $t_{i_\alpha j_\alpha}^{a_\alpha b_\alpha}$ ,  $t_{i_\beta j_\beta}^{a_\beta b_\beta}$ , and  $t_{i_\alpha j_\beta}^{a_\alpha b_\beta}$ ).

Several researchers have recently devoted considerable effort to the derivation and efficient implementation of techniques based on spin-restricted reference determinants that reduce the computational discrepancy between closed- and open-shell systems.<sup>33,38,171–173</sup> This emphasis on spin-restricted techniques has resulted in part from a bias toward reference wavefunctions that maintain the spin symmetry of the exact wavefunction (such as the ROHF determinant), but also because of the possible efficiency advantages of spin-restricted methods over unrestricted techniques. Thus, since the component molecular orbitals are constrained to have identical spatial parts for each spin function, it should be possible to construct the correlated wavefunction in a manner that takes advantage of this symmetry.

It should be noted, however, that the use of a spin-symmetry-adapted determinant such as the ROHF wavefunction as a reference in a coupled cluster calculation does produce a spin-pure energy,<sup>x</sup> but does not imply that the correlated wavefunction itself is an eigenfunction of  $\hat{S}^2$  as well.<sup>27,35</sup> For the spin-orbital definition of  $\hat{T}$  described here, spin contamination can still enter into the coupled cluster wavefunction through the nonlinear contributions of cluster operators to the amplitude equations,<sup>37</sup> though the importance of this

<sup>w</sup>We emphasize that the present discussion focuses only on *high-spin* open-shell systems to which a single-determinant reference wavefunction is applicable. Coupled cluster techniques for low-spin cases, such as open-shell singlets, have been pursued in the literature for many years, however, and provide a fertile area of research (Refs. 158, 167–170).

<sup>x</sup>The ROHF-CCSD energy is indeed completely spin-projected, as discussed in Refs. 35, 27, and 37, but is still different from that computed using a spin-adapted coupled cluster wavefunction.

contamination has been questioned.<sup>174</sup> A great deal of effort has been devoted recently to the efficient construction of spin-adapted open-shell coupled cluster wavefunctions and/or correct spin expectation value equations.<sup>36–42,158</sup>

### Spin-Restricted Triple-Excitation Corrections

The (T) correction discussed earlier beginning with the presentation of Eq. [214] is derived via a perturbational decomposition of the coupled cluster energy and amplitude equations. This decomposition depends on a particular partitioning of the electronic Hamiltonian,  $\hat{H}_N$ , into a zeroth-order component and a fluctuation potential—that is, a particular definition of many-body perturbation theory. When based upon the canonical Hartree–Fock orbitals of an RHF or UHF reference determinant, this partitioning is simple, and  $\hat{H}^{(0)}$  is taken to be the (diagonal) Fock matrix. For ROHF reference wavefunctions, however, the choice of partitioning is less obvious, and a variety of spin-restricted open-shell theories have been reported in the literature in recent years.<sup>127–134,175</sup> For example, in the RMP<sup>129</sup> or ROHF-MBPT<sup>130</sup> method, the diagonal occupied and virtual blocks of the Fock operator are chosen as  $\hat{H}^{(0)}$ , and the off-diagonal occupied-virtual blocks are included in  $\hat{H}^{(1)}$  along with  $\hat{V}_N$ . The resulting perturbed energy and wavefunction equations have much in common with the conventional ROHF-CCSD energy and amplitude equations, leading to a convenient form for the ROHF-CCSD(T) method.<sup>29</sup> One drawback of this approach, however, is that the off-diagonal  $f_{ij}$  and  $f_{ab}$  components of the Fock matrix (contained in the first and second diagrams in Figure 2) are nonzero. Thus, Eq. [224] presented earlier takes on a more general form,<sup>29,31</sup>

$$\begin{aligned} D_{ijk}^{abc} t_{ijk}^{abc} = & P(i/jk)P(a/bc) \left[ \sum_d \langle bc || di \rangle t_{jk}^{ad} - \sum_i \langle la || jk \rangle t_{il}^{bc} + t_i^a \langle bc || jk \rangle + f_{ia} t_{jk}^{bc} \right] \\ & - P(i/jk) \sum_l (1 - \delta_{il}) f_{il} t_{jkl}^{abc} + P(a/bc) \sum_d (1 - \delta_{ad}) f_{ad} t_{ijk}^{bcd} \end{aligned} \quad [250]$$

The presence of  $f_{il}$  and  $f_{ad}$  components requires an iterative solution of this equation—an approach that necessitates storage of the  $\hat{T}_3$  amplitudes in each iteration! This scheme is unreasonable because the number of such amplitudes would rapidly become the computational bottleneck as the size of the molecular system increased. This problem may be circumvented, however, by utilizing the so-called semicanonical molecular orbital basis in which the occupied-occupied and virtual-virtual blocks of the Fock matrix are diagonal.<sup>29,129,130</sup> In this basis, the two final terms in the  $\hat{T}_3$  equation above vanish, and the conventional noniterative computational procedure described earlier in the chapter may be employed.

The use of semicanonical orbitals does have a drawback, however, in that one is necessarily forced to use a computational procedure comparable to that

of the UHF-CCSD(T) approach. Since the ROHF-based spin-orbital Fock matrix contains different  $\alpha$  and  $\beta$  components, rotation to the semicanonical basis breaks the spin restriction on the molecular orbitals.<sup>7</sup> Thus, the integrals used in Eq. [250] are broken into UHF-like  $\alpha - \alpha$ ,  $\beta - \beta$ , and  $\alpha - \beta$  spin cases with a requisite threefold increase in storage requirements.

This problem can be avoided, however, if an appropriate open-shell perturbation theory is defined such that the zeroth-order Hamiltonian is diagonal in the truly spin-restricted molecular orbital basis. The “Z-averaged” perturbation theory (ZAPT) defined by Lee and Jayatilaka<sup>132</sup> fulfills this requirement. ZAPT takes advantage of the symmetric spin orbital basis. For each doubly occupied spatial orbital and each unoccupied spatial orbital, the usual  $\alpha$  and  $\beta$  spin functions are used, but for the singly occupied orbitals, new spin functions,

$$\sigma^+ = \frac{1}{\sqrt{2}}(\alpha + \beta) \quad [251]$$

and

$$\sigma^- = \frac{1}{\sqrt{2}}(\alpha - \beta) \quad [252]$$

are assigned. By convention,  $\sigma^+$  functions are associated with occupied spin orbitals, and  $\sigma^-$  functions with unoccupied spin orbitals. In this basis, the spin orbital Fock operator takes on the schematic form,

$$\hat{F}^{\text{ZAPT}} = \begin{matrix} d_\alpha & \left| \begin{array}{cccccc} \hat{F}_{L\alpha}^{M\alpha} & \hat{F}_{L\beta}^{M\alpha} & \hat{F}_{T\sigma^+}^{L\alpha} & 0 & 0 & \hat{F}_{L\alpha}^{D\beta} \\ \hat{F}_{L\beta}^{M\alpha} & \hat{F}_{L\alpha}^{M\alpha} & \hat{F}_{T\sigma^+}^{L\alpha} & 0 & \hat{F}_{L\alpha}^{D\beta} & 0 \\ \hat{F}_{T\sigma^+}^{L\alpha} & \hat{F}_{T\sigma^+}^{L\alpha} & \hat{F}_{T\sigma^+}^{U\sigma^+} & 0 & 0 & 0 \end{array} \right| \\ d_\beta & \\ s_{\sigma^+} & \\ \hat{F}^{\text{ZAPT}} = s_{\sigma^-} & \left| \begin{array}{cccccc} 0 & 0 & 0 & \hat{F}_{T\sigma^-}^{U\sigma^-} & \hat{F}_{T\sigma^-}^{D\alpha} & -\hat{F}_{T\sigma^-}^{D\alpha} \\ 0 & \hat{F}_{L\alpha}^{D\beta} & 0 & \hat{F}_{T\sigma^-}^{D\alpha} & \hat{F}_{D\alpha}^{E\alpha} & \hat{F}_{D\alpha}^{E\beta} \\ \hat{F}_{L\alpha}^{D\beta} & 0 & 0 & -\hat{F}_{T\sigma^-}^{D\alpha} & \hat{F}_{D\alpha}^{E\beta} & \hat{F}_{D\alpha}^{E\alpha} \end{array} \right| \\ v_\alpha & \\ v_\beta & \end{matrix} \quad [253]$$

where capital letters  $L$  and  $M$  denote doubly occupied spatial orbitals,  $T$  and  $U$  denote singly occupied spatial orbitals, and  $D$  and  $E$  denote unoccupied spatial orbitals. Using a standard definition of ROHF orbitals, the diagonal blocks of

---

<sup>7</sup>This diagonalization affects neither the ROHF determinant itself nor the ROHF or CCSD energies, owing to the well-known invariance of those methods with respect to certain classes of orbital rotations (Ref. 134).

this Fock matrix are themselves diagonal when the theory is applied to conventional high-spin, open-shell systems.<sup>132,134</sup>

With the diagonal blocks of the Fock operator above taken as the ZAPT zeroth-order Hamiltonian, the various excitation operators of coupled cluster theory may be decomposed into perturbational orders, as described earlier in the chapter. The same  $\hat{T}_3$  contributions used to define the conventional (T) correction can then be constructed to produce a ZAPT-based triples correction—denoted (zT).<sup>33</sup> This analysis is complicated by the fact that the theory requires one to distinguish the singly occupied orbitals from the doubly occupied and unoccupied orbitals. Hence, the particle–hole formalism used throughout this chapter must be generalized such that there are two types of hole (doubly occupied and singly occupied) and two types of particle (unoccupied and singly occupied). The tedious algebraic approach to the derivation of the (zT) correction was carried out in Ref. 33 by the construction of a symbolic manipulation program (designed for the Mathematica interface<sup>176</sup>) for the application of Wick's theorem to second-quantized operator strings. This program is described in detail in Ref. 118. The related diagrammatic analysis involves essentially the same rules outlined earlier in the chapter with the complication that cluster operators and Hamiltonian fragments must be factored such that the diagrams differentiate between the two types of hole and particle lines. The rather complicated equations for the (zT) correction are presented in an Appendix in Ref. 33.

The performance of the (zT) correction is essentially identical to that of the conventional ROHF-CCSD(T) method. Application of both to a series of diatomic molecules in ground and excited states indicates insignificant differences between the two in the prediction of bond lengths, harmonic vibrational frequencies, anharmonic constants, and so on. Unfortunately, the complicated equations associated with the (zT) correction have thus far precluded its large scale implementation and, as a result, further systematic studies involving larger basis sets have not yet been carried out.

## Brueckner Orbitals in Coupled Cluster Theory

In 1958, Nesbet extended Brueckner's theory for infinite nuclear matter<sup>177</sup> to nonuniform systems of atoms and molecules.<sup>178</sup> By consideration of the CISD problem in which the electronic Hamiltonian is diagonalized within the basis of the reference and all singly and doubly excited determinants, Nesbet explained that Brueckner theory allows one to construct a set of orthonormal molecular orbitals for which the correlated wavefunction coefficients for all singly excited determinants vanish. Unfortunately, the construction of the set of orbitals that fulfill this “Brueckner condition” can be determined only a posteriori from the single excitation coefficients computed in a given orbital basis. As a result, the practical implementation of Brueckner-orbital-based methods has

usually required the repeated construction of the correlated wavefunction (along with the associated integral transformation). Despite this drawback, Brueckner orbitals have found new life within coupled cluster theory in recent years.<sup>173,179–192</sup> In 1981, Chiles and Dykstra<sup>179</sup> introduced the first molecular application of the Brueckner coupled cluster doubles (B-CCD) method, which they referred to as CCD( $\hat{T}_1=0$ ). Some years later, Handy and coworkers<sup>182–184</sup> also implemented B-CCD energies, along with a perturbational triple-excitation correction [known as B-CCD(T)] and analytic energy gradients. Since these important theoretical developments, perhaps the most significant work in this area has been reported by Hampel, Peterson, and Werner,<sup>160</sup> who explained that the special form of the B-CCD amplitude equations allows one to avoid the repeated transformation of certain classes of two-electron integrals. This advantage, when coupled to specially designed extrapolation schemes that converge the Brueckner orbitals and cluster amplitudes simultaneously, permits significant reduction in the computational expense of the method, such that B-CCD may cost no more than a conventional CCSD calculation.

Perhaps the greatest need for Brueckner-orbital-based methods arises in systems suffering from artificial symmetry-breaking orbital instabilities,<sup>140,193–196</sup> where the approximate wavefunction fails to maintain the selected spin and/or spatial symmetry characteristics of the exact wavefunction. Such instabilities arise in SCF-like wavefunctions as a result of a competition between valence-bond-like solutions to the Hartree–Fock equations; these solutions typically allow for localization of an unpaired electron onto one of two or more symmetry-equivalent atoms in the molecule. In the ground  $^2\Pi_g$  state of  $O_2^-$ , for example, a pair of symmetry-broken Hartree–Fock wavefunctions may be constructed with the unpaired electron localized onto one oxygen atom or the other. Though symmetry-broken wavefunctions have sometimes been exploited to produce providentially correct results in a few systems, they are often not beneficial or even acceptable,<sup>197</sup> and the question of whether to relax constraints in the presence of an instability was originally described by Löwdin as the “symmetry dilemma.”<sup>198</sup>

The effects of symmetry-breaking orbital instabilities on properties computed using correlated wavefunctions built from a single-determinant reference has recently been investigated<sup>140</sup> for a number of finite-order MBPT and coupled cluster methods. Owing to a corresponding singularity in the molecular orbital Hessian,<sup>193,196,199–201</sup> nearby orbital instabilities can produce sometimes dramatically distorted results for second-order properties such as harmonic vibrational frequencies and polarizabilities. However, one important conclusion of Ref. 140 is that the choice of reference wavefunction can significantly affect the location of this Hessian singularity on the potential energy surface, and, as a result, a properly selected set of molecular orbitals can often eliminate the symmetry-breaking problem by moving the instability out of the region of interest. In recent years, Brueckner orbitals have been utilized in conjunction with coupled cluster theory for precisely this purpose for a number

of “difficult” molecular systems,<sup>185,186,202–205</sup> such as the nitrate radical,<sup>186</sup> the O<sub>4</sub><sup>+</sup> ion,<sup>192,202</sup> the hydrogen peroxide radical cation,<sup>203,204</sup> and the C<sup>2</sup>A<sub>2</sub> excited state of NO<sub>2</sub>.<sup>205</sup>

The implementation of B-CC methods for open-shell systems (where symmetry-breaking instabilities are the most likely to occur<sup>195</sup>) is straightforward when either a UHF or an ROHF reference wavefunction is used as the initial guess for the Brueckner determinant. Unfortunately in the ROHF case, it is not possible to maintain spin restriction on the molecular orbitals because the single-excitation amplitudes, which may be used as the rotation parameters for the iterative construction of the Brueckner orbitals, are not symmetric in the spin indices owing to the uneven exchange interaction between the open- and closed-shell electrons discussed earlier. As a result, the repeated construction of the coupled cluster wavefunction requires the transformation and storage of roughly three times the number of two-electron integrals needed for the initial ROHF-CCSD calculation. This difficulty, which is directly comparable to the problem of semicanonical orbitals described in the last section, represents a significant obstacle for open-shell B-CCD implementations.

The symmetric spin-orbital basis, which was also used to construct the spin-restricted (zT) correction, also provides a route to a spin-restricted open-shell B-CC theory (RB-CC).<sup>173</sup> In this spin basis, the  $\hat{T}_1$  amplitudes may be shown to have the symmetries

$$t_{I_\alpha}^{A_\beta} = t_{I_\beta}^{A_\alpha} \quad [254]$$

$$t_{I_\alpha}^{A_\alpha} = t_{I_\beta}^{A_\beta} \quad [255]$$

$$t_{I_\alpha}^{W_{\sigma^-}} = -t_{I_\beta}^{W_{\sigma^-}} \quad [256]$$

and

$$t_{W_\sigma^{\alpha}}^{A_\beta} = t_{W_\sigma^{\beta}}^{A_\alpha} \quad [257]$$

where  $I$ ,  $A$ , and  $W$  indicate doubly occupied, unoccupied, and singly occupied spatial orbitals, respectively. The “spin-flip”  $\hat{T}_1$  amplitudes of the type  $t_{I_\alpha}^{A_\beta}$  are generally nonzero in the symmetric spin-orbital basis, but it may be argued<sup>132</sup> that these amplitudes should instead be classified as double excitations. The remaining three classes of  $\hat{T}_1$  amplitudes may be used to carry out a series of first-order rotations among the orbital subspaces, namely,

$$\tilde{\phi}_I = \phi_I + t_{I_\alpha}^{A_\alpha} \phi_A + t_{I_\alpha}^{W_{\sigma^-}} \phi_W \quad [258]$$

$$\tilde{\phi}_W = \phi_W + t_{W\sigma^+}^{A_\alpha} \phi_A - t_{I_\alpha}^{W\sigma^-} \phi_I \quad [259]$$

At convergence, the orbitals will obey the Brueckner conditions

$$t_{I_\alpha}^{A_\alpha} = t_{W\sigma^+}^{A_\alpha} = t_{I_\alpha}^{W\sigma^-} = 0 \quad [260]$$

These equations provide the basis for the RB-CC method, since they do not imply any loss of spin restriction on the molecular orbitals as the rotation is applied. Furthermore, the RB-CC method may be trivially implemented within existing ROHF-CCSD programs by a simple “symmetrization” of the standard  $(\alpha, \beta) \tilde{T}_1$  amplitudes into the new spin basis<sup>173</sup> prior to the rotation.

The performance of the RB-CCD method (which is analogous to the conventional unrestricted B-CCD method) has been tested on the nitrate radical, NO<sub>3</sub>, and the  $\tilde{C}^2A_2$  state of NO<sub>2</sub>, both of which have presented difficulties for a variety of theoretical methods due in part to symmetry-breaking instabilities in the Hartree–Fock reference wavefunction. The RB-CCD method was found to provide results in excellent agreement with the B-CCD method, including the correct prediction of  $C_s$  symmetry for the equilibrium geometry of the  $\tilde{C}$  state of NO<sub>2</sub>.<sup>205,206</sup> Work is presently under way for extension of the RB-CCD method to include triples [i.e., a RB-CCD(T) method where the triples correction is defined similarly to the (zT) correction described above] and analytical energy gradients.

## Future Research Prospects

Thanks in part to the computational advances described in the preceding section, coupled cluster theory has developed into arguably the most accurate and computationally affordable method of modern computational quantum chemistry. The results of coupled cluster calculations are commonly found in the chemical physics literature, and, when the accuracy of experimental results is questioned, the CCSD(T) method is often used to settle the debate. In spite of this success, coupled cluster theory is far from applicable to all problems of chemical interest. The majority of the current research efforts may be divided into four overlapping categories:

- **Large molecules and extended systems.** As noted near the beginning of the section on Factorization of Coupled Cluster Equations, the CCSD(T) method scales as  $\mathcal{O}(N^7)$ , where  $N$  is the number of basis functions. This implies that a factor of two increase in the size of the molecular system involves a ca. 128 increase in the CPU cost of the calculation. For example, a high accuracy CCSD(T) energy calculation for the amino acid alanine requires approximately 5 days on modern workstations; an equivalent calculation for the alanine dimer would require nearly *two years* to complete. In addition, the storage requirements of the CCSD(T) method scale roughly as  $\mathcal{O}(N)^4$ , leading to rapidly insurmountable disk space limitations as the size of the system increases. Our own

recent CCSD(T) calculations on isomers of [10]annulene (molecular formula C<sub>10</sub>H<sub>10</sub>) involving more than 300 basis functions and low symmetry may represent the current limit of “conventional” coupled cluster programs.<sup>207</sup>

One of the most promising approaches to overcoming the scaling problems of the coupled cluster method lies in the local correlation concept developed primarily by Sæbø and Pulay.<sup>208–212</sup> This scheme relies on the use of a set of localized, nonorthogonal molecular orbitals to drastically reduce the number of nonnegligible parameters in the correlated wave function. Some effort in this direction has been reported by Hampel and Werner,<sup>213</sup> and it is likely that new implementations and extensions of the “local-CC” method will appear in the next few years. In addition, the storage bottleneck associated with large molecules has been examined by several researchers, leading to “integral direct”<sup>163,164</sup> and “resolution of the identity” methods,<sup>165</sup> described earlier in the section on Atomic-Orbital-Basis Algorithms.

- **Excited electronic states.** One deficiency of the conventional coupled cluster methods is that they apply only to ground electronic states (or, more accurately, to the lowest energy states of a given spin and spatial symmetry). The equation-of-motion coupled cluster method<sup>5,60–63,65</sup> and related methods such as SAC-CI<sup>106–108</sup> and STEOM-CC<sup>74,114</sup> have been devised such that higher lying electronic states may be studied. These methods have proven to provide reliable accuracy (on the order of 0.2 eV) in the prediction of electronic excitation spectra for states that are well described by promotion of a single electron from the ground state. Perhaps the most important work in excited state coupled cluster theory in the next several years will be the development of methods for treating “doubly excited” states and the improvement of the accuracy of EOM-CC to better than 0.1 eV through extension of existing methods for the efficient inclusion of triply excited determinants in the diagonalization space of  $\bar{H}$ .<sup>70,71,105,214–217</sup>

- **Potential energy surfaces.** All coupled cluster methods depend implicitly upon a reference wavefunction (usually the single-configuration Hartree–Fock determinant). However, for cases in which this reference fails dramatically, even the CCSD(T) method cannot be expected to provide reliable results. Bond breaking provides an excellent example of this behavior; as a  $\sigma$  bond is separated, for instance, a single determinant fails to properly include both electronic configurations [ $(\sigma)^2$  and  $(\sigma^*)^2$ ] needed to describe the dissociation process with even qualitative accuracy. Since a complete potential energy surface is vital to research efforts in reaction dynamics, for instance, much effort has been devoted to the construction of multireference coupled cluster (MRCC) schemes based primarily on multiconfigurational SCF (MCSCF) reference wavefunctions.<sup>76,78,125,218–223</sup> Of particular interest is the work by Piecuch, Adamowicz, and coworkers,<sup>218,219,223</sup> in which a MRCCSD wavefunction, for example, is obtained via selected triple and quadruple excitations from a full CCSDTQ wavefunction constructed from a single electronic configuration. This approach is similar to that used earlier in multireference configuration

interaction methods.<sup>86,224</sup> By retaining a single-determinant reference formalism, one avoids many of the difficulties of a “true” MCSCF-based approach, and automated techniques for the construction of higher excitation levels (i.e., beyond quadruples) are promising. In addition, multideterminantal coupled cluster methods such as the unitary group approach<sup>39,158,167,168</sup> have been actively pursued in recent years<sup>41,42,169,170</sup> for describing biradicals and other “low-spin” electronic states for which a single-determinant reference is inadequate.

- **High accuracy methods.** For properties such as dissociation and fragmentation energies, coupled cluster theory used in conjunction with large basis sets is often expected to provide “chemical accuracy,” that is,  $\pm 1$  kcal/mol. In recent years, many researchers have asked what would be required to obtain “spectroscopic accuracy,” that is,  $\pm 1$  cm<sup>-1</sup>.<sup>z</sup> It has been shown in numerous studies in the past decade<sup>226–231</sup> that the convergence of the coupled cluster (as well as CI and perturbation theory) energies toward a “basis set limit” is much slower than that possible with Hartree–Fock. That is, for a given level of electron correlation (e.g., CCSD), one must use much more complete basis sets (perhaps including high levels of orbital angular momentum, *s*, *p*, *d*, *f*, etc.) relative to Hartree–Fock before additional improvements to the basis set make no significant contributions to the computed energy. The source of this problem is a well-known failure by correlated techniques such as coupled cluster when used with common Gaussian-type basis functions to describe the behavior of many-electron wavefunctions as electrons approach one another closely.<sup>232</sup> One technique for overcoming this difficulty is to include terms that explicitly involve the interelectronic distance,  $1/r_{12}$ , in the correlated wavefunction. When applied in coupled cluster theory, such an approach has the advantage that the conventional formalism and implementation remain largely intact, with a number of sophisticated modifications needed to account for the additional mathematical term(s). The recent work on the linear  $r_{12}$ -CCSD method by Klopper, Kutzelnigg, Noga, and coworkers<sup>232</sup> and on Gaussian geminals by Persson and Taylor<sup>229</sup> is promising, and further impressive developments are likely to be reported in the next several years.

---

## ACKNOWLEDGMENTS

Our understanding of coupled cluster theory as described in this chapter has been cultivated by conversations and collaborations with numerous colleagues over the past several years. In particular, we would like to acknowledge many fruitful interactions with Professor John F. Stanton of the University of Texas, Dr. Timothy J. Lee of NASA Ames Research Center, Professor Marcel

---

<sup>z</sup>It should be noted that the goal of true spectroscopic accuracy may be unattainable because of the implicit errors associated with the use of a Born–Oppenheimer, nonrelativistic Hamiltonian to describe molecular systems (Ref. 225).

Nooijen of Princeton University, and Professor Rodney J. Bartlett of the University of Florida. We thank Sullivan Beck of the University of Florida for the use of his diag program used to typeset the many diagrams in the chapter. We also thank Drs. Rollin A. King and Matthew L. Leininger of the University of Georgia and Dr. C. David Sherrill of the University of California at Berkeley for their critical reading of the manuscript. Finally, TDC wishes to express his sincere appreciation to Emily A. Crawford for her work in the development of the contract LaTeX package for typesetting complicated Wick's theorem expressions, and for her patience and support during the preparation of the manuscript.

---

## REFERENCES

1. J. Čížek, *J. Chem. Phys.*, **45**, 4256 (1966). On the Correlation Problem in Atomic and Molecular Systems. Calculation of Wavefunction Components in Ursell-Type Expansion Using Quantum-Field Theoretical Methods.
2. J. Čížek, *Adv. Chem. Phys.*, **14**, 35 (1969). On the Use of the Cluster Expansion and the Technique of Diagrams in Calculations of Correlation Effects in Atoms and Molecules.
3. J. Čížek and J. Paldus, *Int. J. Quantum Chem.*, **5**, 359 (1971). Correlation Problems in Atomic and Molecular Systems. III. Rederivation of the Coupled-Pair Many-Electron Theory Using the Traditional Quantum Chemical Methods.
4. A. C. Hurley, *Electron Correlation in Small Molecules*, Academic Press, London, 1976.
5. H. J. Monkhorst, *Int. J. Quantum Chem. Symp.*, **11**, 421 (1977). Calculation of Properties with the Coupled-Cluster Method.
6. J. A. Pople, R. Krishnan, H. B. Schlegel, and J. S. Binkley, *Int. J. Quantum Chem. Symp.*, **14**, 545 (1978). Electron Correlation Theories and Their Application to the Study of Simple Reaction Potential Surfaces.
7. R. J. Bartlett and G. D. Purvis, *Int. J. Quantum Chem.*, **14**, 561 (1978). Many-Body Perturbation Theory, Coupled-Pair Many-Electron Theory, and the Importance of Quadruple Excitations for the Correlation Problem.
8. G. D. Purvis and R. J. Bartlett, *J. Chem. Phys.*, **76**, 1910 (1982). A Full Coupled-Cluster Singles and Doubles Model: The Inclusion of Disconnected Triples.
9. G. D. Purvis and R. J. Bartlett, *J. Chem. Phys.*, **75**, 1284 (1981). The Reduced Linear Equation Method in Coupled Cluster Theory.
10. G. E. Scuseria, T. J. Lee, and H. F. Schaefer, *Chem. Phys. Lett.*, **130**, 236 (1986). Accelerating the Convergence of the Coupled-Cluster Approach. The Use of the DIIS Method.
11. G. E. Scuseria, A. C. Scheiner, T. J. Lee, J. E. Rice, and H. F. Schaefer, *J. Chem. Phys.*, **86**, 2881 (1987). The Closed-Shell Coupled-Cluster Single and Double Excitation (CCSD) Model for the Description of Electron Correlation. A Comparison with Configuration Interaction (CISD) Results.
12. T. J. Lee and J. E. Rice, *Chem. Phys. Lett.*, **150**, 406 (1988). An Efficient Closed-Shell Singles and Doubles Coupled-Cluster Method.
13. G. E. Scuseria, C. L. Janssen, and H. F. Schaefer, *J. Chem. Phys.*, **89**, 7382 (1988). An Efficient Reformulation of the Closed-Shell Coupled-Cluster Single and Double Excitation (CCSD) Equations.
14. J. F. Stanton, J. Gauss, J. D. Watts, and R. J. Bartlett, *J. Chem. Phys.*, **94**, 4334 (1991). A Direct Product Decomposition Approach for Symmetry Exploitation in Many-Body Methods. I. Energy Calculations.
15. R. J. Bartlett, H. Sekino, and G. D. Purvis, *Chem. Phys. Lett.*, **98**, 66 (1983). Comparison of MBPT and Coupled-Cluster Methods with Full CI. Importance of Triplet Excitations and Infinite Summations.
16. Y. S. Lee, S. A. Kucharski, and R. J. Bartlett, *J. Chem. Phys.*, **81**, 5906 (1984). A Coupled-Cluster Approach with Triple Excitations.

17. J. A. Pople, M. Head-Gordon, and K. Raghavachari, *J. Chem. Phys.*, **87**, 5968 (1987). Quadratic Configuration Interaction. A General Technique for Determining Electron Correlation Energies.
18. M. Urban, J. Noga, S. J. Cole, and R. J. Bartlett, *J. Chem. Phys.*, **83**, 4041 (1985). Towards a Full CCSDT Model for Electron Correlation.
19. M. R. Hoffmann and H. F. Schaefer, *Adv. Quantum Chem.*, **18**, 207 (1986). A Full Coupled-Cluster Singles, Doubles, and Triples Model for the Description of Electron Correlation.
20. S. A. Kucharski and R. J. Bartlett, *Adv. Quantum Chem.*, **18**, 281 (1986). Fifth-Order Many-Body Perturbation Theory and Its Relationship to Various Coupled-Cluster Approaches.
21. J. Noga, R. J. Bartlett, and M. Urban, *Chem. Phys. Lett.*, **134**, 126 (1987). Towards a Full CCSDT Model for Electron Correlation. CCSDT-*n* Models.
22. J. Noga and R. J. Bartlett, *J. Chem. Phys.*, **86**, 7041 (1987); Erratum: **89**, 3401 (1988). The Full CCSDT Model for Molecular Electronic Structure.
23. G. E. Scuseria and H. F. Schaefer, *Chem. Phys. Lett.*, **152**, 382 (1988). A New Implementation of the Full CCSDT Model for Molecular Electronic Structure.
24. K. Raghavachari, G. W. Trucks, J. A. Pople, and M. Head-Gordon, *Chem. Phys. Lett.*, **157**, 479 (1989). A Fifth-Order Perturbation Comparison of Electron Correlation.
25. R. J. Bartlett, J. D. Watts, S. A. Kucharski, and J. Noga, *Chem. Phys. Lett.*, **165**, 513 (1990); Erratum: **167**, 609 (1990). Non-iterative Fifth-Order Triple and Quadruple Excitation Energy Corrections in Correlated Methods.
26. J. D. Watts and R. J. Bartlett, *J. Chem. Phys.*, **93**, 6104 (1990). The Coupled-Cluster Single, Double, and Triple Excitation Model for Open-Shell Single Reference Functions.
27. G. E. Scuseria, *Chem. Phys. Lett.*, **176**, 27 (1991). The Open-Shell Restricted Hartree–Fock Singles and Doubles Coupled-Cluster Method Including Triple Excitations CCSD(T): Application to C<sub>3</sub><sup>+</sup>.
28. S. A. Kucharski and R. J. Bartlett, *J. Chem. Phys.*, **97**, 4282 (1992). The Coupled-Cluster Single, Double, Triple, and Quadruple Excitation Method.
29. J. D. Watts, J. Gauss, and R. J. Bartlett, *J. Chem. Phys.*, **98**, 8718 (1993). Coupled-Cluster Methods with Noniterative Triple Excitations for Restricted Open-Shell Hartree–Fock and Other General Single Determinant Reference Functions. Energies and Analytical Gradients.
30. M. J. O. Deegan and P. J. Knowles, *Chem. Phys. Lett.*, **227**, 321 (1994). Perturbative Corrections to Account for Triple Excitations in Closed- and Open-Shell Coupled-Cluster Theories.
31. T. D. Crawford and H. F. Schaefer, *J. Chem. Phys.*, **104**, 6259 (1996). A Comparison of Two Approaches to Perturbational Triple Excitation Corrections to the Coupled-Cluster Singles and Doubles Method for High-Spin Open-Shell Systems.
32. J. F. Stanton, *Chem. Phys. Lett.*, **281**, 130 (1997). Why CCSD(T) Works: A Different Perspective.
33. T. D. Crawford, T. J. Lee, and H. F. Schaefer, *J. Chem. Phys.*, **107**, 7943 (1997). A New Spin-Restricted Triple Excitation Correction for Coupled Cluster Theory.
34. T. D. Crawford and J. F. Stanton, *Int. J. Quantum Chem. Symp.*, **70**, 601 (1998). Investigation of an Asymmetric Triple-Excitation Correction for Coupled Cluster Energies.
35. M. Rittby and R. J. Bartlett, *J. Phys. Chem.*, **92**, 3033 (1988). An Open-Shell Spin-Restricted Coupled-Cluster Method: Application to Ionization Potentials in N<sub>2</sub>.
36. C. L. Janssen and H. F. Schaefer, *Theor. Chim. Acta*, **79**, 1 (1991). The Automated Solution of Second Quantization Equations with Applications to the Coupled-Cluster Approach.
37. P. J. Knowles, C. Hampel, and H.-J. Werner, *J. Chem. Phys.*, **99**, 5219 (1993). Coupled-Cluster Theory for High-Spin, Open-Shell Reference Wave Functions.
38. P. Neogrády, M. Urban, and I. Hubač, *J. Chem. Phys.*, **100**, 3706 (1994). Spin Adapted Restricted Hartree–Fock Reference Coupled-Cluster Theory for Open-Shell Systems.

39. X. Li and J. Paldus, *J. Chem. Phys.*, **101**, 8812 (1994). Automation of the Implementation of Spin-Adapted Open-Shell Coupled-Cluster Theories Relying on the Unitary Group Formalism.
40. X. Li and J. Paldus, *J. Chem. Phys.*, **102**, 2013 (1995). Spin-Adapted Open-Shell State-Selective Coupled-Cluster Approach and Doublet Stability of Its Hartree–Fock Reference.
41. M. Nooijen and R. J. Bartlett, *J. Chem. Phys.*, **104**, 2652 (1996). General Spin Adaptation of Open-Shell Coupled Cluster Theory.
42. P. G. Szalay and J. Gauss, *J. Chem. Phys.*, **107**, 9028 (1997). Spin-Restricted Open-Shell Coupled-Cluster Theory.
43. P. Jørgensen and J. Simons, *J. Chem. Phys.*, **79**, 334 (1983). Ab Initio Analytical Molecular Gradients and Hessians.
44. L. Adamowicz, W. D. Laidig, and R. J. Bartlett, *Int. J. Quantum Chem. Symp.*, **18**, 245 (1984). Analytical Gradients for the Coupled-Cluster Method.
45. G. Fitzgerald, R. Harrison, W. D. Laidig, and R. J. Bartlett, *Chem. Phys. Lett.*, **117**, 433 (1985). Analytical Gradient Evaluation in Coupled-Cluster Theory.
46. R. J. Bartlett, in *Geometrical Derivatives of Energy Surfaces and Molecular Properties*, P. Jørgensen and J. Simons, Eds., D. Reidel, Dordrecht, 1986, pp. 35–61. Analytical Evaluation of Gradients in Coupled-Cluster and Many-Body Perturbation Theory.
47. G. Fitzgerald, R. J. Harrison, and R. J. Bartlett, *J. Chem. Phys.*, **85**, 5143 (1986). Analytic Energy Gradients for General Coupled-Cluster Methods and Fourth-Order Many-Body Perturbation Theory.
48. A. C. Scheiner, G. E. Scuseria, J. E. Rice, T. J. Lee, and H. F. Schaefer, *J. Chem. Phys.*, **87**, 5361 (1987). Analytic Evaluation of Energy Gradients for the Single and Double Excitation Coupled Cluster (CCSD) Wave Function: Theory and Application.
49. E. A. Salter, G. W. Trucks, and R. J. Bartlett, *J. Chem. Phys.*, **90**, 1752 (1989). Analytic Energy Derivatives in Many-Body Methods. I. First Derivatives.
50. J. Gauss, J. F. Stanton, and R. J. Bartlett, *J. Chem. Phys.*, **95**, 2623 (1991). Coupled-Cluster Open-Shell Analytic Gradients: Implementation of the Direct Product Decomposition Approach in Energy Gradient Calculations.
51. J. Gauss, W. J. Lauderdale, J. F. Stanton, J. D. Watts, and R. J. Bartlett, *Chem. Phys. Lett.*, **182**, 207 (1991). Analytic Energy Gradients for Open-Shell Coupled-Cluster Singles and Doubles Calculations Using Restricted Open-Shell Hartree–Fock (ROHF) Reference Functions.
52. J. Gauss, J. F. Stanton, and R. J. Bartlett, *J. Chem. Phys.*, **95**, 2639 (1991). Analytic Evaluation of Energy Gradients at the Coupled-Cluster Singles and Doubles Level Using Quasi-Restricted Hartree–Fock Open-Shell Reference Functions.
53. G. E. Scuseria, *J. Chem. Phys.*, **94**, 442 (1991). Analytic Evaluation of Energy Gradients for the Singles and Doubles Coupled-Cluster Method Including Perturbative Triple Excitations: Theory and Applications to FOOF and Cr<sup>2</sup>.
54. T. J. Lee and A. P. Rendell, *J. Chem. Phys.*, **94**, 6229 (1991). Analytic Gradients for Coupled-Cluster Energies That Include Noniterative Connected Triple Excitations: Application to *cis*- and *trans*-HONO.
55. E. A. Salter and R. J. Bartlett, *J. Chem. Phys.*, **90**, 1767 (1989). Analytic Energy Derivatives in Many-Body Theory. II. Second Derivatives.
56. H. Koch, H. J. Aa. Jensen, P. Jørgensen, T. Helgaker, G. E. Scuseria, and H. F. Schaefer, *J. Chem. Phys.*, **92**, 4924 (1990). Coupled-Cluster Energy Derivatives. Analytic Hessian for the Closed-Shell Coupled-Cluster Singles and Doubles Wave Functions: Theory and Applications.
57. J. F. Stanton and J. Gauss, in *Recent Advances in Coupled-Cluster Methods*, R. J. Bartlett, Ed., World Scientific Publishing, Singapore, 1997, pp. 49–79. Analytic Evaluation of Second Derivatives of the Energy: Computational Strategies for the CCSD and CCSD(T) Approximations.

58. J. Gauss and J. F. Stanton, *Chem. Phys. Lett.*, **276**, 70 (1997). Analytic CCSD(T) Second Derivatives.
59. P. G. Szalay, J. Gauss, and J. F. Stanton, *Theor. Chim. Acta*, **100**, 5 (1998). Analytic UHF-CCSD(T) Second Derivatives: Implementation and Application to the Calculation of the Vibration–Rotation Interaction Constants of NCO and NCS.
60. D. Mukherjee and P. K. Mukherjee, *Chem. Phys.*, **39**, 325 (1979). A Response–Function Approach to the Direct Calculation of the Transition-Energy in a Multiple-Cluster Expansion Formalism.
61. K. Emrich, *Nucl. Phys. A*, **351**, 379 (1981). An Extension of the Coupled Cluster Formalism to Excited States (I).
62. S. Ghosh and D. Mukherjee, *Proc. Indian Acad. Sci. (Chem. Sci.)*, **93**, 947 (1984). Use of Cluster Expansion Techniques in Quantum Chemistry. A Linear Response Model for Calculating Energy Differences.
63. H. Sekino and R. J. Bartlett, *Int. J. Quantum Chem. Symp.*, **18**, 255 (1984). A Linear Response, Coupled-Cluster Theory for Excitation Energy.
64. L. Meissner and R. J. Bartlett, *J. Chem. Phys.*, **94**, 6670 (1991). Transformation of the Hamiltonian in Excitation Energy Calculations: Comparison Between Fock-Space Multi-reference Coupled-Cluster and Equation-of-Motion Coupled-Cluster Methods.
65. J. F. Stanton and R. J. Bartlett, *J. Chem. Phys.*, **98**, 7029 (1993). The Equation of Motion Coupled-Cluster Method. A Systematic Biorthogonal Approach to Molecular Excitation Energies, Transition Probabilities, and Excited State Properties.
66. J. F. Stanton and J. Gauss, *J. Chem. Phys.*, **99**, 8840 (1993). Many-Body Methods for Excited State Potential Energy Surfaces. I. General Theory of Energy Gradients for the Equation-of-Motion Coupled-Cluster Method.
67. J. F. Stanton and J. Gauss, *J. Chem. Phys.*, **101**, 8938 (1994). Analytic Energy Derivatives for Ionized States Described by the Equation-of-Motion Coupled-Cluster Method.
68. J. F. Stanton, J. Gauss, N. Ishikawa, and M. Head-Gordon, *J. Chem. Phys.*, **103**, 4160 (1995). A Comparison of Single Reference Methods for Characterizing Stationary Points of Excited State Potential Energy Surfaces.
69. H. Koch and P. Jørgensen, *J. Chem. Phys.*, **93**, 3333 (1990). Coupled Cluster Response Functions.
70. H. Koch, O. Christiansen, P. Jørgensen, and J. Olsen, *Chem. Phys. Lett.*, **244**, 75 (1995). Excitation Energies of BH, CH<sub>2</sub>, and Ne in Full Configuration Interaction and the Hierarchy CCS, CC2, CCSD, and CC3 of Coupled-Cluster Models.
71. J. D. Watts, S. R. Gwaltney, and R. J. Bartlett, *J. Chem. Phys.*, **105**, 6979 (1996). Coupled-Cluster Calculations of the Excitation Energies of Ethylene, Butadiene, and Cyclopentadiene.
72. O. Christiansen, H. Koch, A. Halkier, P. Jørgensen, T. Helgaker, and A. S. De Merás, *J. Chem. Phys.*, **105**, 6921 (1996). Large-Scale Calculations of Excitation Energies in Coupled-Cluster Theory: The Singlet Excited States of Benzene.
73. M. Head-Gordon and T. J. Lee, in *Recent Advances in Coupled-Cluster Methods*, R. J. Bartlett, Ed., World Scientific Publishing, Singapore, 1997, pp. 221–253. Single Reference Coupled Cluster and Perturbation Theories of Electronic Excitation Energies.
74. M. Nooijen and R. J. Bartlett, *J. Chem. Phys.*, **106**, 6441 (1997). A New Method for Excited States: Similarity Transformed Equation-of-Motion Coupled-Cluster Theory.
75. O. Sinanoğlu, *Adv. Chem. Phys.*, **6**, 315 (1964). Many-Electron Theory of Atoms, Molecules, and Their Interactions.
76. R. J. Bartlett, *J. Phys. Chem.*, **93**, 1697 (1989). Coupled-Cluster Approach to Molecular Structure and Spectra: A Step Toward Predictive Quantum Chemistry.
77. R. J. Bartlett and J. F. Stanton, in *Reviews in Computational Chemistry*, K. B. Lipkowitz and D. B. Boyd, Eds., VCH Publishers, New York, 1994, Vol. 5, pp. 65–169. Applications of Post-Hartree–Fock Methods: A Tutorial.

78. R. J. Bartlett, in *Modern Electronic Structure Theory*, Vol. 2 of *Advanced Series in Physical Chemistry*, D. R. Yarkony, Ed., World Scientific Publishing, Singapore, 1995, pp. 1047–1131. Coupled-Cluster Theory: An Overview of Recent Developments.
79. T. J. Lee and G. E. Scuseria, in *Quantum Mechanical Electronic Structure Calculations with Chemical Accuracy*, S. R. Langhoff, Ed., Kluwer Academic Publishers, Dordrecht, 1995, pp. 47–108. Achieving Chemical Accuracy with Coupled-Cluster Theory.
80. F. E. Harris, H. J. Monkhorst, and D. L. Freeman, *Algebraic and Diagrammatic Methods in Many-Fermion Theory*, Oxford University Press, New York, 1992.
81. P. R. Taylor, in *Lecture Notes in Quantum Chemistry: European Summer School II*, Vol. 64 of *Lecture Notes in Chemistry*, B. O. Roos, Ed., Springer-Verlag, Berlin, 1994, pp. 125–202. Coupled-Cluster Methods in Quantum Chemistry.
82. A. Szabo and N. S. Ostlund, *Modern Quantum Chemistry: Introduction to Advanced Electronic Structure Theory*, 1st ed., McGraw-Hill, New York, 1989.
83. W. Kutzelnigg, in *Methods of Electronic Structure Theory*, H. F. Schaefer, Ed., Plenum Press, New York, 1977, pp. 129–188. Pair-Correlation Theories.
84. P. Jørgensen and J. Simons, *Second Quantization-Based Methods in Quantum Chemistry*, Academic Press, New York, 1981.
85. I. Shavitt, in *Methods of Electronic Structure Theory*, H. F. Schaefer, Ed., Plenum Press, New York, 1977, pp. 189–275. The Method of Configuration Interaction.
86. C. D. Sherrill and H. F. Schaefer, *Adv. Quantum Chem.*, **34**, 143 (1999). The Configuration Interaction Method: Advances in Highly Correlated Approaches.
87. R. J. Bartlett, *Annu. Rev. Phys. Chem.*, **32**, 359 (1981). Many-Body Perturbation Theory and Coupled-Cluster Theory for Electron Correlation in Molecules.
88. M. Nooijen, Ph.D. Thesis, Vrije Universiteit Amsterdam, 1992. The Coupled Cluster Green's Function.
89. J. A. Pople, in *Energy, Structure, and Reactivity*, D. W. Smith and W. B. McRae, Eds., Wiley, New York, 1973, pp. 51–61. Theoretical Models for Chemistry.
90. R. J. Bartlett, C. E. Dykstra, and J. Paldus, in *Advanced Theories and Computational Approaches to the Electronic Structure of Molecules*, C. E. Dykstra, Ed., D. Reidel, Dordrecht, 1984, pp. 127–159. Coupled-Cluster Methods for Molecular Calculations.
91. E. Merzbacher, *Quantum Mechanics*, 2nd ed., Wiley, New York, 1970.
92. J. F. Stanton, unpublished notes, Austin, TX, 1996. Fundamentals of Second Quantization.
93. W. Kutzelnigg, *Mol. Phys.*, **94**, 65 (1998). Almost Variational Coupled Cluster Theory.
94. M. R. Hoffmann and J. Simons, *J. Chem. Phys.*, **88**, 993 (1988). A Unitary Coupled-Cluster Method: Theory and Applications.
95. M. R. Hoffmann and J. Simons, *Chem. Phys. Lett.*, **142**, 451 (1987). Analytical Energy Gradients for a Unitary Coupled-Cluster Theory.
96. R. J. Bartlett and J. Noga, *Chem. Phys. Lett.*, **150**, 29 (1988). The Expectation Value Coupled-Cluster Method and Analytical Energy Derivatives.
97. J. S. Arponen, *Ann. Phys.*, **151**, 311 (1983). Variational Principles and Linked-Cluster Exp S Expansions for Static and Dynamic Many-Body Problems.
98. R. F. Bishop and J. S. Arponen, *Int. J. Quantum Chem. Symp.*, **24**, 197 (1990). Correlations in Extended Systems: A Microscopic Multilocal Method for Describing Both Local and Global Properties.
99. R. J. Bartlett, S. A. Kucharski, J. Noga, J. D. Watts, and G. W. Trucks, in *Lecture Notes in Quantum Chemistry*, Vol. 52 of *Lecture Notes in Chemistry*, U. Kaldor, Ed., Springer-Verlag, Berlin, 1989, pp. 125–149. Some Consideration of Alternative Ansätze in Coupled-Cluster Theory.
100. P. G. Szalay, M. Nooijen, and R. J. Bartlett, *J. Chem. Phys.*, **103**, 281 (1995). Alternative Ansätze in Single Reference Coupled-Cluster Theory. III. A Critical Analysis of Different Methods.

101. J. F. Stanton, unpublished notes, Austin, TX, 1998. Coupled Cluster Theory for the Ambidextrous.
102. H. Koch, H. J. Aa. Jensen, P. Jørgensen, and T. Helgaker, *J. Chem. Phys.*, **93**, 3345 (1990). Excitation Energies from the Coupled Cluster Singles and Doubles Linear Response Function (CCSDLR). Applications to Be, CH<sup>+</sup>, CO, and H<sub>2</sub>O.
103. R. J. Rico and M. Head-Gordon, *Chem. Phys. Lett.*, **213**, 224 (1993). Single-Reference Theories of Molecular Excited States with Single and Double Substitutions.
104. O. Christiansen, H. Koch, and P. Jørgensen, *Chem. Phys. Lett.*, **243**, 409 (1995). The Second-Order Approximate Coupled Cluster Singles and Doubles Model CC2.
105. O. Christiansen, H. Koch, and P. Jørgensen, *J. Chem. Phys.*, **103**, 7429 (1995). Response Functions in the CC3 Iterative Triple Excitation Model.
106. H. Nakatsuji and K. Hirao, *J. Chem. Phys.*, **68**, 2053 (1978). Cluster Expansion of the Wavefunction. Symmetry-Adapted-Cluster Expansion, Its Variational Determination, and Extension of Open-Shell Orbital Theory.
107. H. Nakatsuji, *Chem. Phys. Lett.*, **59**, 362 (1978). Cluster Expansion of the Wavefunctions. Excited States.
108. H. Nakatsuji, *Chem. Phys. Lett.*, **67**, 329 (1979). Cluster Expansion of the the Wavefunction. Electron Correlations in Ground and Excited States by SAC (Symmetry-Adapted-Cluster) and SAC CI Theories.
109. U. Kaldor, *Theor. Chim. Acta*, **80**, 427 (1991). The Fock Space Coupled Cluster Method: Theory and Application.
110. D. Mukhopadhyay, S. Mukhopadhyay, R. Chaudhuri, and D. Mukherjee, *Theor. Chim. Acta*, **80**, 441 (1991). Aspects of Separability in the Coupled Cluster Based Direct Method for Energy Differences.
111. C. M. L. Rittby and R. J. Bartlett, *Theor. Chim. Acta*, **80**, 469 (1991). Multireference Coupled Cluster Theory in Fock Space.
112. J. F. Stanton, R. J. Bartlett, and C. M. L. Rittby, *J. Chem. Phys.*, **97**, 5560 (1992). Fock Space Multireference Coupled-Cluster Theory for General Single Determinant Reference Functions.
113. M. Nooijen and R. J. Bartlett, *J. Chem. Phys.*, **102**, 3629 (1995). Equation-of-Motion Coupled-Cluster Method for Electron Attachment.
114. M. Nooijen and R. J. Bartlett, *J. Chem. Phys.*, **106**, 6449 (1997). Similarity Transformed Equation-of-Motion Coupled-Cluster Study of Ionized, Electron Attached, and Excited States of Free Base Porphyrin.
115. K. F. Freed, *Annu. Rev. Phys. Chem.*, **22**, 313 (1971). Many-Body Theories of the Electronic Structure of Atoms and Molecules.
116. G. C. Wick, *Phys. Rev.*, **80**, 268 (1950). The Evaluation of the Collision Matrix.
117. J. Paldus and J. Čížek, *Adv. Quantum Chem.*, **9**, 105 (1975). Time-Independent Diagrammatic Approach to Perturbation Theory of Fermion Systems.
118. T. D. Crawford, Ph.D. Thesis, University of Georgia, 1996. Many-Body Perturbation Theory and Perturbational Triple Excitation Corrections to the Coupled-Cluster Singles and Doubles Method for High-Spin Open-Shell Systems.
119. R. J. Bartlett and D. M. Silver, *Int. J. Quantum Chem. Symp.*, **9**, 183 (1975). Some Aspects of Diagrammatic Perturbation Theory.
120. R. J. Bartlett, unpublished notes, Gainesville, FL, 1994. Systematic Derivation of Coupled-Cluster Equations.
121. E. R. Davidson, in *The World of Quantum Chemistry*, R. Daudel and B. Pullman, Eds., D. Reidel, Dordrecht, 1974, pp. 17–30. Configuration Interaction Description of Electron Correlation.
122. S. R. Langhoff and E. R. Davidson, *Int. J. Quantum Chem.*, **8**, 61 (1974). Configuration Interaction Calculations on the Nitrogen Molecule.

123. R. J. Bartlett, I. Shavitt, and G. D. Purvis, *J. Chem. Phys.*, **71**, 281 (1979). The Quartic Force Field of H<sub>2</sub>O Determined by Many-Body Methods That Include Quadruple Excitation Effects.
124. F. L. Pilar, *Elementary Quantum Chemistry*, 2nd ed., McGraw-Hill, New York, 1990.
125. M. Urban, I. Černušák, V. Kellö, and J. Noga, in *Electron Correlation in Atoms and Molecules*, Vol. 1 of *Methods in Computational Chemistry*, S. Wilson, Ed., Plenum Press, New York, 1987, pp. 117–250. Electron Correlation in Molecules.
126. C. Møller and M. S. Plesset, *Phys. Rev.*, **46**, 618 (1934). Note on an Approximation Treatment for Many-Electron Systems.
127. I. Hubač and P. Čársky, *Phys. Rev.*, **A22**, 2392 (1980). Correlation Energy of Open-Shell Systems. Application of the Many-Body Rayleigh–Schrödinger Perturbation Theory in the Restricted Roothaan–Hartree–Fock Formalism.
128. R. D. Amos, J. S. Andrews, N. C. Handy, and P. J. Knowles, *Chem. Phys. Lett.*, **185**, 256 (1991). Open-Shell Møller-Plesset Perturbation Theory.
129. P. J. Knowles, J. S. Andrews, R. D. Amos, N. C. Handy, and J. A. Pople, *Chem. Phys. Lett.*, **186**, 130 (1991). Restricted Møller-Plesset Theory for Open-Shell Molecules.
130. W. J. Lauderdale, J. F. Stanton, J. Gauss, J. D. Watts, and R. J. Bartlett, *Chem. Phys. Lett.*, **187**, 21 (1991). Many-Body Perturbation Theory with a Restricted Open-Shell Hartree–Fock Reference.
131. C. Murray and E. R. Davidson, *Chem. Phys. Lett.*, **187**, 451 (1991). Perturbation Theory for Open-Shell Systems.
132. T. J. Lee and D. Jayatilaka, *Chem. Phys. Lett.*, **201**, 1 (1993). An Open-Shell Restricted Hartree–Fock Perturbation Theory Based on Symmetric Spin Orbitals.
133. P. M. Kozlowski and E. R. Davidson, *Chem. Phys. Lett.*, **226**, 440 (1994). Construction of Open-Shell Perturbation Theory Invariant with Respect to Orbital Degeneracy.
134. T. D. Crawford, H. F. Schaefer, and T. J. Lee, *J. Chem. Phys.*, **105**, 1060 (1996). On the Energy Invariance of Open-Shell Perturbation Theory with Respect to Unitary Transformations of Molecular Orbitals.
135. R. Krishnan and J. A. Pople, *Int. J. Quantum Chem.*, **14**, 91 (1978). Approximate Fourth-Order Perturbation Theory of the Electron Correlation Energy.
136. R. Krishnan, M. J. Frisch, and J. A. Pople, *J. Chem. Phys.*, **72**, 4244 (1980). Contribution of Triple Substitutions to the Electron Correlation Energy in Fourth Order Perturbation Theory.
137. J. R. Thomas, B. J. DeLeeuw, G. Vacek, and H. F. Schaefer, *J. Chem. Phys.*, **98**, 1336 (1993). A Systematic Study of the Harmonic Vibrational Frequencies for Polyatomic Molecules: The Single, Double, and Perturbative Triple Excitation Coupled-Cluster [CCSD(T)] Method.
138. J. R. Thomas, B. J. DeLeeuw, G. Vacek, T. D. Crawford, Y. Yamaguchi, and H. F. Schaefer, *J. Chem. Phys.*, **99**, 403 (1993). The Balance Between Theoretical Method and Basis Set Quality: A Systematic Study of Equilibrium Geometries, Dipole Moments, Harmonic Vibrational Frequencies, and Infrared Intensities.
139. R. J. Bartlett and I. Shavitt, *Chem. Phys. Lett.*, **50**, 190 (1977). Comparison of High-Order Many-Body Perturbation Theory and Configuration Interaction for H<sub>2</sub>O.
140. T. D. Crawford, J. F. Stanton, W. D. Allen, and H. F. Schaefer, *J. Chem. Phys.*, **107**, 10626 (1997). Hartree–Fock Orbital Instability Envelopes in Highly Correlated Single-Reference Wavefunctions.
141. T. J. Lee, A. P. Rendell, and P. R. Taylor, *J. Phys. Chem.*, **94**, 5463 (1990). Comparison of the Quadratic Configuration Interaction and Coupled-Cluster Approaches to Electron Correlation Including the Effect of Triple Excitations.
142. A. P. Rendell, T. J. Lee, and A. Komornicki, *Chem. Phys. Lett.*, **178**, 462 (1991). A Parallel Vectorized Implementation of Triple Excitations in CCSD(T): Application to the Binding Energies of the AlH<sub>3</sub>, AlH<sub>2</sub>F, AlHF<sub>2</sub>, and AlF<sub>3</sub> Dimers.

143. K. Raghavachari, J. A. Pople, E. S. Replogle, and M. Head-Gordon, *J. Phys. Chem.*, **94**, 5579 (1990). Fifth-Order Møller-Plesset Perturbation Theory: Comparison of Existing Correlation Methods and Implementation of New Methods Correct to Fifth Order.
144. A. L. L. East, Ph.D. Thesis, Stanford University, 1994. Selected Theoretical Studies of Vibrational Anharmonicity and Thermochemistry.
145. S. A. Kucharski and R. J. Bartlett, *J. Chem. Phys.*, **108**, 5243 (1998). Noniterative Energy Corrections Through Fifth-Order to the Coupled Cluster Singles and Doubles Method.
146. V. Kvasnička, V. Lurinc, S. Biskupič, and M. Haring, *Adv. Chem. Phys.*, **52**, 181 (1983). Coupled-Cluster Approach in the Electronic-Structure Theory of Molecules.
147. S. A. Kucharski and R. J. Bartlett, *Theor. Chim. Acta*, **80**, 387 (1991). Recursive Intermediate Factorization and Complete Computational Linearization of the Coupled-Cluster Single, Double, Triples, and Quadruple Excitation Equations.
148. C. L. Janssen, E. T. Seidl, G. E. Scuseria, T. P. Hamilton, Y. Yamaguchi, R. B. Remington, Y. Xie, G. Vacek, C. D. Sherrill, T. D. Crawford, J. T. Fermann, W. D. Allen, B. R. Brooks, G. B. Fitzgerald, D. J. Fox, J. F. Gaw, N. C. Handy, W. D. Laidig, T. J. Lee, R. M. Pitzer, J. E. Rice, P. Saxe, A. C. Scheiner, and H. F. Schaefer, PSI 2.0.8, PSITECH, Inc., Watkinsville, GA 30677, 1995. E-mail: psi@ccqc.uga.edu. This program is available for a handling fee of \$100.
149. MOLPRO is a package of ab initio programs written by H.-J. Werner and P. J. Knowles with contributions from R. D. Amos, A. Berning, D. L. Cooper, M. J. O. Deegan, A. J. Dobbyn, F. Eckert, C. Hampel, T. Leininger, R. Lindh, A. W. Lloyd, W. Meyer, M. E. Mura, A. Nicklass, P. Palmieri, K. Peterson, R. Pitzer, P. Pulay, G. Rauhut, M. Schütz, H. Stoll, A. J. Stone, and T. Thorsteinsson. E-mail: molpro-support@tc.bham.ac.uk.
150. J. F. Stanton, J. Gauss, J. D. Watts, W. J. Lauderdale, and R. J. Bartlett, ACES II. The package also contains modified versions of the MOLECULE Gaussian integral program of J. Almlöf and P. R. Taylor, the ABACUS integral derivative program written by T. U. Helgaker, H. J. Aa. Jensen, P. Jørgensen and P. R. Taylor, and the PROPS property evaluation integral code of P. R. Taylor. E-mail: aces2@qpp.ufl.edu.
151. K. Dowd, *High Performance Computing: RISC Architectures, Optimization, and Benchmarks*, O'Reilly and Associates, Sebastopol, CA, 1993.
152. P. Čársky, L. J. Schaad, B. A. Hess, M. Urban, and J. Noga, *J. Chem. Phys.*, **87**, 411 (1987). Use of Molecular Symmetry in Coupled-Cluster Theory.
153. M. Häser, *J. Chem. Phys.*, **95**, 8259 (1991). Molecular Point-Group Symmetry in Electronic Structure Calculations.
154. F. Haase and R. Ahlrichs, *J. Comput. Chem.*, **14**, 907 (1993). Semidirect MP2 Gradient Evaluation on Workstation Computers—The MPGRAD Program.
155. M. Kollwitz, M. Häser, and J. Gauss, *J. Chem. Phys.*, **108**, 8295 (1998). Non-Abelian Point Group Symmetry in Direct Second-Order Many-Body Perturbation Theory Calculations of NMR Chemical Shifts.
156. R. Pauncz, *Spin Eigenfunctions: Construction and Use*, Plenum Press, New York, 1979.
157. R. Pauncz, *The Symmetric Group in Quantum Chemistry*, CRC Press, Boca Raton, FL, 1995.
158. X. Li and J. Paldus, *J. Chem. Phys.*, **103**, 6536 (1995). Unitary Group Based Open-Shell Coupled-Cluster Approach and Triplet and Open-Shell Singlet Stabilities of Hartree–Fock References.
159. S. Wilson, in *Electron Correlation in Atoms and Molecules*, Vol. 1 of *Methods in Computational Chemistry*, S. Wilson, Ed., Plenum Press, New York, 1987, pp. 251–309. Four-Index Transformations.
160. C. Hampel, K. A. Peterson, and H.-J. Werner, *Chem. Phys. Lett.*, **190**, 1 (1992). A Comparison of the Efficiency and Accuracy of the Quadratic Configuration Interaction (QCISD), Coupled-Cluster (CCSD), and Brueckner Coupled-Cluster (BCCD) Methods.
161. P. R. Taylor, *Int. J. Quantum Chem.*, **31**, 521 (1987). Integral Processing in Beyond-Hartree–Fock Calculations.

162. M. J. Frisch, M. Head-Gordon, and J. A. Pople, *Chem. Phys. Lett.*, **166**, 281 (1990). Semi-Direct Algorithms for the MP2 Energy and Gradient.
163. H. Koch, O. Christiansen, R. Kobayashi, P. Jørgensen, and T. Helgaker, *Chem. Phys. Lett.*, **228**, 233 (1994). A Direct Atomic Orbital Driven Implementation of the Coupled Cluster Singles and Doubles (CCSD) Model.
164. H. Koch, A. S. De Merás, T. Helgaker, and O. Christiansen, *J. Chem. Phys.*, **104**, 4157 (1996). The Integrals-Direct Coupled-Cluster Singles and Doubles Model.
165. A. P. Rendell and T. J. Lee, *J. Chem. Phys.*, **101**, 400 (1994). Coupled-Cluster Theory Employing Approximate Integrals: An Approach to Avoid the Input/Output and Storage Bottlenecks.
166. J. M. L. Martin, *J. Chem. Phys.*, **100**, 8186 (1994). On the Performance of Correlation Consistent Basis Sets for the Calculation of Total Atomization Energies, Geometries and Harmonic Frequencies.
167. J. Paldus, in *New Horizons of Quantum Chemistry: Proceedings of the Fourth International Congress of Quantum Chemistry*, P.-O. Löwdin and B. Pullman, Eds., D. Reidel, Dordrecht, 1983, pp. 31–60. Coupled Cluster Approaches to the Many-Electron Correlation Problem.
168. J. Paldus, in *Methods in Computational Molecular Physics*, S. Wilson and G. H. F. Diercksen, Eds., Plenum Press, New York, 1992, pp. 99–194. Coupled Cluster Theory.
169. A. Balkova and R. J. Bartlett, *Chem. Phys. Lett.*, **193**, 364 (1992). Coupled-Cluster Method for Open-Shell Singlets.
170. A. Balkova and R. J. Bartlett, *J. Chem. Phys.*, **99**, 7907 (1993). The 2-Determinant Coupled-Cluster Method for Electric Properties of Excited Electronic States: The Lowest  $^1B_1$  and  $^3B_1$  States of the Water Molecule.
171. D. Jayatilaka and T. J. Lee, *Chem. Phys. Lett.*, **199**, 211 (1992). The Form of Spin Orbitals for Open-Shell Restricted Hartree–Fock Reference Functions.
172. D. Jayatilaka and T. J. Lee, *J. Chem. Phys.*, **98**, 9734 (1993). Open-Shell Coupled-Cluster Theory.
173. T. D. Crawford, T. J. Lee, and H. F. Schaefer, *J. Chem. Phys.*, **107**, 9980 (1997). Spin-Restricted Brueckner Orbitals for Coupled-Cluster Wavefunctions.
174. J. F. Stanton, *J. Chem. Phys.*, **101**, 371 (1994). On the Extent of Spin Contamination in Open-Shell Coupled-Cluster Wave Functions.
175. T. J. Lee, A. P. Rendell, K. G. Dyall, and D. Jayatilaka, *J. Chem. Phys.*, **100**, 7400 (1994). Open-Shell Restricted Hartree–Fock Perturbation Theory: Some Considerations and Comparisons.
176. S. Wolfram, *Mathematica: A System for Doing Mathematics by Computer*, 2nd ed., Addison-Wesley, New York, 1991.
177. K. A. Brueckner, *Phys. Rev.*, **96**, 508 (1954). Nuclear Saturation and Two-Body Forces. II. Tensor Forces.
178. R. K. Nesbet, *Phys. Rev.*, **109**, 1632 (1958). Brueckner's Theory and the Method of Superposition of Configurations.
179. R. A. Chiles and C. E. Dykstra, *J. Chem. Phys.*, **74**, 4544 (1981). An Electron Pair Operator Approach to Coupled-Cluster Wave Functions. Application to  $\text{He}_2$ ,  $\text{Be}_2$ , and  $\text{Mg}_2$  and Comparison with CEPA Methods.
180. L. Z. Stolarczyk and H. J. Monkhorst, *Int. J. Quantum Chem. Symp.*, **18**, 267 (1984). Coupled-Cluster Method with Optimized Reference State.
181. G. E. Scuseria and H. F. Schaefer, *Chem. Phys. Lett.*, **142**, 354 (1987). The Optimization of Molecular Orbitals for Coupled Cluster Wavefunctions.
182. N. C. Handy, J. A. Pople, M. Head-Gordon, K. Raghavachari, and G. W. Trucks, *Chem. Phys. Lett.*, **164**, 185 (1989). Size-Consistent Brueckner Theory Limited to Double Substitutions.
183. R. Kobayashi, N. C. Handy, R. D. Amos, G. W. Trucks, M. J. Frisch, and J. A. Pople, *J. Chem. Phys.*, **95**, 6723 (1991). Gradient Theory Applied to the Brueckner Doubles Method.

184. R. Kobayashi, R. D. Amos, and N. C. Handy, *Chem. Phys. Lett.*, **184**, 195 (1991). The Analytic Gradient of the Perturbative Triple Excitations Correction to the Brueckner Doubles Method.
185. T. J. Lee, R. Kobayashi, N. C. Handy, and R. D. Amos, *J. Chem. Phys.*, **96**, 8931 (1992). Comparison of the Brueckner and Coupled-Cluster Approaches to Electron Correlation.
186. J. F. Stanton, J. Gauss, and R. J. Bartlett, *J. Chem. Phys.*, **97**, 5554 (1992). On the Choice of Orbitals for Symmetry Breaking Problems with Application to  $\text{NO}_3$ .
187. R. Kobayashi, H. Koch, P. Jørgensen, and T. J. Lee, *Chem. Phys. Lett.*, **211**, 94 (1993). Comparison of Coupled-Cluster and Brueckner Coupled-Cluster Calculations of Molecular Properties.
188. V. A. Kozlov and V. I. Pupyshev, *Chem. Phys. Lett.*, **206**, 151 (1993). Self-Consistent Brueckner Theory for Molecular Orbitals.
189. R. Kobayashi, R. D. Amos, and N. C. Handy, *J. Chem. Phys.*, **100**, 1375 (1994). Large Basis Set Calculations Using Brueckner Theory.
190. J. D. Watts and R. J. Bartlett, *Int. J. Quantum Chem. Symp.*, **28**, 195 (1994). Coupled-Cluster Singles, Doubles, and Triples Calculations with Hartree–Fock and Brueckner Orbital Reference Determinants: A Comparative Study.
191. G. E. Scuseria, *Int. J. Quantum Chem.*, **55**, 165 (1995). On the Connections Between Brueckner-Coupled-Cluster, Density-Dependent Hartree–Fock, and Density Functional Theory.
192. C. D. Sherrill, A. I. Krylov, E. F. C. Byrd, and M. Head-Gordon, *J. Chem. Phys.*, **109**, 4171 (1998). Energies and Analytic Gradients for a Coupled-Cluster Doubles Model Using Variational Brueckner Orbitals. Application to Symmetry Breaking in  $\text{O}_4^+$ .
193. J. Čížek and J. Paldus, *J. Chem. Phys.*, **47**, 3976 (1967). Stability Conditions for the Solutions of the Hartree–Fock Equations for Atomic and Molecular Systems. Application to the Pi-Electron Model of Cyclic Polyenes.
194. J. Paldus and J. Čížek, *Chem. Phys. Lett.*, **3**, 1 (1969). Stability Conditions for the Solutions of the Hartree–Fock Equations for the Simple Open-Shell Case.
195. E. R. Davidson and W. T. Borden, *J. Phys. Chem.*, **87**, 4783 (1983). Symmetry Breaking in Polyatomic Molecules: Real and Artifactual. See also: T. Bally and W. T. Borden, in *Reviews in Computational Chemistry*, K. B. Lipkowitz and D. B. Boyd, Eds., Wiley-VCH, New York, Vol. 13, pp. 1–97. Calculations on Open-Shell Molecules: A Beginner’s Guide.
196. W. D. Allen, D. A. Horner, R. L. DeKock, R. B. Remington, and H. F. Schaefer, *Chem. Phys.*, **133**, 11 (1989). The Lithium Superoxide Radical: Symmetry Breaking Phenomena and Potential Energy Surfaces.
197. O. Goscinski, *Int. J. Quantum Chem. Symp.*, **19**, 51 (1986). Are Localized Broken Symmetry Solutions Acceptable in Molecular Calculations?
198. P.-O. Löwdin, *Rev. Mod. Phys.*, **35**, 496 (1963). Discussion on the Hartree–Fock Approximation.
199. K. Deguchi, K. Nishikawa, and S. Aono, *J. Chem. Phys.*, **75**, 4165 (1981). Instabilities of the Hartree–Fock Solution and the Vibrational Mode in a Molecule.
200. Y. Yamaguchi, I. L. Alberts, J. D. Goddard, and H. F. Schaefer, *Chem. Phys.*, **147**, 309 (1990). Use of the Molecular Orbital Hessian for Self-Consistent-Field (SCF) Wavefunctions.
201. N. A. Burton, Y. Yamaguchi, I. L. Alberts, and H. F. Schaefer, *J. Chem. Phys.*, **95**, 7466 (1991). Interpretation of Excited State Hartree–Fock Analytic Derivative Anomalies for  $\text{NO}_2$  and  $\text{HCO}_2$  Using the Molecular Orbital Hessian.
202. L. A. Barnes and R. Lindh, *Chem. Phys. Lett.*, **223**, 207 (1994). Symmetry Breaking in  $\text{O}_4^+$ : An Application of the Brueckner Coupled-Cluster Method.
203. Y. Xie, W. D. Allen, Y. Yamaguchi, and H. F. Schaefer, *J. Chem. Phys.*, **104**, 7615 (1996). Is the Oxywater Radical Cation More Stable Than Neutral Oxywater?
204. J. Hrušák and S. Iwata, *J. Chem. Phys.*, **106**, 4877 (1997). The Vibrational Spectrum of  $\text{H}_2\text{O}_2^+$  Radical Cation: An Illustration of Symmetry Breaking.

205. T. D. Crawford, J. F. Stanton, P. G. Szalay, and H. F. Schaefer, *J. Chem. Phys.*, **107**, 2525 (1997). The  $\tilde{C}^2A_2$  Excited State of  $\text{NO}_2$ : Evidence for a  $C_s$  Equilibrium Structure and a Failure of Some Spin-Restricted Reference Wavefunctions.
206. K. Shibuya, C. Terauchi, M. Sugawara, K. Aoki, K. Tsuji, and S. Tsuchiya, *J. Mol. Struct.*, **413–414**, 501 (1997). Vibrational Level Structure of  $\text{NO}_2 \tilde{C}^2A_2$  in the Energy Region of  $16200\text{--}21000\text{ cm}^{-1}$ : Evidence for the Breakdown of  $C_{2v}$  Symmetry.
207. R. A. King, T. D. Crawford, J. F. Stanton, and H. F. Schaefer, *J. Am. Chem. Soc.*, submitted, 1999. Conformations of [10]Annulene. More Bad News for Density-Functional Theory and Perturbation Theory.
208. P. Pulay, *Chem. Phys. Lett.*, **100**, 151 (1983). Localizability of Dynamic Electron Correlation.
209. S. Sæbø and P. Pulay, *Chem. Phys. Lett.*, **113**, 13 (1985). Local Configuration Interaction: An Efficient Approach for Larger Molecules.
210. P. Pulay and S. Sæbø, *Theor. Chim. Acta*, **69**, 357 (1986). Orbital-Invariant Formulation and Second-Order Gradient Evaluation in Møller-Plesset Perturbation Theory.
211. S. Sæbø and P. Pulay, *J. Chem. Phys.*, **86**, 914 (1987). Fourth-Order Møller-Plesset Perturbation Theory in the Local Correlation Treatment. I. Method.
212. S. Sæbø, W. Tong, and P. Pulay, *J. Chem. Phys.*, **98**, 2170 (1993). Efficient Elimination of Basis Set Superposition Errors by the Local Correlation Method: Accurate Ab Initio Studies of the Water Dimer.
213. C. Hampel and H.-J. Werner, *J. Chem. Phys.*, **104**, 6286 (1996). Local Treatment of Electron Correlation in Coupled Cluster Theory.
214. J. D. Watts and R. J. Bartlett, *J. Chem. Phys.*, **101**, 3073 (1994). The Inclusion of Connected Triples Excitations in the Equation-of-Motion Coupled-Cluster Methods.
215. J. D. Watts and R. J. Bartlett, *Chem. Phys. Lett.*, **233**, 81 (1995). Economical Triple Excitation Equation-of-Motion Coupled-Cluster Methods for Excitation-Energies.
216. J. D. Watts and R. J. Bartlett, *Chem. Phys. Lett.*, **258**, 581 (1996). Iterative and Noniterative Triple Excitation Corrections in Coupled-Cluster Methods for Excited Electronic States—The EOM-CCSDT-3 and EOM-CCSD(T) Methods.
217. O. Christiansen, H. Koch, and P. Jørgensen, *J. Chem. Phys.*, **105**, 1451 (1996). Perturbative Triple Excitation Corrections to Coupled Cluster Singles and Doubles Excitation Energies.
218. P. Piecuch, N. Oliphant, and L. Adamowicz, *J. Chem. Phys.*, **99**, 1875 (1993). A State-Selective Multireference Coupled-Cluster Theory Employing the Single-Reference Formalism.
219. P. Piecuch and L. Adamowicz, *J. Chem. Phys.*, **102**, 898 (1995). Breaking Bonds with the State-Selective Multireference Coupled-Cluster Methods Employing the Single-Reference Formalism.
220. A. Banerjee and J. Simons, *J. Chem. Phys.*, **76**, 4548 (1982). Applications of Multiconfigurational Coupled-Cluster Theory.
221. W. D. Laidig and R. J. Bartlett, *Chem. Phys. Lett.*, **104**, 424 (1984). A Multi-Reference Coupled-Cluster Method for Molecular Applications.
222. P. G. Szalay and R. J. Bartlett, *J. Chem. Phys.*, **103**, 3600 (1995). Approximately Extensive Modifications of the Multireference Configuration Interaction Method: A Theoretical and Practical Analysis.
223. K. B. Ghose, P. Piecuch, and L. Adamovicz, *J. Chem. Phys.*, **103**, 9331 (1995). Improved Computational Strategy for the State-Selective Coupled-Cluster Theory with Semi-Internal Triexcited Clusters: Potential Energy Surface of the HF Molecule.
224. J. T. Fermann, C. D. Sherrill, T. D. Crawford, and H. F. Schaefer, *J. Chem. Phys.*, **100**, 8132 (1994). Benchmark Studies of Electron Correlation in Six-Electron Systems.
225. N. C. Handy and A. M. Lee, *Chem. Phys. Lett.*, **252**, 425 (1996). The Adiabatic Approximation.

226. J. Almlöf and P. R. Taylor, *J. Chem. Phys.*, **86**, 4070 (1987). General Contraction of Gaussian Basis Sets. I. Atomic Natural Orbitals for First- and Second-Row Atoms.
227. J. Almlöf, T. Helgaker, and P. R. Taylor, *J. Phys. Chem.*, **92**, 3029 (1988). Gaussian Basis Sets for High-Quality Ab Initio Calculations.
228. T. H. Dunning, *J. Chem. Phys.*, **90**, 1007 (1989). Gaussian Basis Sets for Use in Correlated Molecular Calculations. I. The Atoms Boron Through Neon.
229. B. J. Persson and P. R. Taylor, *J. Chem. Phys.*, **105**, 5915 (1996). Accurate Quantum-Chemical Calculations: The Use of Gaussian-Type Geminal Functions in the Treatment of Electron Correlation.
230. J. M. L. Martin and P. R. Taylor, *J. Chem. Phys.*, **106**, 8620 (1997). Benchmark Quality Total Atomization Energies of Small Polyatomic Molecules.
231. T. Helgaker, W. Klopper, H. Koch, and J. Noga, *J. Chem. Phys.*, **106**, 9639 (1997). Basis-Set Convergence of Correlated Calculations on Water.
232. W. Klopper, Habilitationsschrift, Eidgenössischen Technischen Hochschule, Zürich, 1996.  $r_{12}$ -Dependent Wave Functions.